

Aus der
Klinik und Poliklinik für Hals-Nasen-Ohrenheilkunde
Klinikum der Ludwig-Maximilians-Universität München



**Functional characterization of effectors of EGFR-mediated local
invasion in head and neck carcinomas**

Dissertation
zum Erwerb des Doktorgrades der Medizin
an der Medizinischen Fakultät der
Ludwig-Maximilians-Universität zu München

vorgelegt von
Enxian Shi

aus
Chongqing, China

Jahr
2024

Mit Genehmigung der Medizinischen Fakultät der
Ludwig-Maximilians-Universität München

Erstes Gutachten: Prof. Dr. Olivier Gires
Zweites Gutachten: Prof. Dr. Sebastian Kobold
Drittes Gutachten: Prof. Dr. Andreas Leunig
weitere Gutachten: PD Dr. Maximilian Reiter

Promovierter Mitbetreuer: Prof. Philipp Baumeister
Dekan: Prof. Dr. med. Thomas Gudermann

Tag der mündlichen Prüfung: 31.07.2024

Affidavit



Promotionsbüro
Medizinische Fakultät



Affidavit

Shi, Enxian

Surname, first name

Street

Zip code, town, country

I hereby declare, that the submitted thesis entitled:

Functional characterization of effectors of EGFR-mediated local invasion in head and neck carcinomas

.....

is my own work. I have only used the sources indicated and have not made unauthorized use of services of a third party. Where the work of others has been quoted or reproduced, the source is always given.

I further declare that the dissertation presented here has not been submitted in the same or similar form to any other institution for the purpose of obtaining an academic degree.

Chongqing, 31.07.2024

place, date

Enxian Shi

Signature doctoral candidate

Table of content

Affidavit	3
Table of content.....	4
Zusammenfassung	7
Abstract.....	9
List of abbreviations	11
1. Introduction.....	14
1. 1 Head and neck squamous cell carcinoma	14
1.1.1 Molecular heterogeneity of HNSCC	15
1.2 Epithelial-to-mesenchymal transition (EMT)	16
1.2.1 EMT in cancer.....	17
1.2.2 Molecular regulation of EMT in HNSCC.....	20
1.3 Epidermal growth factor receptor (EGFR).....	21
1.3.1 EGFR biology and targeted therapies in HNSCC	22
1.3.2 An EGFR-mediated EMT gene signature in HNSCC	24
1.4 Integrin β 4 (ITG β 4)	26
1.4.1 Structure and biology of ITG β 4	26
1.4.2 ITG β 4 in cancer	28
1.5 CD73.....	30
1.5.1 Biology of CD73	30
1.5.2 CD73 in cancer	32
2. Materials and Methods.....	33
2.1 Human samples and ethics statement	33
2.2 Immunohistochemistry, immunofluorescence and scoring	33
2.3 Tumor budding	34
2.4 Cell lines and treatments	34
2.5 Generation of ITG β 4 knockdown cells	34
2.6 Generation of CD73 knockdown and overexpression cells.....	35
2.8 Primers used for qPCR quantification	35
2.9 Flow cytometry.....	36
2.10 Cytotoxicity assay	36
2.11 2D migration, invasion and wound healing assay	37
2.12 3D invasion assay	37
2.13 Data source and gene set variation analysis (GSVA)	37

2.14 Statistical analysis	38
3. Results	39
3.1 EGF ^{high} induces EMT in HNSCC cell lines	39
3.1.1 EGFR expression in FaDu and Kyse30 cells	39
3.1.2 EGF ^{high} induces EMT morphology change in FaDu and Kyse30.....	40
3.2 ITGβ4 and its ligand laminin 5 are up-regulated in HNSCC.....	41
3.2.1 Upregulation of <i>ITGβ4</i> and laminin 5 in 2D transcriptomic analysis.....	41
3.2.2 EGF ^{high} treatment upregulates ITGβ4 expression in HNSCC cell lines..	41
3.2.3 ITGβ4 is upregulated in HNSCC tumor tissues.....	42
3.2.4 ITGβ4 and laminin 5 expression in TCGA cohort and scRNA-seq dataset	45
3.2.5 ITGβ4 and LAMA3 co-expression in HNSCC tumor tissues.....	46
3.3 ITGβ4 correlates with EGFR activity in malignant HNSCC cells	48
3.4 ITGβ4 promotes migration and invasion in HNSCC.....	50
3.4.1 Validation of ITGβ4 knockdown in HNSCC cells.....	50
3.4.2 Knockdown of ITGβ4 decreases EGFR-mediated 2D migration and invasion in HNSCC cells	51
3.4.3 Knockdown of ITGβ4 decreases EGFR-mediated 3D invasion in HNSCC cells.....	54
3.4.4 Antagonizing ITGβ4 inhibits local invasion in HNSCC cells	55
3.5 ITGβ4 is strongly expressed in locally invasive cells and tumor budding	57
3.5.1 ITGβ4 and laminin 5 genes are upregulated at the leading edge of HNSCC	57
3.5.2 ITGβ4 availability in the leading edge of invasion in EGF-treated spheroids.....	59
3.5.3 Edge localization of ITGβ4 is associated with stronger tumor budding intensity	61
3.6 Laminin 5-ITGβ4 promotes EGFR-mediated local invasion	62
3.7 CD73 expression is upregulated via the EGFR-MAPK axis in HNSCC65	
3.8 Functional role of CD73 in EGFR-mediated migration and invasion in HNSCC	68
3.8.1 CD73 blocking does not impacts on EGFR-EMT induction	68
3.8.2 Inhibition of CD73 impacts on EGFR-mediated 2D migration and invasion.....	70
3.8.3 Blocking CD73 represses EGFR-mediated local invasion	72
3.9 CD73 serves an effector of EGFR-mediated EMT.....	76
3.9.1 Proliferation-independent effect of CD73 inhibition on EGFR-mediated local invasion.....	76
3.9.2 Functional characterization of CD73 on EGFR-EMT-mediated local invasion.....	78
3.10 CD73 is highly expressed in budding cells in HNSCC	83

3.11 CD73 expression as a predictive marker of Cetuximab response.....	87
4. Discussion	90
4.1 Functional characterization of ITGβ4 and CD73 in EGFR-mediated EMT in HNSCC.....	91
4.1.1 ITGβ4 binding to laminin 5 promotes EGFR-mediated local invasion in HNSCC	91
4.1.2 CD73 supports EGFR-mediated invasion in HPV-neg HNSCC	93
4.2 ITGβ4 and CD73 as predictive biomarkers in HNSCC	96
4.3 Rationale for ITGβ4 and CD73 as therapeutic targets in HNSCC	97
5. References.....	99
6. Contribution statement	125
7. List of publications.....	126
8. Acknowledge.....	127

Zusammenfassung

In Plattenepithelkarzinomen des Kopf- und Halsbereichs (HNSCC) spielt die molekulare Heterogenität eine entscheidende Rolle bei schlechten klinischen Ergebnissen und Therapieresistenz. Das Vorhandensein intratumoraler Heterogenität bildet die Grundlage für die Förderung eines epithelial-mesenchymalen Übergangs (Epithelial-mesenchymal transition; EMT) oder einer partiellen EMT, die zentrale Faktoren für Tumorprogression, Metastasierung und Therapieresistenz in humanen Papillomavirus-negativen (HPV-negativen) HNSCC darstellen. Der epidermale Wachstumsfaktorrezeptor (EGFR) ist häufig überexprimiert und dient als therapeutisches Ziel in fortgeschrittenen HNSCC. Die Antwort auf die EGFR-Behandlung in HNSCC ist jedoch begrenzt und es fehlen Biomarker für die Vorhersage der Therapieantwort und neue therapeutische Ziele, um die Wirksamkeit der EGFR-Therapie in einer kombinierten therapeutischen Modalität zu verbessern. Unsere Gruppe hat zuvor berichtet, dass EGFR eine duale Rolle bei der Regulation von Proliferation und EMT in HNSCC spielt und einen invasionsfördernden Subtyp von EMT durch eine anhaltende Überaktivierung von EGFR induziert, der durch eine EGFR-EMT-Gensignatur charakterisiert ist. Des Weiteren wurde eine prognostische 5-Gensignatur aus der identifizierten EGFR-EMT-Gensignatur erstellt, welche mit dem Gesamtüberleben bei HNSCC-Patienten assoziiert.

Ziel dieser vorliegenden Studie war es, eine funktionelle Charakterisierung zweier Genprodukte aus der EGFR-EMT-Gensignatur, Integrin beta 4 (ITG β 4) und CD73, im Prozess der EGFR-vermittelten lokalen Invasion in HNSCC durchzuführen und zu untersuchen, ob diese beiden Oberflächenproteine als prädiktive Biomarker und potenzielle therapeutische Ziele in HNSCC dienen.

Im ersten Teil dieser Arbeit wurde ITG β 4, ein Bestandteil der 5-Gensignatur des EGFR-EMT in HNSCC, ausgewählt, um eine funktionelle Charakterisierung in der EGFR-vermittelten lokalen Invasion durchzuführen. Die Hochregulation von ITG β 4 wurde in primären HNSCC und Lymphknotenmetastasen durch Immunhistochemie-Färbung validiert und war mit der EGFR-MAPK-Signalkaskade in Zelllinien und in der TCGA-Kohorte assoziiert. ITG β 4 und sein Ligand Laminin 5 waren an Tumorrändern im Vergleich zum Tumorkern hochreguliert, und ITG β 4 wurde in invasiven Zellen in einem 3D-Sphäroid-Modell stark exprimiert. Die funktionelle Charakterisierung von ITG β 4 in der EGFR-vermittelten lokalen Invasion wurde in 2D- und 3D-Zellmodellen für

Migration und Invasion untersucht. Die Hemmung der ITG β 4 Expression unterdrückte die EGFR-vermittelte Migration und Invasion. Das Blockieren der Bindung von ITG β 4 an Laminin-5 durch den ASC8-Antikörper reduzierte ebenfalls die EGFR-vermittelte lokale Invasion, während die Ergänzung von Laminin 5 die lokale Invasion in 3D förderte.

Im zweiten Teil konzentrierten wir uns darauf, die Regulation von CD73 durch die EGFR-Signalkaskade und ihre funktionelle Rolle in der EGFR-vermittelten lokalen Invasion in HNSCC zu erforschen. Es wurde validiert, dass CD73 durch die EGFR-MAPK-Achse hochreguliert und durch Cetuximab und MEK-Inhibitor gehemmt wurde. Die CD73-Expression war mit der Aktivität des EGFR-Signalwegs, der EMT- und der partiellen EMT-Signatur (pEMT) in einzelnen malignen HNSCC Zellen und in großen Kohorten von HNSCC assoziiert. Der neu entwickelte, antagonistische CD73-Antikörper 22E6 reduzierte die EGFR-vermittelte Migration und Invasion, was mit der Wirkung der alleinigen Cetuximab-Behandlung vergleichbar war. Interessanterweise beobachteten wir, wenn nicht-inhibierende Konzentrationen von Cetuximab und 22E6 kombiniert wurden, eine bemerkenswert starke Hemmung der lokalen Invasion, wodurch die funktionelle IC50 Konzentration von Cetuximab im Hinblick auf die lokale Invasion erheblich gesenkt wurde. In-vitro-Experimente zum Funktionsgewinn- und -verlust von CD73, zusammen mit der starken Expression von CD73 in einzelnen, abgesonderten Tumorzellen in primären HNSCC, bekräftigen weiterhin eine Rolle von CD73 als Effektor der EGFR-vermittelten lokalen Invasion. Im Gegensatz zu veröffentlichten Daten erwies sich CD73 nicht als prognostischer Marker für das Gesamtüberleben (overall survival OS) in der TCGA-HNSCC-Kohorte, wenn die Patienten nach ihrem HPV-Status stratifiziert wurden. Allerdings prognostizierte CD73 das OS von Mundhöhlenkarzinomen. Darüber hinaus korrelierten das CD73-Expressionsniveaus mit der Antwort auf Cetuximab bei HPV-negativen fortgeschrittenen, metastasierten HNSCC-Patienten.

Zusammenfassend lässt sich sagen, dass diese Studie zu dem Schluss führt, dass ITG β 4 und CD73 als Bestandteile der EGFR-EMT-Signatur eine entscheidende Rolle bei der EGFR-vermittelten lokalen Invasion in HNSCC spielen. ITG β 4 und CD73 wurden als potenzielle Indikatoren für den EGFR-EMT-Status in Zellen identifiziert, die möglicherweise als Sensoren für aggressive, invasive Krebszellen dienen, die auf Cetuximab ansprechen, und als therapeutische Ziele in Kombination mit Cetuximab in der Behandlung von fortgeschrittenen HNSCC.

Abstract

In head and neck squamous cell carcinomas (HNSCCs), molecular heterogeneity exerts a crucial influence on unfavorable clinical prognosis and resistance to treatment. Intratumoral heterogeneity serves as a foundation to promote epithelial-mesenchymal transition (EMT) or pEMT (pEMT), which are prominent factors contributing to tumor progression, metastasis and therapy resistance in human papillomavirus-negative (HPV-negative) HNSCC. Epidermal growth factor receptor (EGFR) is frequently overexpressed in advanced HNSCC and serves as a therapeutic target. However, the effectiveness of EGFR-targeted treatments in HNSCC is not consistent, and there is a lack of reliable biomarkers to predict treatment outcomes and novel therapeutic targets to enhance the effectiveness of targeting EGFR in combinatorial therapies. Our group previously reported that EGFR presents a dual role in governing both proliferation and EMT in HNSCC, and identified an invasion-promoting subtype of EMT induced by sustained hyper-activation of EGFR, which is characterized by an EGFR-EMT gene signature. A 5-gene prognostic signature, derived from the identified EGFR-EMT gene signature, exhibited a correlation with the overall survival in HNSCC patients. The aim of this thesis was to explore the functional characterization of two effectors, ITG β 4 and CD73, integral components of the EGFR-EMT gene signature, in the context of EGFR-mediated local invasion in HNSCC. Additionally, the study aimed to evaluate whether these two effectors could function as predictive biomarkers and potential therapeutic targets in HNSCC.

The first part of this thesis focused on ITG β 4, identified within the EGFR-EMT 5-gene prognostic signature in HNSCC, to explore its functional characterization in EGFR-mediated local invasion. Upregulation of ITG β 4 was validated in both primary HNSCC and lymph node metastases by immunohistochemistry staining, and exhibited an association with EGFR-MAPK signaling in single malignant cells and in the HPV-negative TCGA HNSCC cohort. Furthermore, in the leading edge area, *ITG β 4* and its associated ligand, laminin 5, showed increased expression compared with tumor core areas, and ITG β 4 was strongly expressed in leading invasive tumor cells in a 3D spheroid model. ITG β 4 co-localized with laminin 5 at the boundary between tumor and stromal regions, which was associated with enhanced tumor budding in HNSCC. Functional characterization of ITG β 4 in EGFR-mediated local invasion was assessed using 2D and

3D models to study migration and invasion processes. *ITGβ4* knock-down suppressed migration and invasion mediated by EGFR activation. Blocking *ITGβ4* binding to laminin by ASC8 antibody likewise reduced EGFR-mediated local invasion, whereas supplementation of laminin 5 further promoted EGF-mediated local invasion in 3D.

In the second part, we focused on exploring CD73 regulation via EGFR signaling pathway and CD73's function in EGFR-mediated local invasion in HNSCC. CD73 was upregulated through the EGFR-MAPK pathway and inhibited by treatment with Cetuximab and MEK inhibitor. Furthermore, CD73 expression was associated with EGFR activation, EMT hallmark, and Puram's common pEMT signature in single malignant cells and across broad cohorts of HNSCC. Inhibiting CD73's enzymatic activity showed no impact on EMT induction, however, the antagonizing CD73 antibody 22E6 reduced migration and invasion mediated to a comparable extent than Cetuximab mono-treatment. Interestingly, when combining ineffective concentrations of Cetuximab and 22E6, we observed a remarkably potent inhibition of local invasion, substantially lowering the functional IC50 of Cetuximab with respect local invasive. Loss- and gain-of-function experiments in vitro, coupled with the observed strong expression of CD73 in tumor budding in primary HNSCC, further corroborated CD73's role as a key factor in EGFR-mediated local invasion.

Contrary to previous findings, CD73 did not serve as a predictor of overall survival (OS) when patients were categorized based on their HPV status in the TCGA-HNSCC group. However, CD73 was indicative of OS in cases of oral cavity cancer. Additionally, in patients with HPV-negative recurrent or metastatic HNSCC, the levels of CD73 expression were linked with their responsiveness to Cetuximab treatment.

In summary, this study led to the conclusion that as parts of EGFR-EMT signature, *ITGβ4* and CD73 is crucial for EGFR-mediated local invasion in HNSCC. Furthermore, *ITGβ4* and CD73 were identified as potential indicators of the EGFR-EMT activity, potentially acting as detectors for aggressive, invasive cancer cells responsive to Cetuximab, and as therapeutic targets for combined therapy with Cetuximab in the treatment of recurrent and advanced HNSCC.

List of abbreviations

ADO	Adenosine
AJCC	American Joint Committee on Cancer
AMP	Adenosine Monophosphate
APCP	Adenosine 5'-(α,β -methylene)diphosphate
AREG	Amphiregulin
AUC	Area Under the Curve
BTC	Betacellulin
CAF	Cancer-associated Fibroblast
CAR-T	Chimeric Antigen Receptor T Cell
CDKN2A	Cyclin-Dependent Kinase Inhibitor 2A
CNV	Copy Number Variation
CSC	Cancer Stem Cells
DDIT4	DNA Damage Inducible Transcript 4
EBV	Epstein-Barr Virus
ECM	Extracellular Matrix
EGF	Epidermal Growth Factor
EGFR	Epidermal Growth Factor Receptor
EMT	Epithelial-mesenchymal Transition
EMT-TFs	Epithelial-Mesenchymal Transition Transcription Factors
EPGN	Epigen
EREG	Epiregulin
ERK	Extracellular Signal-Regulated Kinase
FADD	Fas-Associated Protein with Death Domain
FDA	Food and Drug Administration
FGFR1	Fibroblast Growth Factor Receptor 1
FHCRC	Fred Hutchinson Cancer Research Center
GEO	Gene Expression Omnibus
GPI	Glycosyl-phosphatidylinositol

GSVA	Gene Set Variation Analysis
HB-EGF	Heparin-binding EGF-like Growth Factor
HCC	Hepatocellular Carcinoma
HER2	Human Epidermal Growth Factor Receptor 2
HNSCC	Head and Neck <i>Squamous</i> Cell Carcinoma
HPV	Human Papillomavirus
IA	Invasive Area
ID	Invasive Distance
IF	Immunofluorescence
IHC	Immunohistochemistry
IL-17	Interleukin-17
ITGB4/ITGβ4	Integrin β4
ITH	Inter-tumor Heterogeneity
LE	Leading Edge
LN5	Laminin 5
MAPK	Mitogen-Activated Protein Kinase
MEK	Mitogen-Activated Protein Kinase Kinase
MET	Mesenchymal-epithelial Transition
MFI	Mean Fluorescence Intensity
MSigDB	Molecular Signatures Database
NCEH1	Neutral Cholesterol Ester Hydrolase 1
NF- κB	Nuclear Factor-κB
NT5E	5'-Nucleotidase
OD	Optical Density
OS	Overall Survival
OSCC	Oral Squamous Cell Cancer
PCR	Polymerase Chain Reaction
PD-1	programmed cell death protein 1
PD-L1	Programmed Death-Ligand 1

PDX	Patient-derived Xenografts
pEMT	Partial Epithelial-mesenchymal Transition
PFS	Progression-free Survival
PI3K	Phosphoinositide 3-Kinase
PIK3CA	Phosphatidylinositol-4,5-bisphosphate 3-kinase Catalytic Subunit Alpha
PKC	Protein kinase C
PLC	Phospholipase C
PRRX1	Paired-related Homeobox 1
RTK	Receptors Tyrosine Kinases
scRNA-seq	Single-Cell RNA Sequencing
TC	Tumor Core
TCGA	Cancer Genome Atlas
TCGA	The Cancer Genome Atlas
TGF- α	Transforming Growth Factor- α
TGF- β	Transforming Growth Factor- β
TIMP1	Tissue Inhibitor of Metaloproteinases 1
TISCH2	Tumor Immune Single-Cell Hub 2
TKI	Tyrosine Kinase Inhibitor
TME	Tumor Microenvironment
TNBC	Triple Negative Breast Cancer
TNM	Tumour-Node-Metastasis
TRAF3	Tumor Necrosis Factor Receptor-Associated Factor 3
UICC	Union for International Cancer Control
WT	Wild Type

1. Introduction

1.1 Head and neck squamous cell carcinoma

Head and neck squamous cell carcinoma (HNSCC) encompasses a wide range of cancers that originate from mucosal epithelial cells in the oral cavity, pharynx, larynx and sinonasal tract (Thomas et al., 2022). HNSCC remain the sixth most prevalent malignancy with 600,000 new cases diagnosed each year and a mortality rate of approximately 40–50% (Santos et al., 2021; Siegel et al., 2023; H. Sung et al., 2021). The prevalence of HNSCC differs between various regions and countries, and it has been generally associated with multiple risk factors including excessive tobacco consumption, alcohol abuse, exposure to environmental pollutants, and viral infection with human papillomavirus (HPV) or Epstein-Barr virus (EBV) (Gillison et al., 2008; Mody et al., 2021). HNSCCs that develop within the oropharynx are increasingly associated with chronic infection with HPV, particularly HPV-16 (Rahimi, 2020; Solomon et al., 2018). HPV-induced oropharyngeal cancers are regarded as a distinct disease entity, which has been presented in a modified 8th edition of the UICC tumor staging system. HPV-negative HNSCC typically manifests in the oral cavity and laryngeal regions, and is primarily correlated with acquired mutations and alterations from risk factors such as tobacco and alcohol (Ferris et al., 2021; Leemans et al., 2018; Puram et al., 2023).

There is evidence of histological progression of invasive HNSCC starting from epithelial cell hyperplasia, progresses through various degrees of atypical hyperplasia, carcinoma *in situ*, and finally leading to invasive carcinoma (Johnson et al., 2020). Despite this rather long-lasting sequence of events, most patients are diagnosed with advanced HNSCC in the absence of clinically noticeable precancerous lesions. Traditional HNSCC staging defined by the tumor-node-metastasis (TNM) system has been updated by the 2017 AJCC/UICC staging system, incorporating new details specific to HPV-positive disease and the depth of invasion (Leemans et al., 2018). Predominant factors associated with poor survival in HNSCC include resistance to multimodal therapeutic approach, and high incidence of local recurrence and metastasis. The multimodal treatment approach, which is based on anatomical subdivision, stage, disease characteristics, functional considerations and patient preference, is generally consisting of surgery, radiation, chemotherapy and targeted therapy (Marur & Forastiere, 2016; Mesia et al., 2021). Importantly, epidermal growth factor receptors (EGFR) emerged as a primary molecular target in therapeutic

strategies (Bhatia & Burtress, 2023). The optimal application of EGFR inhibitor-based treatment strategies remains actively under investigation, despite the approval of the anti-EGFR monoclonal antibody Cetuximab for recurrent/metastatic tumors. HNSCC is recognized as an intrinsically immune-suppressive disease, and immune checkpoint inhibitors, such as anti-programmed cell death protein 1 (PD-1) and anti-PD-1 ligand (PD-L1) inhibitors, have been identified as additional therapeutic alternatives for advanced HNSCC (Botticelli et al., 2021; X. Wu et al., 2019). Regardless of these advances, outcomes haven't been improved significantly over the past decades, particularly in HPV-negative HNSCC, and short- and long-term treatment-associated overall survival remain rather poor.

1.1.1 Molecular heterogeneity of HNSCC

HNSCCs represent a heterogeneous group of tumors, and high intra- and inter-tumor heterogeneity (ITH) is a key factor in the progression, metastasis and treatment resistance of HNSCC (Leemans et al., 2011, 2018; Van den Bossche et al., 2022). Extensive research suggests that heterogeneity develops over time when initially healthy epithelial cells undergo genetic and epigenetic alterations, enabling them to differentiate into various tumor cell types, most likely including the formation of tumor-initiating cells. It has been revealed that high ITH fosters substantial cellular diversity, leading to the development of distinct cellular subgroups characterized by unique transcriptomic profiles, which might explain differences in response to standard treatments (Johnson et al., 2020; Rahimy et al., 2023; Sharon et al., 2023).

Large whole-genome sequencing analyses have been performed, deepening our understanding of heterogeneous properties of HNSCC (Leemans et al., 2018). Stransky *et al.* reported on frequent and multiple genomic mutations observed in HNSCC, yielding an average per tumor of 130 mutations in coding sequences (Stransky et al., 2011). The Cancer Genome Atlas (TCGA) is a rich dataset covering aspects such as copy number alterations (CNAs), mutation patterns, and mRNA and miRNA expression derived from cancer samples. The TCGA HNSCC analysis (Cancer Genome Atlas., 2015) presented an in-depth view of somatic genetic variations through the analysis of 279 HNSCCs. This analysis revealed significant genomic instability in HNSCC, characterized by frequent losses or gains of chromosomal regions. In HPV-positive HNSCC, the analysis confirmed the unique enrichment for loss of tumor necrosis factor receptor-associated Factor 3 (TRAF3), a key component of the nuclear factor- κ B (NF- κ B) pathway activation,

amplification of E2F1, and activating mutations of phosphatidylinositol-4,5-bisphosphate 3-kinase catalytic subunit alpha (PIK3CA). HPV-negative HNSCC exhibited amplified cyclin-dependent kinase inhibitor 2A (CDKN2A), TP53 modifications, and enhancement of the genes encoding receptor tyrosine kinases EGFR, HER2 (also termed ERBB2) and fibroblast growth factor receptor 1 (FGFR1) (Cancer Genome Atlas., 2015). Targeting EGFR with therapeutic agents (i.e. Cetuximab) has become an FDA- and EMA-approved approach for blocking EGFR activation in HNSCC, whereas amplification of receptor tyrosine kinases HER2 may potentially enhance resistance to EGFR-targeting treatment in HNSCC (Bhatia & Burtneess, 2023; Kang et al., 2023; M. J. Xu et al., 2017).

Single cell RNA-sequencing (scRNA-seq) of tumor samples has further revealed intra-tumor genetic diversity and its potential clinical significance in HNSCC (Puram et al., 2017). The analysis identified HNSCC tumor cell signatures associated with epithelial differentiation, the cell cycle, cellular stress, hypoxia, and a partial epithelial-mesenchymal transition (pEMT). Tumor cells in pEMT state were often found at the forefront of primary HNSCC, and those with a predominate pEMT signature were positively associated with locoregional metastasis. Notably, pEMT was established as an independent predictor of nodal metastasis, grading and pathologic characteristics (Puram et al., 2017). Further analysis revealed that the pEMT signature was predominantly linked to the expression of the canonical EMT transcription factor, *Slug*, and it prognosticates OS and response to radiation therapy in HNSCC (Schinke, Pan, et al., 2022). These results indicate that the heterogeneity of HNSCC and more specifically tumor cells in pEMT are key factors in driving HNSCC progression, and therefore there is a high demand for identifying molecular biomarkers to determine the molecular abnormalities in HNSCC.

1.2 Epithelial-to-mesenchymal transition (EMT)

During EMT, epithelial cells downregulate epithelial traits and enhance mesenchymal features (Lamouille et al., 2014; Nieto et al., 2016). This cellular phenotype was first identified in the early embryonic development by Elizabeth Hay (Hay & Zuk, 1995). In the process of EMT, epithelial cells undergo a loss of cell polarity and cell-cell junctions, experience changes in the cell signaling pathways that govern cell morphology, and exhibit alterations in gene expression (**Fig 1**). Meanwhile, epithelial cells can acquire increased motility of individual cells, stem-cell like property and enhanced migratory or invasion abilities. The reverse process to EMT is known as mesenchymal-epithelial transition (MET), which leads to loss of migratory capacity, increased expression of

junctional complexes. The process of epithelial cells undergoing EMT and then reverting to MET demonstrates the intrinsic plasticity of the epithelial phenotype (Chaffer et al., 2011; Lambert & Weinberg, 2021; Lamouille et al., 2014; Shibue & Robert A. Weinberg, 2017). EMT is widely recognized to be involved in various non-pathological and pathological processes, including early embryonic development, organogenesis, wound healing, tissue fibrosis, as well as carcinoma progression and development of metastasis (Baumeister et al., 2021; Pastushenko & Blanpain, 2019; Yangguang Ou, Rachael E Wilson, 2018).

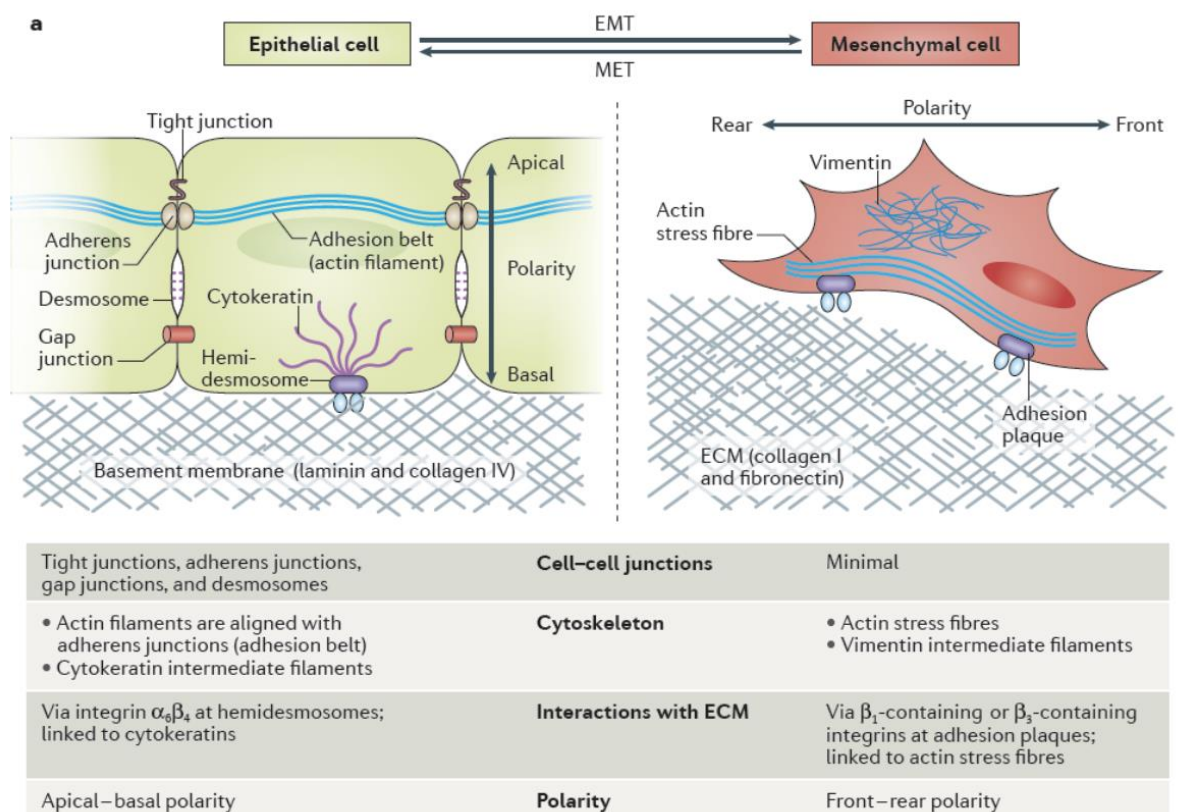


Figure 1. A graphical overview depicting morphological and physiological changes correlated with EMT

Initiation of the EMT program triggers significant alterations in multiple aspects of cell morphology and property, particularly evident in the transformation of cell-cell connections, modifications in the cytoskeletal composition, shifts in cellular interactions within the extracellular matrix (ECM), and adjustments in cellular orientation and organization (Figure 1 was copied from Shibue & Robert A. Weinberg, 2017).

1.2.1 EMT in cancer

EMT has been shown to be linked with oncogenic processes, including tumor initiation, tumor stemness, migration, blood dissemination of cancer cells, metastatic colonization and resistance to therapy (De Craene & Berx, 2013; Tam & Weinberg, 2013; Thiery et al., 2009; N. Zhang et al., 2021). In *LSL-Kras^{G12D}; P53^{loxP/+}; Pdx1-cre; LSL-Rosa26^{YFP/YFP}* (KPCY) mouse cancer models of pancreatic ductal adenocarcinoma (PDAC), half of tumors presented EMT characteristics, including a decrease in the epithelial marker E-cadherin or an increase in the mesenchymal markers Vimentin or Zeb1 (Aiello et al., 2019). Cancer cells that have experienced EMT acquire the ability to detach from primary tumors, migrate and spread to locoregional lymph nodes or vessels, and seed in distant organs (**Fig 2**). It has also been revealed that EMT is essential in the initial phases of tumor metastasis in mouse models of various cancers including HNSCC, prostate cancer, colorectal cancer and breast cancer (Ji et al., 2021; Lengrand et al., 2023; Pu et al., 2009; T. Shen et al., 2018; Zhu et al., 2022). Interestingly, EMT is not a binary process. Some cancer cells may present both epithelial and mesenchymal features, which could be recognized as pEMT (Bakir et al., 2020; Brabletz et al., 2021; T. Chen et al., 2017). Sc-RNA seq analysis also identified a pEMT program in HNSCC, characterized by the incomplete activation of EMT transcription factors (EMT-TFs) and the enrichment of a pEMT signature in cancer cells that is linked to reduced overall survival rates and an elevated risk of developing therapeutic resistance (Pan et al., 2018; Schinke, Pan, et al., 2022). During the EMT process, the expression of EMT-TFs results in a profound restructuring of cell behavior (Saitoh, 2023; Skrypek et al., 2017). For example, upregulated expression of mesenchymal markers like N-Cadherin and Vimentin triggers a polarization of tumor cells in a front-to-back manner, enhancing their migratory capabilities and invasion into the surrounding stroma (Paolillo & Schinelli, 2019; Vu & Datta, 2017). These changes play a crucial role in the initial stage of the metastatic cascade, specifically during local invasion, intravasation, and extravasation.

Numerous studies have corroborated EMT as a crucial regulator of the phenotype of cancer stem cells (CSCs) (Lambert & Weinberg, 2021; Lamouille et al., 2014; Shibue & Weinberg, 2017). CSCs, alternatively known as tumor-initiating cells, represent a subset of tumor cells endowed with the ability for self-renewal and seeding new tumors, and are implicated in the process of tumor initiation, metastasis and therapy resistance (Dawood et al., 2014; Nassar & Blanpain, 2016; Walcher et al., 2020). It has been observed that EMT activation in neoplastic cells is closely associated with transitioning into the CSC

state across various cancer types (Lambert & Weinberg, 2021). Following the EMT process, tumor cells in the non-CSC state gain CSC-like marker expression and acquire enhanced ability to seed tumors. Studies have demonstrated that CSCs exhibit greater resistance to standard cancer therapies compared to non-CSCs. (T. Huang et al., 2020; Walcher et al., 2020). This suggests that cancer cells that have transitioned into the CSC state through the initiation of EMT programs are more likely to develop resistance to standard treatment, thereby leading to CSC-driven clinical relapse. Hence, a profound understanding of the role of key molecules during the EMT process in tumor metastasis is indeed helpful to address tumor progression and drug resistance.

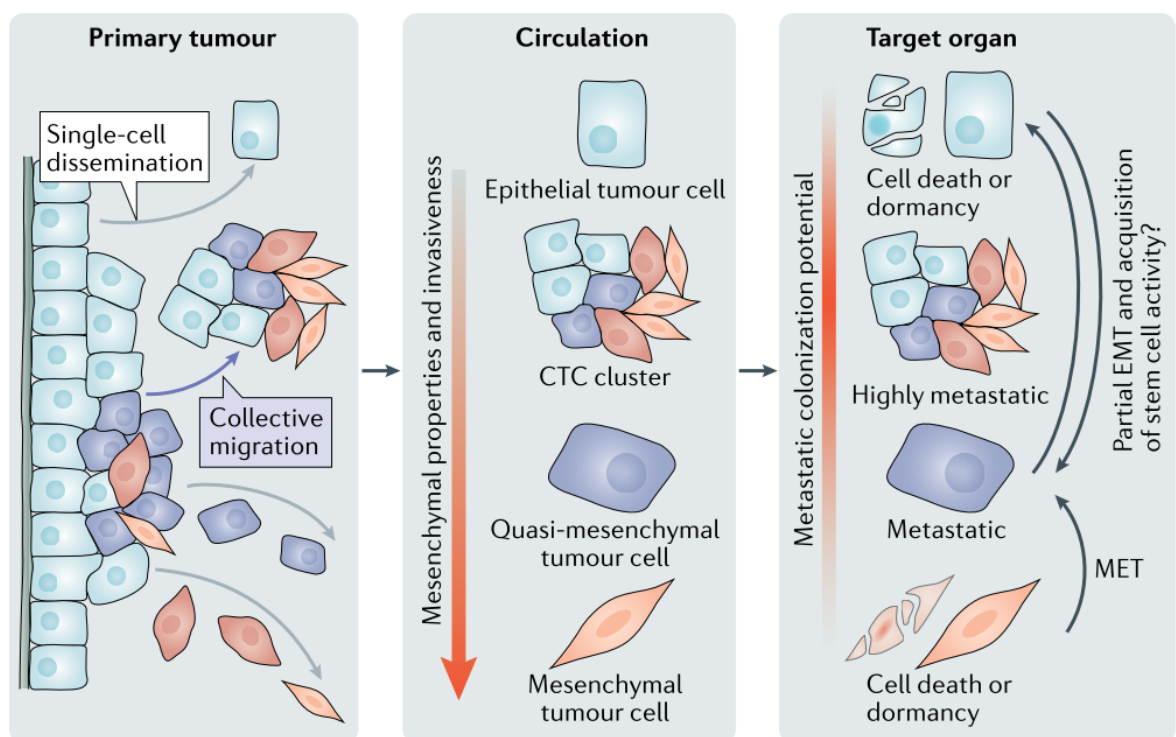


Figure 2. EMT heterogeneity during metastatic progression

Metastatic cancer cells can achieve various extents of EMT during the metastatic cascade. After gaining mesenchymal features, cancer cells may detach from the primary tumor as tumor buds, which have the potential to survive in proximity of the primary tumor or within the circulation and establish colonies in specific target organs. Some epithelial cancer cells in the circulation may undergo EMT or pEMT to acquire metastatic capacity and spread as a multicellular circulating tumor cell (CTC) cluster. After spreading to distant organs, cancer cells with a high mesenchymal phenotype will undergo a mesenchymal-epithelial transition (MET) to effectively initiate metastatic growth (Figure 2 was copied from Lambert & Weinberg, 2021).

1.2.2 Molecular regulation of EMT in HNSCC

EMT-TFs and central signaling pathways, including the transforming growth factor- β (TGF- β), EGFR, NOTCH, and WNT signaling pathways, regulate EMT and pEMT in HNSCC (Baumeister et al., 2021) (**Fig 3**).

Firstly, the intensity of EMT induction is primarily dependent on EMT-TFs that trigger cellular reprogramming. Master EMT-TFs, like SNAIL1, SLUG, ZEB1/2, and TWIST1/2, serve as transcriptional repressors that inhibit the expression of E-cadherin, leading to disruption of junctions between epithelial cells and the loss of cellular polarity (García-Cabo et al., 2020; Georgolios et al., 2006; Nardi et al., 2018). EMT-TFs also promote upregulation of mesenchymal markers, including N-cadherin and Vimentin, which can enhance migration and invasion in tumor cells (Phuong T Nguyen et al., 2011; Phuong Thao Nguyen et al., 2018; Wong et al., 2014). Moreover, EMT-TFs can interact in a network-like manner with various signaling pathways such as TGF-beta and WNT, thus facilitating the regulation of EMT initiation (Caramel et al., 2013; Frey et al., 2022; D. Liu et al., 2019).

Secondly, TGF- β 1 induces EMT via a SMAD-dependent pathway in HNSCC and plays a pivotal role in the formation of tumor buds that dissociate from primary oral squamous cell cancer (OSCC) by activating ZEB1 and paired-related homeobox 1 protein PRRX1 (C. Yu et al., 2011). TGF- β 1 cooperates with PRRX1 to regulate EMT activation, migration and invasion in HNSCC. Moreover, it has been demonstrated that TGF- β 1 originating from cancer-associated fibroblasts (CAFs) within the tumor microenvironment can trigger pEMT in OSCC (Puram et al., 2017). In the TME, TGF- β 1 cooperates with interleukin-17 (IL-17) to activate tumor-associated neutrophils, thereby enhancing EMT and promoting invasion in OSCC (T. Yu et al., 2021).

Lastly, EGFR signaling pathway is also essential in EMT regulation in HNSCC (Holz et al., 2011; Keysar et al., 2013; Psyrris et al., 2013). EGFR induces EMT through activation of the mitogen-activated protein kinase (MAPK) signaling pathway, resulting in a reduction of E-cadherin expression and an increase of N-cadherin and Vimentin expression. Furthermore, our group previously revealed that EGFR signaling presents a dual role in regulating cell proliferation and EMT, with the latter being influenced by the hyper-activation of ERK1/2 (Pan et al., 2018). EGFR-mediated EMT relied on high-dose of EGF treatment that sustained enhanced ERK1/2 activation, whereas low-dose of EGF treatment led to moderate proliferation in HNSCC.

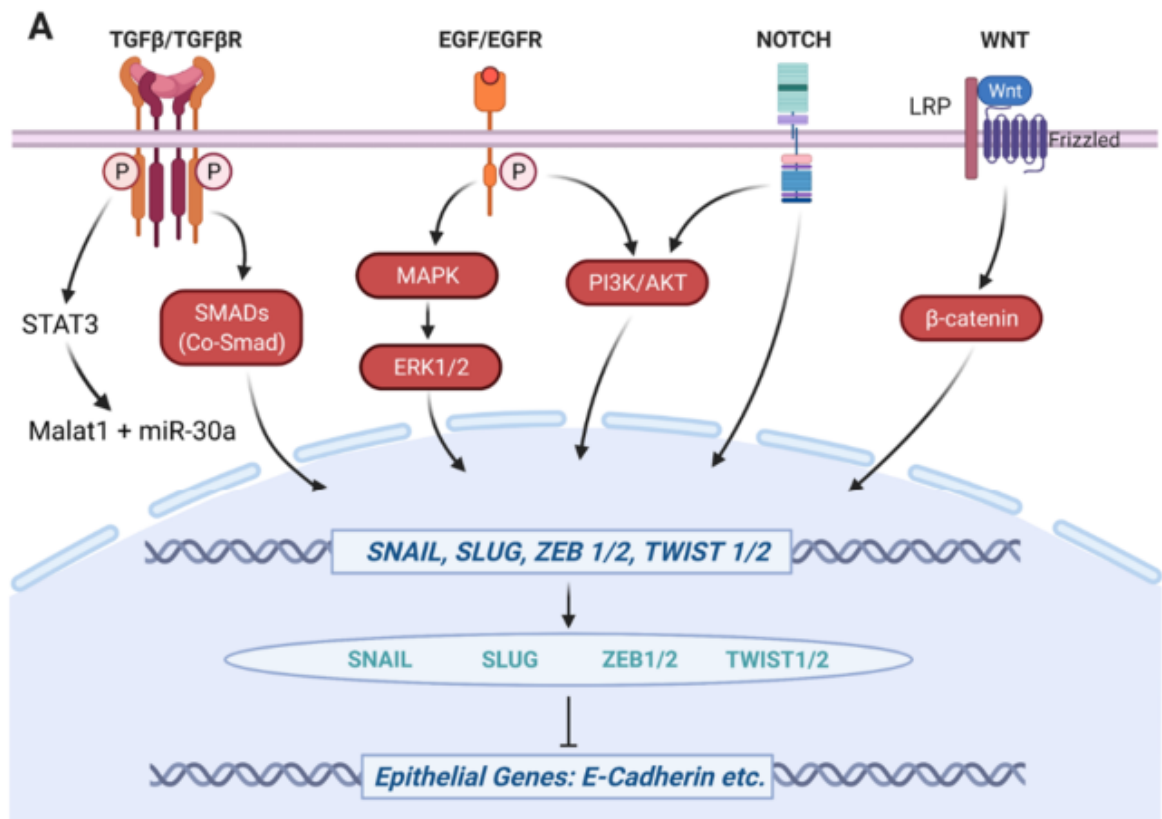


Figure 3. A schematic overview of signaling pathways involved in regulating EMT process in HNSCC

Major signaling pathways involved in EMT or pEMT program in HNSCC includes TGFβ/TGFβR, EGF/EGFR, NOTCH, and WNT signaling pathway. The activation of these central signaling pathway and their downstream signaling can mediate the expression of EMT-TFs such as SNAIL, SLUG, ZEB1/2, and TWIST1/2, further promoting pEMT or EMT induction in HSNCC (Figure 3 was copied from Baumeister et al., 2021).

1.3 Epidermal growth factor receptor (EGFR)

EGFR is a transmembrane receptor that is part of the ErbB/HER family of four receptor tyrosine kinases (RTKs) including the remaining members, namely ErbB2/HER2, ErbB3/HER3, and ErbB4/HER4 (Citri & Yarden, 2006; Hynes & Lane, 2005). Some of the well-known ligands for EGFR include epidermal growth factor (EGF), transforming growth factor-α (TGF-α), amphiregulin (AREG), betacellulin (BTC), epiregulin (EREG), heparin-binding EGF-like growth factor (HB-EGF) and epigen (EPGN) (Harris et al., 2003). Upon ligand binding to a single-chain EGFR, EGFR assembles into a dimer, which activates intracellular signaling by initiating EGFR autophosphorylation via its tyrosine

kinase activity. Ligand-dependent EGFR activation triggers a series of intracellular signaling pathways, including the Ras/MAPK pathway, the PI3K/AKT pathway, and the phospholipase C (PLC)/protein kinase C (PKC) signaling cascade, which are important for cell survival, proliferation, differentiation, angiogenesis and tumor metastasis (Shi et al., 2022)(**Fig 4**). Moreover, EGFR is increasingly acknowledged as an indicator of tumor resistance, given that its genetic alterations have been identified to emerge in response to chemotherapy and radiotherapy (Bossi, Resteghini, et al., 2016; Nicholson et al., 2001; Sun et al., 2016).

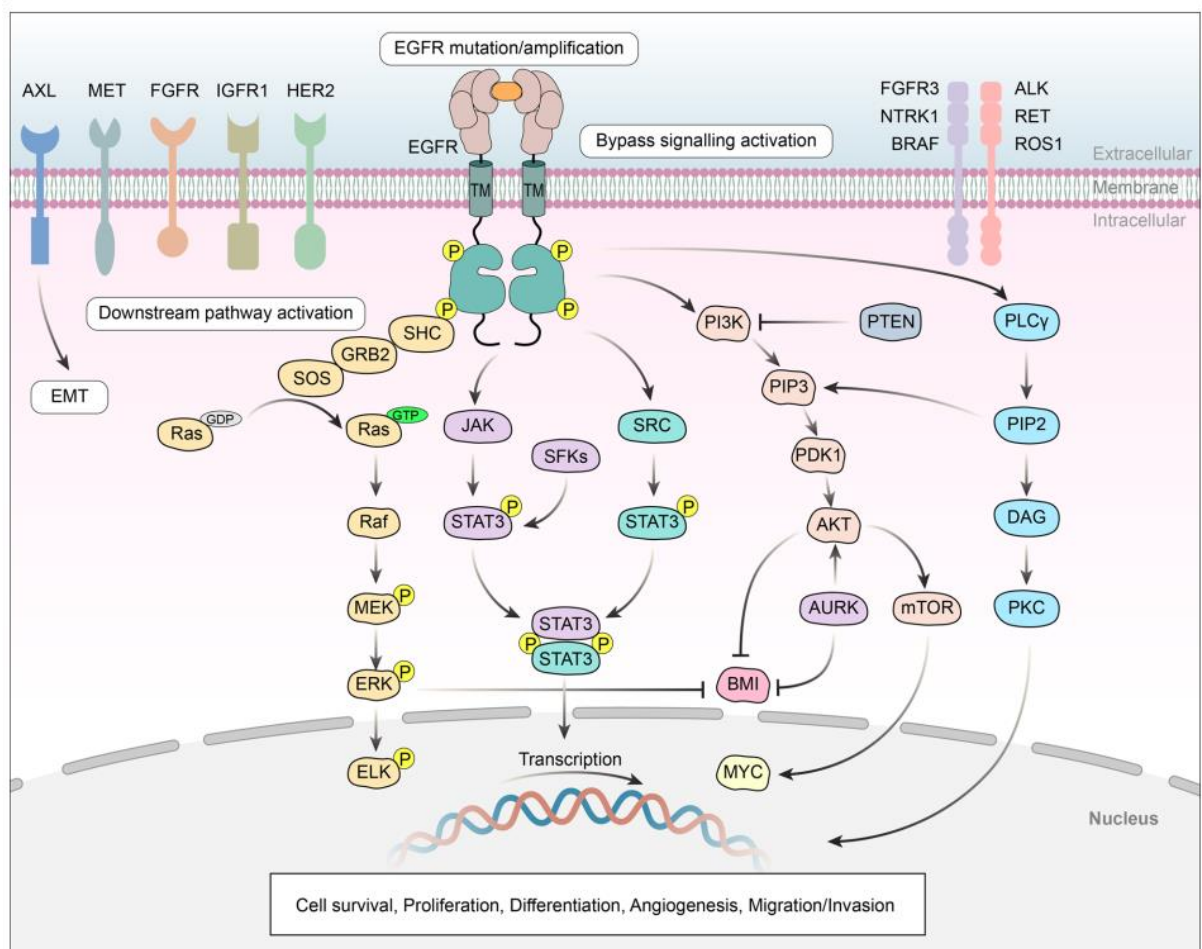


Figure 4. Function of EGFR signaling pathway

The EGFR exon boundaries and their corresponding extracellular, transmembrane, and intracellular protein domains are illustrated. Activation of EGFR signaling pathway is involved in PI3K-AKT-mTOP signaling pathway, Ras-Raf-MAPK signaling and STAT signaling activation, regulating cell survival, angiogenesis, proliferation, invasion, metastasis and treatment resistance (Figure 4 was copied from Shi et al., 2022).

1.3.1 EGFR biology and targeted therapies in HNSCC

EGFR is crucial in HNSCC progression, and EGFR amplification or overexpression is frequently observed in HNSCC (Rehmani & Issaeva, 2020; Zimmermann et al., 2006). It was discovered that EGFR is overexpressed by 92% of the primary tumors at mRNA level and by 38-47% at protein level in HNSCCs (Nair et al., 2022). Moreover, EGFR expression is significantly correlated with worse prognosis and decreased effectiveness of treatment. In a clinical trial, efficacy of radiotherapy is increased in HNSCC patients when combined with EGFR-targeting antibodies treatment. An investigation on primary laryngeal squamous-cell carcinoma (n=140) revealed a substantial disparity in the 5-year survival rate based on EGFR expression: 81% for those with tumors not expressing EGFR, contrasting with 25% for those with tumors that did express EGFR (Rehmani & Issaeva, 2020). Numerous studies have indicated that heightened expression of EGFR can result in enhanced activation of downstream signaling such as ERK1/2 and AKT, which are associated with proliferation, migration and invasion in HNSCC (Citri & Yarden, 2006; Sigismund et al., 2018).

Together, overexpression of EGFR, coupled with transcriptional amplification or excessive production of ligands through autocrine/paracrine mechanisms, result in aberrant EGFR activation, thereby triggering activation of downstream signaling pathways and promoting HNSCC progression. Given that high frequency of EGFR overexpression in most HNSCCs and its link to reduced overall survival in numerous preclinical and clinical studies, two main treatment approaches focusing on targeting EGFR have been established (Ciardiello & Tortora, 2008). The first one involves targeting the extracellular domain of EGFR using monoclonal antibodies such as cetuximab (also known as Erbitux). These antibodies block EGFR activation by endogenous ligands via competitive inhibition. This process then triggers internalization and degradation of the antibody-receptor complex, thereby leading to a decrease in EGFR expression. On the other hand, targeting the intracellular domain of EGFR with small molecular tyrosine kinase inhibitors (TKIs) like gefitinib, erlotinib, or ZD1839 inhibits auto-phosphorylation of EGFR and activation of subsequent signaling pathways. Despite the pronounced expression of EGFR in HSNCC, utilizing EGFR-targeting monotherapies did not meet the clinical expectations and may induce resistance. It has been described that the abundance of EGFR ligands, instead of excessive expression of EGFR, is associated with Cetuximab resistance (C. Huang et al., 2021). A study involving HNSCC patient-derived xenografts (PDX) treated with antibody Cetuximab demonstrated that EGFR ligands exhibited significantly increased expression in the treatment-responder

group than the non-responder group (Klinghammer et al., 2017). Owing to the involvement of EGFR with other oncogenic pathways and heterogeneity of HNSCC, investigating novel therapeutic approaches that target EGFR in combination with other potential druggable targets will be crucial.

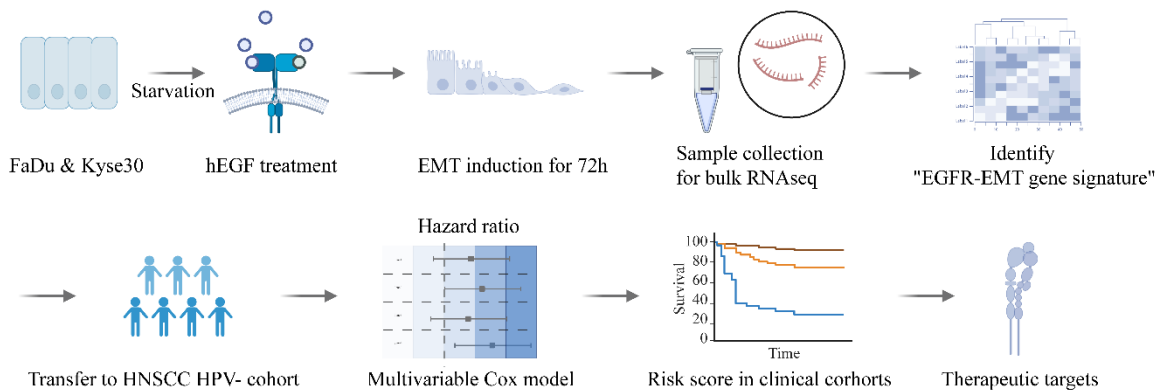
1.3.2 An EGFR-mediated EMT gene signature in HNSCC

Nowadays, genomic and transcriptomic profiling of tumors in bulk or single cells has been conducted to gain a deeper insight into intra-tumoral heterogeneity, invasion and metastasis in HNSCC (Galeano Niño et al., 2022; Qi et al., 2019). Bulk transcriptomic analysis in the TCGA HNSCC cohort revealed basal, mesenchymal-enriched, traditional epithelial-like and atypical categories. A scRNA-seq analysis of 18 OSCC patients performed by Puram et al. also refined the molecular subtypes into the malignant basal (associated with pEMT), the classical and the atypical subtypes (Puram et al., 2017). Interestingly, pEMT signatures identified by Tyler and Tirosh across hundreds of cancers were not associated with metastasis in most cancers, whereas a significant association with metastasis was observed in HNSCC (Tyler & Tirosh, 2021). Moreover, induction of EMT in HSNCC is regulated by key signaling pathways such as TGF- β , EGFR, NOTCH, and WNT signaling pathways (Baumeister et al., 2021). Our group, along with others, have previously revealed EMT induction in HNSCC through hyper-activation of EGFR and MAPK signaling pathways (Egloff et al., 2009; Pan et al., 2018; Rong et al., 2020). Molecular processes underlying EMT mediated by EGFR activation in HNSCC cells were further explored by our group (Schinke, Shi, et al., 2022), resulting in the generation of a transcriptomic profile for genes regulated by EGFR-EMT in HNSCC cells, establishing a gene signature for EGFR-mediated EMT, including 171 genes (**Fig 5A-B**). The gene signature indicative of EGFR-induced EMT showed molecular alterations in cadherin binding, cell-substrate junction, the development of leading edges, and cell division, suggesting a promoted cell migration and invasion, and a decrease in cell proliferation rates. The signature of EGFR-mediated EMT characterized HNSCC cells in an EMT state in a manner comparable to the EMT hallmark from MSigDB (Molecular Signatures Database) and the pEMT gene signatures, yet with distinctions observed at the single cell level. The latter aspect was further fostered by the fact that only 4% (7/171) and 2.3% (4/171) genes overlapped between EGFR-mediated EMT signature and the hallmark of EMT and the pEMT gene signatures, respectively (**Table 1**). This suggested that the identified gene signature of EGFR-mediated EMT was uniquely distinguishable

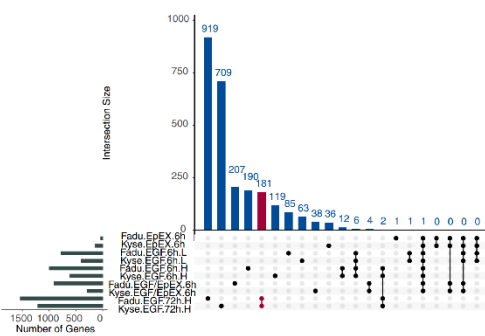
from the standard EMT hallmark and pEMT genes, exhibiting a different pattern of distribution across individual malignant cells.

The gene signature of EGFR-mediated EMT was further applied to a HPV-neg HNSCC cohort in TCGA. Using computational methods, a 5-gene prognostic signature was identified for predicting risk in HNSCC. This signature includes DDIT4 (DNA Damage Inducible Transcript 4), FADD (Fas-Associated protein with Death Domain), ITGB4 (Integrin β 4), NCEH1 (Neutral Cholesterol Ester Hydrolase 1), and TIMP1 (Tissue Inhibitor of Metalloproteinases 1), and it is associated with reduced OS in HNSCC (**Fig 5C-D**). Moreover, when comparing the prognostic value of risk scores based on EGFR-mediated EMT with established EMT signatures, it revealed that both EGFR-mediated and pEMT signature risk scores outperformed other EMT-associated risk scores, indicating a finer classification system of HNSCC.

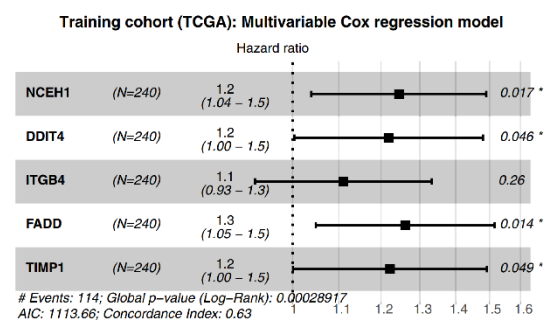
A



B



C



D

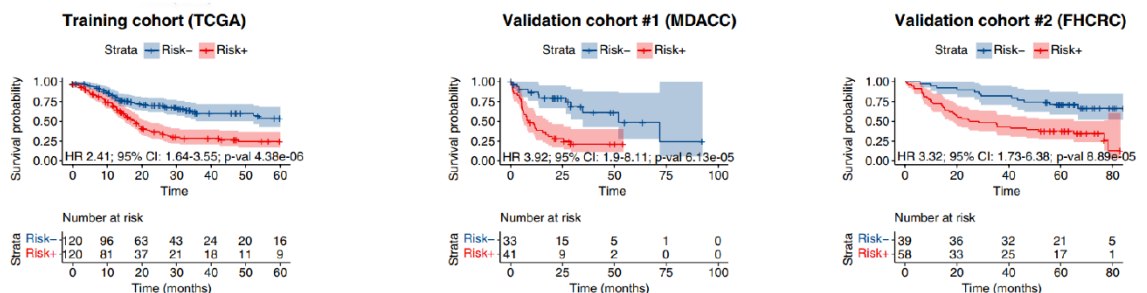


Figure 5. Identification of a gene signature associated with EGFR-mediated EMT

(A). Workflow of RNA-seq analysis focused on EGFR-mediated EMT in HNSCC: cells were treated with serum-free medium as control and high dose of EGF for 72 h to induce EMT, respectively, and RNA samples were collected for 3'-RNA-seq analysis. (B). An upset plot presents exclusive DEGs in the indicated different groups and 181 genes were identified in both FaDu and Kyse30 upon high dose of EGF treatment for 72 h (171 genes of these 181 genes were similarly regulated in both FaDu and Kyse30, and were selected for further analysis). (C). A forest plot displaying the outcomes from a multivariable Cox proportional hazards regression analysis, that incorporates the 5-gene signature, in HPV-neg HNSCC (n=240) in TCGA cohort (Figure 5 was copied from Schinke, Shi, et al., 2022).

Table 1. Overlapping genes in different signatures (Schinke, Shi, et al., 2022)

EGFR-EMT vs. pEMT	EGFR-EMT vs. EMT hallmark
LAMA3	CD44
LAMB3	LAMA3
MMP1	MMP1
SERPINE2	NT5E
	SERPINE2
	TIMP1
	MCM7

1.4 Integrin β 4 (ITG β 4)

1.4.1 Structure and biology of ITG β 4

As a component of the 5-gene prognostic signature related to EGFR-EMT in HNSCC, ITG β 4 is a member of the integrin family. Integrins constitute a vast group of heterodimeric transmembrane receptors for extracellular matrix (ECM) components and are comprised of paired α and β subunits (Kechagia & Ivaska, 2019; Takada et al., 2007). They function as a linkage between the ECM and the cytoskeleton and are bidirectional signaling receptors engaged in both outside-in and inside-out signaling processes (Hamidi & Ivaska, 2018) (**Fig 6A**). ITG β 4 typically pairs with the integrin α 6 subunit to form the

integrin $\alpha6\beta4$. Integrin $\alpha6\beta4$, predominantly expressed in epithelial cells, binds to laminin 5 in the ECM and is located in hemidesmosomes, which are structures that facilitate the stable basal surface adhesion of epithelial cells to basement membrane (Beaulieu, 2019; Stewart & O'Connor, 2015). ITG $\beta4$ has a large cytoplasmic signaling domain that is structurally different from other integrin subunits (Stewart & O'Connor, 2015) (**Fig 6B**). Integrin $\alpha6\beta4$ can be released from hemidesmosomes via phosphorylation of ITG $\beta4$'s cytoplasmic tail stimulated by activation of growth factor receptors like EGFR or by direct effects of protein kinase C. Detachment of integrin $\alpha6\beta4$ from hemidesmosomes can enhance the formation of motility structures by interacting with growth factor receptors and activating central signaling pathways such as PI3K, AKT, and MAPK signaling, thereby promoting tumorigenesis, cell migration and wound healing. Furthermore, studies have demonstrated that integrin $\alpha6\beta4$ is involved in the contextual positioning of cells (S. Li et al., 2023; X. L. Li et al., 2017; Stewart & O'Connor, 2015). When cells fail to adhere to the appropriate ECM, they experience a special form of apoptosis named anoikis, which is activated by the cleavage of the ITG $\beta4$ cytoplasmic tail.

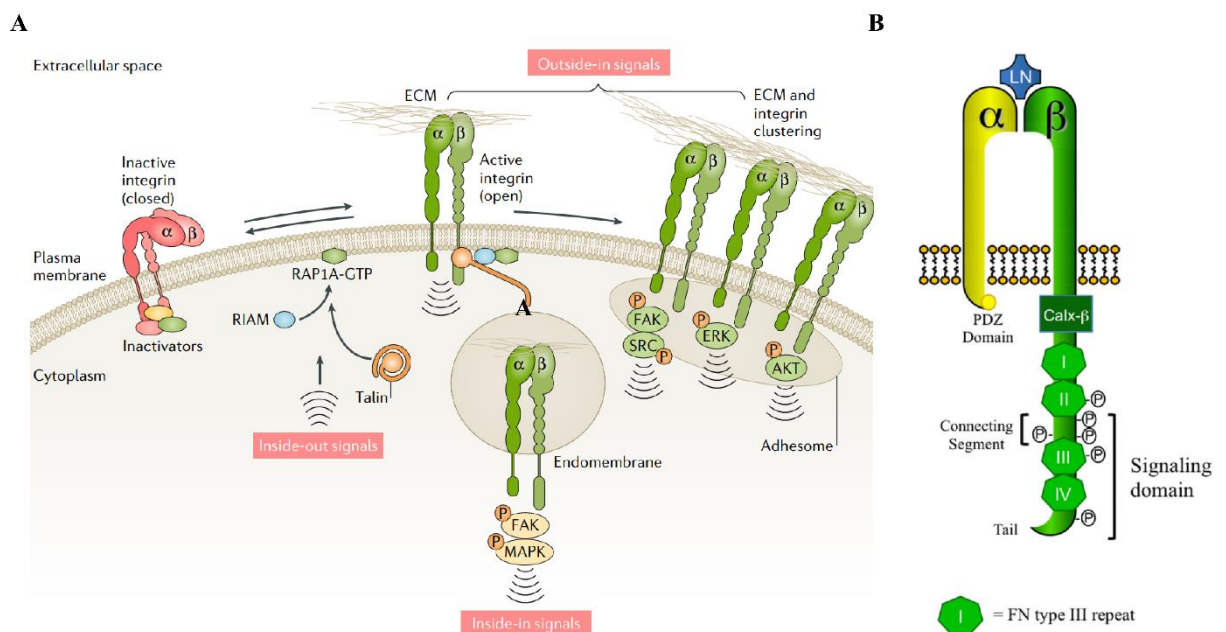


Figure 6. Integrin signaling and the structure of ITG $\beta4$

(A). Integrins are distinctive signaling molecules capable of bidirectional communication, and they are present in various conformational states that govern their affinity towards proteins in the ECM. In the folded (inactive) conformation, integrins are inactive and exhibit low affinity for ECM ligands. Conversely, when completely stretched out (active), integrins become active, enabling them to trigger downstream signaling

pathways and elicit cellular reactions upon ligand binding. The “outside-in” signals activate integrins in a ligand-dependent manner, typically activating phosphorylation of focal adhesion kinase (FAK), ERK and AKT. Some “inside-out” signals like Talin, can bind integrins to trigger recruitment of additional integrin-activating proteins (Hamidi & Ivaska, 2018). (B) The integrin $\beta 4$ subunit exclusively forms a pairing with the $\alpha 6$ subunit. The extended cytoplasmic domain of $\beta 4$ stands out structurally from other recognized receptors and includes several unique segments, such as a Calx- β domain, four fibronectin type III repeats, a connecting segment, and a C-terminal tail (Figure 6 was copied from Stewart & O’Connor, 2015).

1.4.2 ITG β 4 in cancer

Increasing evidence indicates that ITG β 4 binding to laminin 5 is essential for the growth of tumor cells, invasion, and metastasis in various tumors (Bierie et al., 2017; Fang et al., 2023; X. Jiang et al., 2021; Leng et al., 2016; Meng et al., 2020; J. S. Sung et al., 2020b). Frequent reports indicate the overexpression of ITG β 4 in a range of cancers including HNSCC, breast cancer, pancreatic cancer and colorectal cancer (J. F. Beaulieu, 2019; S.-R. Ma et al., 2023; J. S. Sung et al., 2020; Zhuang et al., 2020). The upregulation of ITG β 4 expression was recognized as a marker for prognosis in breast cancer and pancreatic ductal adenocarcinoma (Benesch et al., 2022; Xiao Ling Li et al., 2014). Proteomic analysis of exosomes showed that exosomal ITG β 4 was significantly correlated with lung metastasis (Nie et al., 2020). In triple negative breast cancer (TNBC), cancer cells that overexpress ITG β 4 provided CAFs with ITGB4 via exosomes and cancer cell-derived ITG β 4 mediated metabolic reprogramming in CAFs, which was correlated with poor prognosis (J. S. Sung et al., 2020).

Activation of integrin signaling is also critical for tumor initiation, metastatic reactivation, and shows resistance to therapies targeting oncogenes and the immune system (Cooper & Giancotti, 2019; S. Li et al., 2023). During tumorigenesis, ITG β 4 cooperates with ERBB2 and can downregulate epithelial adhesion and polarity and amplify oncogenic signaling pathways that enhance growth and invasion in tumor (Guo & Giancotti, 2004) (**Fig 7**). It was further reported that ITG β 4 signaling is critical for the proliferation of squamous cell carcinomas (Zhong et al., 2020). Selective inactivation of the ITG β 4 signaling domain inhibits the growth and advancement of prostate tumors in a mouse model. Moreover, ITG β 4 has been shown to be involved in the regulation of CSCs (Bierie et al., 2017; Ruan et al., 2020). It was described that inactivation of the signaling domain

of ITG β 4 reduced self-renewal and enhanced capacity of CSCs in prostate tumor cells. Interestingly, ITG β 4-positive CSCs in prostate and lung cancers exhibited hybrid E/M traits and enhanced metastatic ability. In addition, a few studies have revealed the involvement of ITG β 4 in EMT. In hepatocellular carcinoma (HCC), ITG β 4 stimulates EMT via the regulation of EMT-TF Slug (X.-L. Li et al., 2017). Upregulation of ITG β 4 is associated with downregulated expression of E-cadherin and upregulated expression of Vimentin in pancreatic adenocarcinoma (Masugi et al., 2015). In TNBC, ITG β 4 can serve as a marker to identify CSC-enriched populations within pEMT and was linked to a lower duration of survival without relapse after undergoing chemotherapy (Wang et al., 2019). Despite of that, the role of ITG β 4 in EMT or pEMT, and local invasion in HNSCC remains unclear.

Although integrins have been recognized as promising targets for cancer therapy for an extended period, there is no approved anticancer drugs specifically targeting integrins. Currently, two integrin-specific immunotherapies targeting β 7 and β 3 by conjugation to chimeric antigen receptor (CAR) T-cells are in clinical study (Cobb et al., 2022; Hosen et al., 2021). These therapeutics show treatment potential in melanoma and cholangiocarcinoma. Recently, immune targeting of ITG β 4 has been studied in tumor mice models, showing that targeting ITG β 4 can significantly suppressed tumor growth and metastasis in breast cancer and HNSCC tumor model (Ruan et al., 2020). Therefore, considering the significance of ITG β 4 in tumor progression, a high demand for the development of drugs that specifically target ITG β 4 in cancer remains.

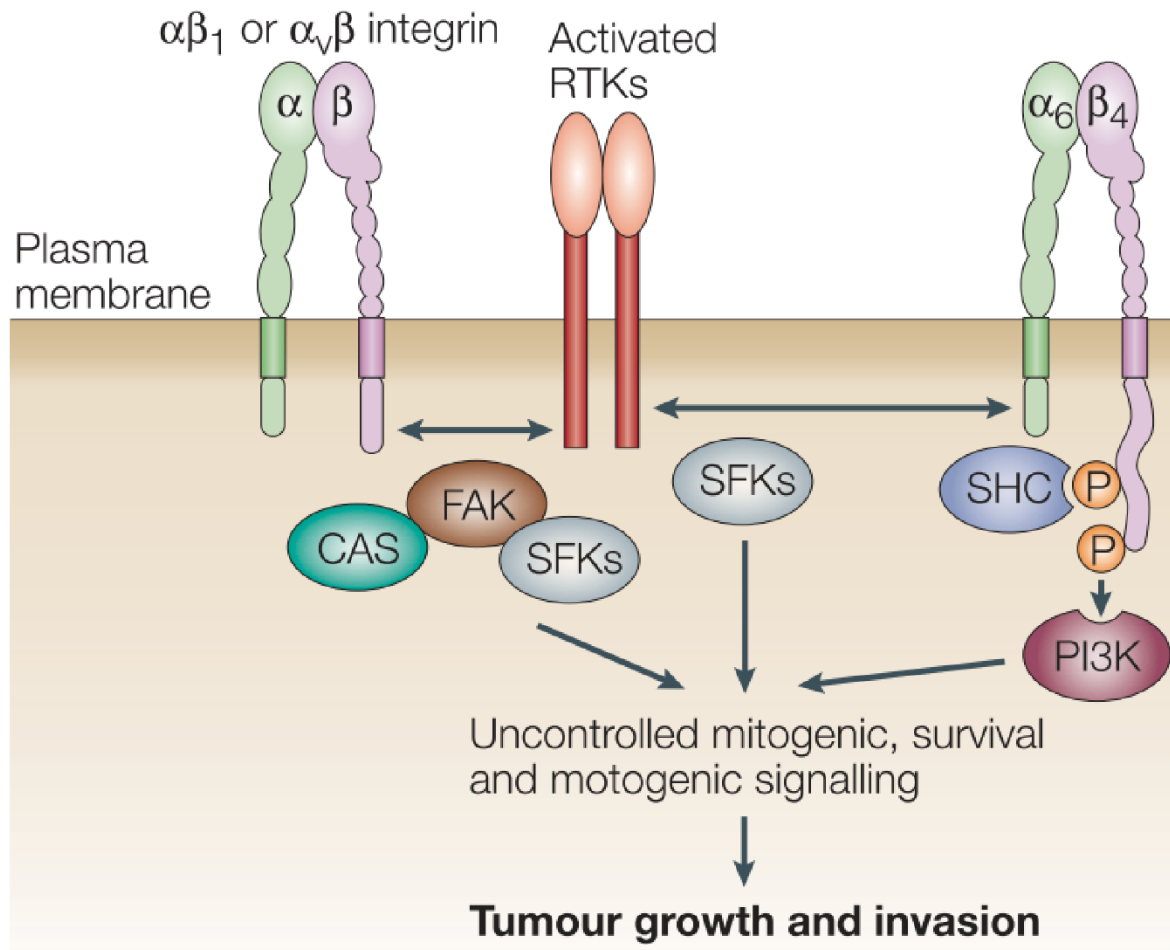


Figure 7. Interaction between ITGβ4 and receptor tyrosine kinases

Receptor tyrosine kinases (RTKs) that undergo constant activation due to genetic mutations or overexpression can initiate the phosphorylation of the cytoplasmic segment of ITGβ4, which establishes binding sites for signaling molecules like SHC and regulators of phosphatidylinositol 3-kinase (PI3K). In this conceptual framework, the cytoplasmic region of ITGβ4 plays the role of a signaling adaptor, enhancing signals associated with cell growth, survival, and motility triggered by the active RTK (Figure 7 was copied from Guo & Giancotti, 2004).

1.5 CD73

1.5.1 Biology of CD73

CD73, alternatively referred to as 5'-nucleotidase (5'-NT), is a cell surface protein anchored by glycosyl-phosphatidylinositol (GPI) in the plasma membrane. It is encoded by the *NT5E* gene and exhibits widespread expression across various cell types including epithelial cells, endothelial cells, T cells, and B cells. The balance between ATP and

adenosine plays a crucial role in inflammation, tissue damage and hypoxic stress (Allard et al., 2017). CD73, an enzyme that hydrolyzes adenosine monophosphate (AMP) to adenosine (ADO), is critical for maintaining tissue homeostasis through converting ATP-driven immune activation to ADO-mediated immunosuppression (Alcedo et al., 2021) (**Fig 8**). CD73-catalyzed ADO can bind to its receptors (A1, A2A, A2B and A3) to suppress the function of immune cells, thereby protecting tissues against ischemia-reperfusion injury and chronic inflammatory diseases. Moreover, CD73-catalyzed ADO also plays a curial role in creating an immunosuppressive TME that promotes metastasis and resistance to immunotherapy in cancers (Hallaj et al., 2021; Leone & Emens, 2018; Vijayan et al., 2017; Yegutkin & Boison, 2022).

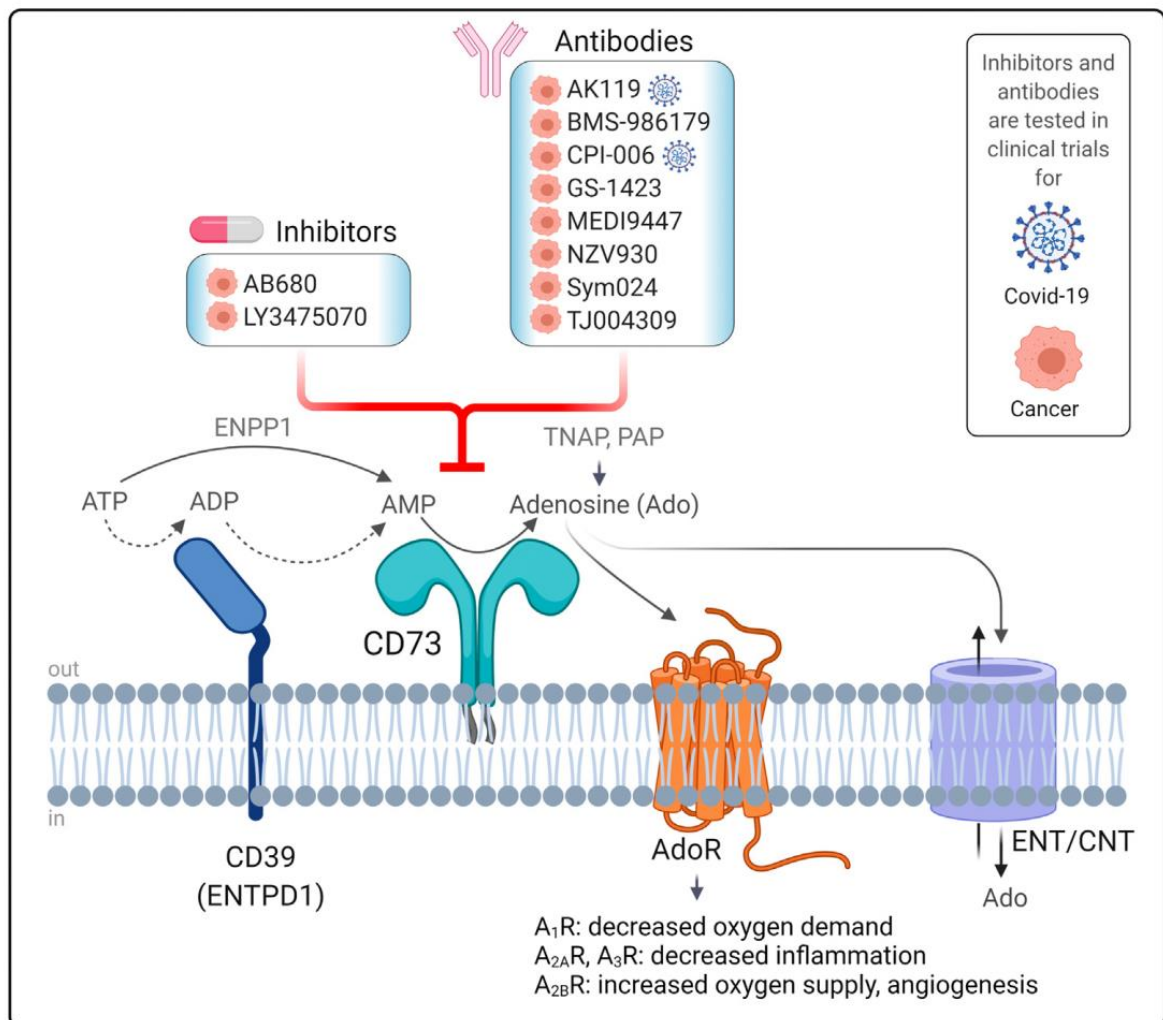


Figure 8. CD73 is a critical enzyme in purinergic signaling

As a glycosylphosphatidylinositol (GPI)-anchored glycoprotein located on the outer membrane of cells, CD73 collaborates with ectonucleoside triphosphate diphosphohydrolase 1 (CD39) to enzymatically convert ATP into ADO through a two-

step process. CD73 plays a pivotal role as the primary enzyme responsible for dephosphorylating AMP, producing extracellular ADO as a result. ADO generated by CD73 directly influences functions specific to different tissues by binding to four distinct types of G protein-coupled adenosine receptors (AdoRs) that are associated with oxygen demand, inflammation and angiogenesis (Figure 8 was copied from Alcedo et al., 2021).

1.5.2 CD73 in cancer

CD73 is highly expressed in a variety of solid tumors and this elevated expression is linked to decreased overall survival (Han et al., 2022; X. L. Ma et al., 2020; Z. Xu et al., 2020). It has been demonstrated that the tumor microenvironment (TME) plays a role in tumorigenesis and cancer progression, and an immunosuppressed TME can enhance neoplastic growth through releasing immunomodulatory factors (Ho et al., 2020; C. Liu et al., 2022). Several studies have revealed that CD73 promotes cancer progression by increasing ADO concentrations in the TME, which mediates immunosuppression (Mastelic-Gavillet et al., 2019; Pang et al., 2021; Xia et al., 2023). Upregulation of extracellular ADO can regulate immune evasion, accelerating tumor growth and metastasis. Therefore, CD73 is regarded as an emerging immune checkpoint molecule and holds promise as a target for monoclonal antibody inhibition in cancer therapy. (Allard et al., 2017).

Moreover, non-enzymatic functions of CD73 are associated with EMT regulation (Z. Gao et al., 2014). CD73 can facilitate the interaction between cancer cells and the ECM, consequently augmenting cell-cell adhesion, migration, invasion, and the stem-like properties of malignant cells. A few studies in lung and breast cancers showed that CD73 facilitates EMT and promotes the early stage of tumor progression through PI3K/AKT signaling or RICS/Rho GTPase signaling pathway activation (Cadassou et al., 2021; Petruk et al., 2021). It also was reported that CD73 expression is correlated with hallmarks of EMT and metastasis in HNSCC. Moreover, it was documented that CD73 enhanced the EGFR signaling pathway activation in HNSCC (A. Shen et al., 2022; F. Xue et al., 2022). Nevertheless, the upregulation of CD73 upon EGFR activation, as well as the functional significance of CD73 in EGFR-mediated EMT and local invasion, require more exploration in HPV-neg HNSCC.

2. Materials and Methods

2.1 Human samples and ethics statement

The cohort from Ludwig-Maximilians-University Munich in Germany, focusing on HNSCC (referred to as the LMU cohort), consisted of tumor samples collected from 109 patients diagnosed with HNSCC. Among them, p16 staining was HPV-negative in 43 patients, HPV-positive in 41 patients, and 25 patients could not be clearly identified. Clinical samples were gathered during standard surgical procedures, following the authorization of the local medical faculties' Ethics Committee (Ethikkommission der Medizinischen Fakultät der LMU; 087–03; 197–11; 426–11, EA 448–13, and 17–116). This collection adhered to the ethical standards set forth in the WMA Declaration of Helsinki and complied with the Department of Health and Human Services' guidelines as detailed in the Belmont Report.

2.2 Immunohistochemistry, immunofluorescence and scoring

Clinical samples were obtained using 8 mm punch biopsies from surgically removed primary tumors and normal mucosal areas located beyond the resection margins. The specimens were preserved via rapid freezing in tissue-Tek® (Sakura, Finetek, The Netherlands) and later sectioned into 5 µm thick slices for staining. For immunohistochemical and immunofluorescence staining, antibodies like ITGβ4 (439-9B, 1:200, Thermo Fisher Scientific, Germany), laminin 5 (P3H9, 1:500, Abcam, Germany), Ki67 (SP6, 1:250, Abcam, Germany), and anti-CD73 (22E6, 1:100) were employed, along with the avidin-biotin-peroxidase technique (Vectastain, Vector Laboratories, Burlingame, CA, USA) or with secondary antibodies conjugated to Alexa Fluor-488 and Alexa Fluor-594. The immunofluorescence images were captured using a Leica TCS-SP8 scanning system (Leica, Nussloch, Germany). Immunohistochemical analysis was conducted using a dual-parameter evaluation system and all samples are scored according to percentage of cells (tumor) and staining intensity is rated on a scale of 0 to 3 (0 = negative, 1 = mild, 2 = moderate, 3 = strong, score = sum (% x intensity) as described. IHC scoring was assessed independently by a minimum of two experienced scorers blinded for sample identities and clinical endpoint information. Immunohistochemical score is determined by multiplying the antigen intensity by the percentage of cells.

2.3 Tumor budding

Tumor budding was defined by the separation of single tumor cells or small groups of less than five cells from the main tumor body. The intensity of budding was assessed by two skilled scientists or pathologists, who conducted their evaluations independently and without considering clinicopathological information. The budding was then categorized into four levels: negative (where no budding was seen), weak, moderate, and severe.

2.4 Cell lines and treatments

The HPV-negative cell lines Kyse30, FaDu, and Cal27 (sourced from ATCC, Manassas, VA, USA) underwent regular validation using STR typing. They were cultured in DMEM or RPMI with 10% FCS and 1% penicillin/streptomycin, in a 5% CO₂ environment at 37°C. Under serum-free conditions, these cells were subjected to various treatments, which included EGF (ranging from 1.8 to 9 nM, sourced from PromoCell PromoKine, Heidelberg, Germany), Cetuximab (concentrations from 0.5 to 10 µg/mL, Erbitux by Merck Serono, Darmstadt, Germany), anti-ITGβ4 (10 µg/mL, ASC8, Merck, Germany), anti-GFP antibody (10 µg/mL, Thermo Fisher Scientific, Germany), the inhibitors AZD6244 and MK2206 (both at 1 µM, from Selleckchem, Munich, Germany), laminin 5 (0.1-10 µg/mL, BioLamina, Sundbyberg, Stockholm, SE), antagonizing CD73 antibody 22E6 (0.5-10 µg/ml, kind gift from Prof. R. Zeidler, Dept. of Otorhinolaryngology, LMU Munich, Germany) and rat IgG isotype control antibody (5 µg/mL, Biolegend, San Diego, CA).

2.5 Generation of ITGβ4 knockdown cells

To achieve knockdown of ITGβ4 in Kyse30 and FaDu cells, shRNA targeting ITGβ4 (shITGβ4: 5'-CGAGAAGCTTCACACCTAT-3') was delivered via lentiviral transduction. Additionally, a scrambled shRNA (shControl: 5'-CCTAAGGTTAAGTCGCCCT-3') was used as a negative control. The lentiviral vector pLVX-shRNA1 (Clontech, Saint-Germain-en-Laye, France) was employed for this purpose, and it was packaged in 293T cells using the plasmids psPAX2 and phCMV-VSV-G. For the transfection process, 50,000 cells/well were plated in 500 µL of culture medium in a 24-well plate and unconcentrated supernatant containing lentiviral particles was introduced as control. Stable ITGβ4 knockdown (ITGβ4-KD) cells were chosen by

treating them with 1 µg/mL of puromycin. Negative control and *ITGβ4*-KD cells in FaDu and Kyse30 were further confirmed by flow cytometry.

2.6 Generation of CD73 knockdown and overexpression cells

Knock-down of CD73 in FaDu was achieved via transferring CD73-specific shRNA expression plasmids. These plasmids included shRNA targeting hNT5E (5'-TAA GTT TAC GTG TCC AAA TTT-3') and a control plasmid with an irrelevant scramble shRNA (5'-CCT AAG GTT AAG TCG CCC TCG-3'). The transfection was carried out using Lipofectamine 3000 transfection reagent (Thermo Fisher Scientific, Germany). GFP-positive cells following transfection were enriched by FACS and cultured in medium with 2 µg/mL puromycin. For CD73 overexpression and re-expression, cells were transfected with a pRP[Exp]-Hygro-CAG > hNT5E plasmid to generate stable bulk transfectants. All plasmids were sourced from VectorBuilder (Neu-Isenburg, Germany)

2.7 Reverse transcription qPCR analysis

Total RNA extraction was performed using the RNeasy Mini Kit (Qiagen, Germany), followed by reverse transcription using the Quantiect Reverse Transcription Kit (Qiagen, Germany) following the manufacturer's instructions. Measurement of cDNAs in triplicates were analyzed using gene-specific primers and qRT-PCR SYBR-Green Master PCR Mix on a QuantStudio3 device (Thermo Fisher Scientific, Germany). To ensure consistency, all mRNA quantifications were normalized to GAPDH or TBP.

2.8 Primers used for qPCR quantification

ITGβ4-FW 5'-CTC CAC CGA GTC AGC CTT C-3'

ITGβ4-BW 5'-CGG GTA GTC CTG TGT CCT GTA-3'

E-cadherin-FW5'- CGA GAG CTA CAC GTT CAC GG-3'

E-cadherin-BW5'- GGG TGT CGA GGG AAA AAT AG-3'

N-cadherin-FW5'- TCA GGC GTC TGT AGA GGC TT-3'

N-cadherin-BW5'- ATG CAC ATC CTT CGA TAA GA-3'

TWIST1-FW5'- ACA AGC TGA GCA AGA TTC AGA CC-3'

TWIST1-BW5'- TCC AGA CCG AGA AGG CGT AG-3'

Vimentin-FW5'-GAG AAC TTT GCC GTT GAA GC-3'

Vimentin-BW5'-GCT TCC TGT AGG TGG CAA TC-3'

TBP-FW 5'-CCA CTC ACA GAC TCT CAC AAC-3'

TBP-BW 5'-CTG CGG TAC AAT CCC AGA ACT-3'

GAPDH-FW5'-AGG TCG GAG TCA ACG GAT TT-3'

GAPDH-BW5'-TAG TTG AGG TCA ATG AAG GG-3'

2.9 Flow cytometry

After trypsinization, 500,000 cells were incubated for 60 min on ice with anti-ITG β 4 (1:200 in PBS-3% FCS, 439-9B, Thermo Fisher Scientific, Germany), anti-EGFR (1:200 in PBS-3% FBS, Cell Signaling Technology, Danvers, Massachusetts, US), either anti-CD73 Alexa Fluor® 647-conjugated antibody or primary anti-CD73 22E6 (diluted at 1:100 in PBS-3% FBS) or isotype-matched control IgG antibody. Subsequently, cells were subjected to three washes with PBS-3% FCS and then subjected to staining with either FITC-conjugated secondary antibody (diluted at 1:50, Vector Laboratories/Biozol, Eching, Germany, FI-4001, 45 min at 4°C) or Alexa Fluor® 647-conjugated secondary antibody (diluted at 1:100, Jackson Immuno Research, 60 min at 4°C) or Alexa Fluor® 594-conjugated secondary antibody (diluted at 1:100, Molecular Probes, 60 min at 4 °C). Following three washes with PBS-3% FCS, we assessed fluorescence intensity using a CytoFlex instrument equipped with CytExpert Software, Version 2.2 (Beckman Coulter, Krefeld, Germany). Subsequently, all collected data underwent analysis using FlowJo software, specifically version 10.8.1 (FlowJo, Ashland, OR, USA).

2.10 Cytotoxicity assay

FaDu and Kyse30 cells were plated in 96-well plate at a density of 3,000 cells/well overnight for full attachment. After washing with PBS, the cells were subjected to one of two conditions: untreated as a control or treated with varying concentrations of the 22E6 antibody and Mitomycin C (Bioreagent, Schwerte, Germany) for 24 h, 48 h and 72 h. Cellular cytotoxicity was further assessed by applying the Cell Counting Kit-8 (Dojindo, Kumamoto, Japan) following the instructions provided by the manufacturer, and was quantified by absorbance measurement at 450 nm with a colorimeter (VersaMax Microplate Reader, Molecular Devices, San Jose, CA, USA).

2.11 2D migration, invasion and wound healing assay

We performed migration and invasion assays in a 2D setting using Boyden chambers (8.0 μm pore size, Merck Millipore Ltd., Germany), without or with Matrigel coating. Matrigel (Corning, Germany) was diluted in serum-free medium to a concentration of 1 mg/mL. After starvation for 18 h, cells were seeded in the upper well with 300 μL serum-free medium at a density of 2.5×10^5 , and indicated treatment were added to the lower chamber. Quantification of migrating and invasive cells was conducted after 24 hours in a colorimeter (VersaMax Microplate Reader, Molecular Devices, San Jose, CA, USA) using the QCM™ 24-Well Colorimetric Cell Migration Assay Kit (Merck Millipore Ltd., Germany).

In wound healing assays, Kyse30 and FaDu were cultured in 6-well plates to achieve a 90% confluence overnight. Following starvation in serum-free condition for 18 h, the wound was created by scratching cell layers with a 200 μL pipette tip. Cells were then cultured in the indicated treatment for 24 h or 48 h. Wound closure was quantified at specified time points by using the ImageJ in conjunction with MRI wound healing tool (NIH, Bethesda, MD, USA).

2.12 3D invasion assay

FaDu cells were seeded at a density of 1,500-3,000 cells per well, while Cal27 cells were seeded at 5,000 cells per well in 96-well low-adherent plates. These cells were allowed to incubate for 72 hours to facilitate the formation of spheroids. Spheroids were then embedded in 200 μL of Matrigel (diluted with serum-free medium, 3 mg/mL) or Collagen I (diluted with serum-free medium, 2 mg/mL) supplemented with different concentration of laminin 5 (0, 0.1, 1 and 10 $\mu\text{g}/\text{mL}$), and were plated onto glass bottom dishes (35 mm, Ibbidi, Germany) and incubated at 37 °C for 1 h. After the polymerization of Matrigel/Collagen I, spheroids were treated with the specified treatments in serum-free medium. After 72 h, spheroids in different groups were captured using imaging equipment (Leica, Nussloch, Germany). The invasive area, determined as the difference between the total cell-covered area and the central area of the spheroids, as well as the invasive distance, representing the average distance of the 10-15 cells located farthest from the spheroid's center, were quantified using the Image J software.

2.13 Data source and gene set variation analysis (GSVA)

We obtained normalized gene expression data and clinical information for HNSCC patients from the Cancer Genome Atlas (TCGA) cohort through the cBioPortal website (<https://www.cbioportal.org/>). Additionally, we retrieved two microarray datasets related to HNSCC from the Gene Expression Omnibus (GEO): GSE65858 and the Fred Hutchinson Cancer Research Center (FHCRC) cohort (GSE41613). \log_2 transformation of all gene expressions was performed before proceeding with the analysis. Subsequently, we focused exclusively on HPV-negative HNSCC patients for in-depth investigation, comprising 415 patients in TCGA, 97 patients in FHCRC cohort, and 196 patients in GSE65858 dataset. GSE65021 and GSE84713, two datasets containing information about HNSCC patients treated with cetuximab, were retrieved from GEO. Additionally, we downloaded an HNSCC scRNA sequencing dataset, GSE103322, from GEO to facilitate subsequent analysis.

EGFR activity and gene signatures of EMT hallmark were acquired from MSigDB (<https://www.gsea-msigdb.org/gsea/msigdb/>). The pEMT gene signatures and gene signatures associated with EGFR-mediated EMT were obtained from previous data (Puram et al., 2017; Schinke et al., 2022). R ‘gsva’ package was applied for computing GSVA scores for individual sample in bulk-seq or for single malignant cell sequencing. R ‘corrgram’ package was applied for analyzing and visualizing associations between CD73 expression and GSVA scores.

2.14 Statistical analysis

All results are presented as mean value with accompanying standard deviations from three or more independent experiments. Comparisons between two groups were performed by t test, and significant differences between more than two groups were determined by using One-way or Two-way ANOVA analysis. Differences in survival between groups were evaluated using the Kaplan-Meier method and the log-rank test. R ‘pROC’ package was applied for calculating and visualizing the area under the curve (AUC). The Fisher’s exact test was used to examine associations between CD73 expression and clinical parameters in the LMU cohort. Multivariable logistic regression was applied to assess the relationship between CD73 expression and relapse after cetuximab treatment. In this thesis, statistical significance was defined as p-values ≤ 0.05 .

3. Results

As mentioned in the introduction, our group has previously demonstrated that EGFR activation and EMT shift are critical for tumor progression in patients with HNSCC. We established a transcriptomic profile to characterize EGFR-mediated EMT, identifying an EGFR-mediated EMT gene signature that comprised a 5-gene prognostic signature. *ITGβ4* is a component of this 5-gene signature, and it has been reported that *ITGβ4* plays a role in the migration, invasion, and EMT processes in various carcinomas. Based on this, we assessed if *ITGβ4* could serve as an effective target to suppress tumor invasion mediated by EGFR-EMT, and as a predictive marker of tumorigenesis and response to Cetuximab in HNSCC.

3.1 EGF^{high} induces EMT in HNSCC cell lines

3.1.1 EGFR expression in FaDu and Kyse30 cells

EGFR expression and activity are critical parameters for clinical endpoints of HNSCCs and copy number aberrations and irregular *EGFR* expression patterns are observed in HNSCC, especially in HPV-negative tumors. Data from the cancer cell line encyclopedia (CCLE) revealed that the absolute copy number variations (CNV) were assessed as CNV+7 in Kyse30 cells and CNV+2 in FaDu cells (**Fig 9A**), which indicated that higher CNV in Kyse30 is associated with enhanced *EGFR* gene expression compared with FaDu. Consistent with this, it was shown that EGFR protein expression in Kyse30 cells was 3.2 times higher than that in FaDu cells (**Fig 9B**).

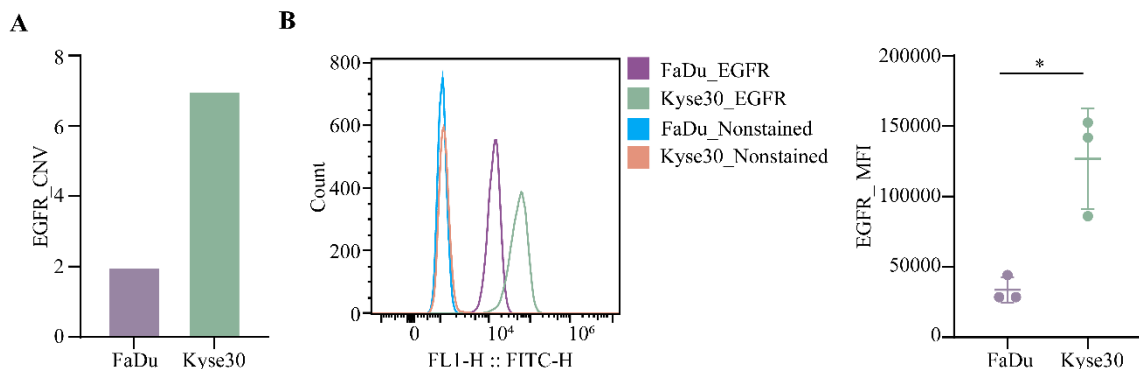


Figure 9 Expression of EGFR in head and neck squamous cell carcinoma cells

(A) CNV analysis of EGFR in HNSCC cell lines was retrieved from CCLE. (B) Kyse30 and FaDu cells were subjected to staining with EGFR-specific antibodies and FITC-labelled secondary antibody. The figure displays representative histograms (left panel) along with the mean expression values and standard deviations derived from three independent experiments (right panel). Significant differences are denoted by asterisks (*), with p -values less than 0.05 as determined by a t -test.

3.1.2 EGF^{high} induces EMT morphology change in FaDu and Kyse30

As reported by our lab, EGF^{high} induces EMT in HNSCC cells via hyper-activating EGFR signaling pathway (Pan et al., 2018). To validate previous findings, FaDu and Kyse30 cell lines, which express high level of EGFR, were cultured in high dose of EGF (9 nM) treatment or in serum-free medium as control. After 72 h treatment, cells with EGF^{high} treatment displayed a spindle-shaped mesenchymal phenotype and exhibited decreased cell-cell junctions, while cells in serum-free control condition appeared in a cobblestone-like epithelial morphology with tight cell-cell junctions (**Fig 10**). This observation indicated that EGF^{high} treatment for 72 h resulted in EMT induction in HNSCC cells.

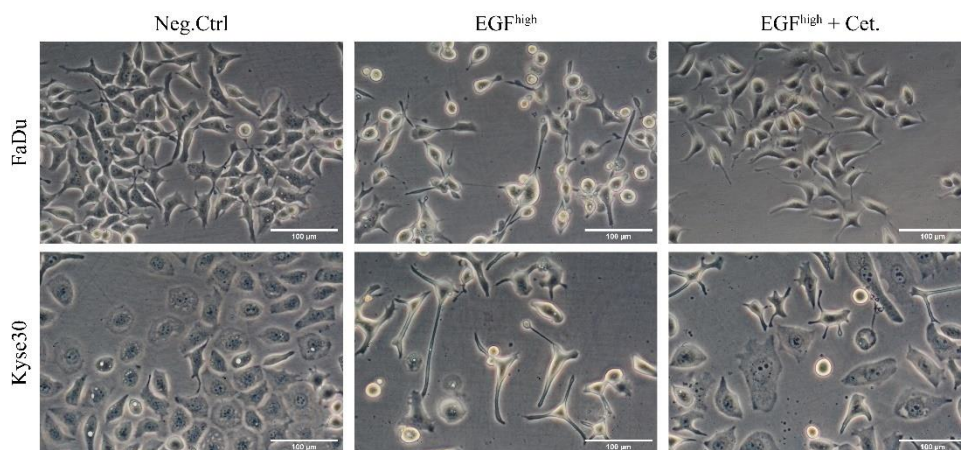


Figure 10 Microscopic images illustrating the morphology of Kyse30 and FaDu cells

FaDu and Kyse30 cells were subjected to various treatments including Negative Control (Neg.Ctrl), EGF^{high}, or a combination of EGF^{high} with Cetuximab. EGF^{high}: 9 nM EGF; Scalebars represent 100 μm. Shown are representative micrographs from three independent experiments.

3.2 ITGβ4 and its ligand laminin 5 are up-regulated in HNSCC

3.2.1 Upregulation of *ITGβ4* and laminin 5 in 2D transcriptomic analysis

Previous transcriptomic analysis focusing on EGFR-mediated EMT identified a gene signature comprising exclusively regulated genes, totaling 181 genes, which included notable genes such as *ITGβ4*, as well as the laminin 5 genes *LAMA3*, *LAMB3*, and *LAMC2*. Compared with untreated ctrl samples, the Log2FC values for *ITGβ4* in FaDu and Kyse30 cells treated with EGF^{high} were notably significant at 0.81 ± 0.21 and 2.02 ± 0.30 , respectively (**Fig 11**). *ITGβ4* ligand laminin 5 genes *LAMA3*, *LAMB3*, and *LAMC2* exhibited up-regulation after EGF^{high} treatment in both FaDu and Kyse30 cells. As shown in **Fig 11**, EGF^{high} treated FaDu and Kyse30 presented a significant Log2FC of 1.91 ± 0.70 and 1.68 ± 0.38 of *LAMA3*, 2.42 ± 0.33 and 1.94 ± 0.39 of *LAMB3*, and 3.24 ± 0.51 and 2.83 ± 0.29 of *LAMC2*, respectively.

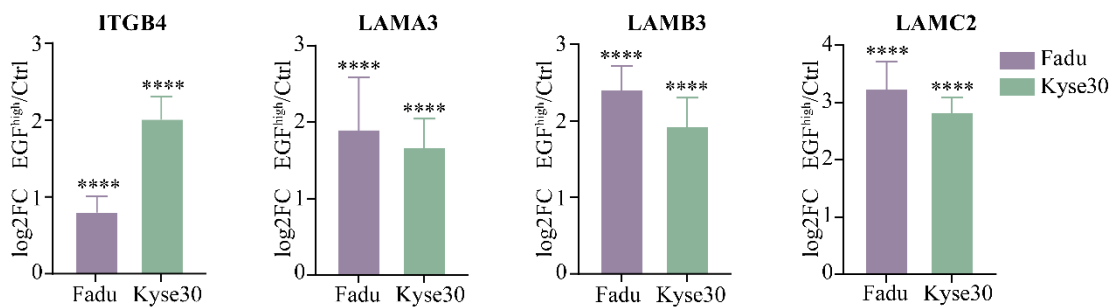


Figure 11 *ITGβ4*, *LAMA3*, *LAMB3* and *LAMC2* expression in EGFR-mediated EMT

Relative mRNA expressions of *ITGβ4*, *LAMA3*, *LAMB3* and *LAMC2* are presented as mean log2 fold (Log2FC) ratios of EGF^{high}-treated relative to negative control samples, along with the standard error of the mean (SEM). These results were obtained from bulk RNAseq analysis of FaDu and Kyse30 cells subjected to EGF^{high} treatment (EGF at 9 nM for 72 h) based on data from four independent experiments. Significance is denoted by **** with a *p*-value < 0.0001.

3.2.2 EGF^{high} treatment upregulates *ITGβ4* expression in HNSCC cell lines

To further validate the upregulation of *ITGβ4* observed in the transcriptomic analysis, induction of *ITGβ4* by EGFR activation was addressed at RNA and protein level in FaDu and Kyse30 cells. The results showed that compared with untreated control, *ITGβ4*

relative mRNA expression was enhanced 1.71-fold and 4.40-fold upon EGF^{high} treatment in FaDu and Kyse30 cells, respectively (**Fig 12A-B**). Besides that, after EGF^{high} treatment, ITGβ4 expression at cell surface was upregulated 4.62-fold and 2.52-fold in FaDu and Kyse30 cells, respectively (**Fig 12C-D**). Hence, ITGβ4 is significantly upregulated upon EGF^{high} treatment in HNSCC cells.

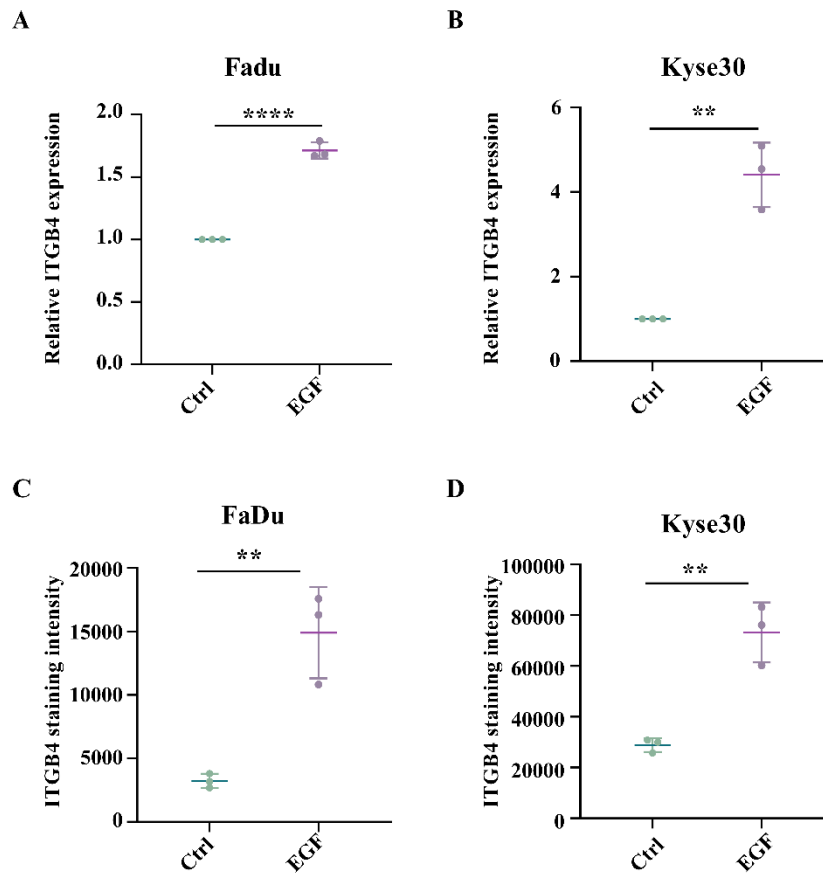


Figure 12 EGF^{high} treatment upregulates ITGβ4 expression in HNSCC cell lines

(A-B) Quantitative RT-PCR (qRT-PCR) analysis of ITGβ4 expression in FaDu and Kyse30 cell lines upon EGF treatment. (C-D) Cell surface expression of ITGβ4 in FaDu and Kyse30 cell lines upon EGF treatment measure by flow cytometry. All data was presented as the mean values along with standard deviation (SD) from a total of three independent experiments ($n = 3$). ** p -value < 0.01 (t -test).

3.2.3 ITGβ4 is upregulated in HNSCC tumor tissues

ITGβ4 protein expression was investigated in HPV-negative and -positive HNSCC patients of the cohort of 109 patients with HPV-negative and HPV-positive HNSCC at the Head and Neck Department at the Ludwig-Maximilians- University of Munich,

Germany (clinical parameters information in **Table 2**). As shown in **Fig 13A**, IHC staining showed strong ITG β 4 expression within the initial suprabasal cell layers near the basal lamina. Conversely, primary HNSCC tumors exhibited an elevated expression of ITG β 4. IHC scoring was applied to evaluate ITG β 4 expression in mucosa and tumor tissues, demonstrating a significant overexpression in 80 primary HNSCCs compared with 64 normal mucosa tissues (**Fig 13B**). Moreover, ITG β 4 staining showed a significant overexpression in primary HNSCC tumor and lymph node metastases in comparison to normal mucosa in matched triplets (n=26) (**Fig 13C**). Patients were further clustered into HPV-negative and HPV-positive groups, revealing that ITG β 4 was significantly upregulated in 43 HPV-negative and 41 HPV-positive HNSCC tumor tissues compared to non-malignant mucosa (**Fig 13D-E**).

Table 2: Clinical parameters of LMU HNSCC cohort (n=109)

LMU HNSCC cohort				
Age	≤63	>63		
%	47.71	52.29		
Absolute	52	57		
Gender	Female	Male		
%	21.10	78.90		
Absolute	23	86		
P16	Negative	Positive	Unknown	
%	39.45	37.61	22.94	
Absolute	43	41	25	
Smoking	Never	Former	Current	Unknown
%	11.01	42.20	41.28	5.50
Absolute	12	46	45	6
Localization	Oral Cavity	Oropharynx	Hypopharynx & Larynx	
%	61.47	23.85	14.68	

Absolute	67	26	16	
T stage	pT1-2	pT3-4	pTx	Unknown
%	46.79	48.62	1.83	2.75
Absolute	51	53	2	3
N stage	N0	N+	Nx	Unknown
%	25.69	57.80	13.76	2.75
Absolute	28	63	15	3
M stage	M0	M1	Unknown	
%	54.13	0.92	44.95	
Absolute	59	1	49	

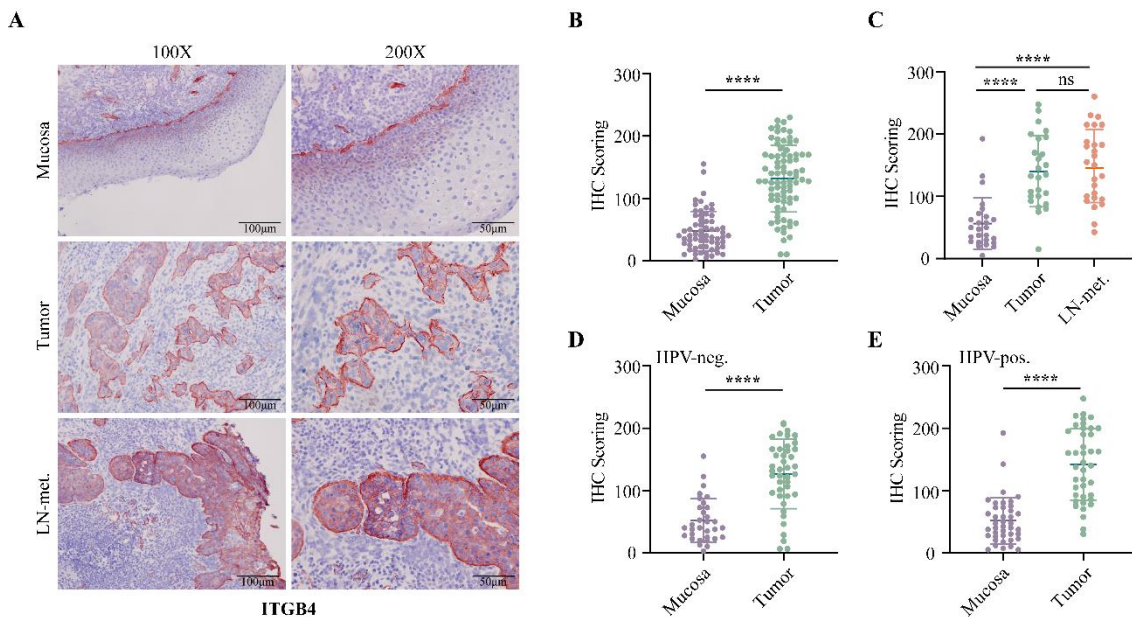


Figure 13 *ITGB4 is upregulated in HNSCC tumor tissues*

(A) Illustrative instances of *ITGB4* expression in normal mucosa (64 cases) and primary HNSCC (80 cases) from a total of 84 patients are depicted. Additionally, matched triplets, which included lymph node metastases in 26 cases, were analyzed in both HPV-negative and HPV-positive HNSCC cases within the LMU cohort. (B-E) The scatter dot plots display the IHC quantification of *ITGB4* expression, presenting the mean and SD values for all samples. Additionally, the plots in D-E are stratified based on the HPV-status for

comparison. Ns: No statistical significance, **** $p \leq 0.0001$ (determined by *t*-test and One-way ANOVA).

3.2.4 ITG β 4 and laminin 5 expression in TCGA cohort and scRNA-seq dataset

Expression levels of *ITG β 4* along with the genes encoding laminin 5, including *LAMA3*, *LAMB3* and *LAMC2* in HNSCC tumor were confirmed in the scRNA-seq dataset GSE103322 using TISCH2 (Tumor Immune Single-Cell Hub 2). TISCH2 represents an online scRNA-seq database that offers comprehensive cell-type annotations at the individual cell level. It allows for the investigation of gene expression and correlations within both malignant and non-malignant cells across 18 different cancer types, including HNSCC (<http://tisch.comp-genomics.org/home/>). The analysis demonstrated that *ITG β 4* exhibited predominant expression in malignant cells and endothelial cells ($\log(\text{TPM}/10 + 1) > 0.5$) and revealed the strongest expression of *ITG β 4* in individual malignant HNSCC cells compared to non-malignant cells (**Fig 14A**). Interestingly, *LAMA3*, *LAMB3* and *LAMC2* presented a similar expression pattern to *ITG β 4* and were mostly expressed in malignant individual HNSCC cells. Moreover, overexpression of *ITG β 4* along with the genes encoding laminin 5, including *LAMA3*, *LAMB3* and *LAMC2*, were assessed in the TCGA HNSCC dataset using the TIMER 2.0 online tool. TIMER is a comprehensive resource designed for systematical analysis of tumor immunological, clinical, and genomic features across diverse cancer types in TCGA dataset (<http://timer.cistrome.org/>). The analysis in the HNSCC cohort from TCGA showed that *ITG β 4* and laminin 5 genes were significantly overexpressed in HNSCC tumor compared to non-tumor tissue, and enhanced expressed in HPV-negative HNSCC tumor in comparison of HPV-positive HNSCC tumor (**Fig 14B**). Hence, *ITG β 4* and its laminin 5 ligand genes are upregulated in HNSCC.

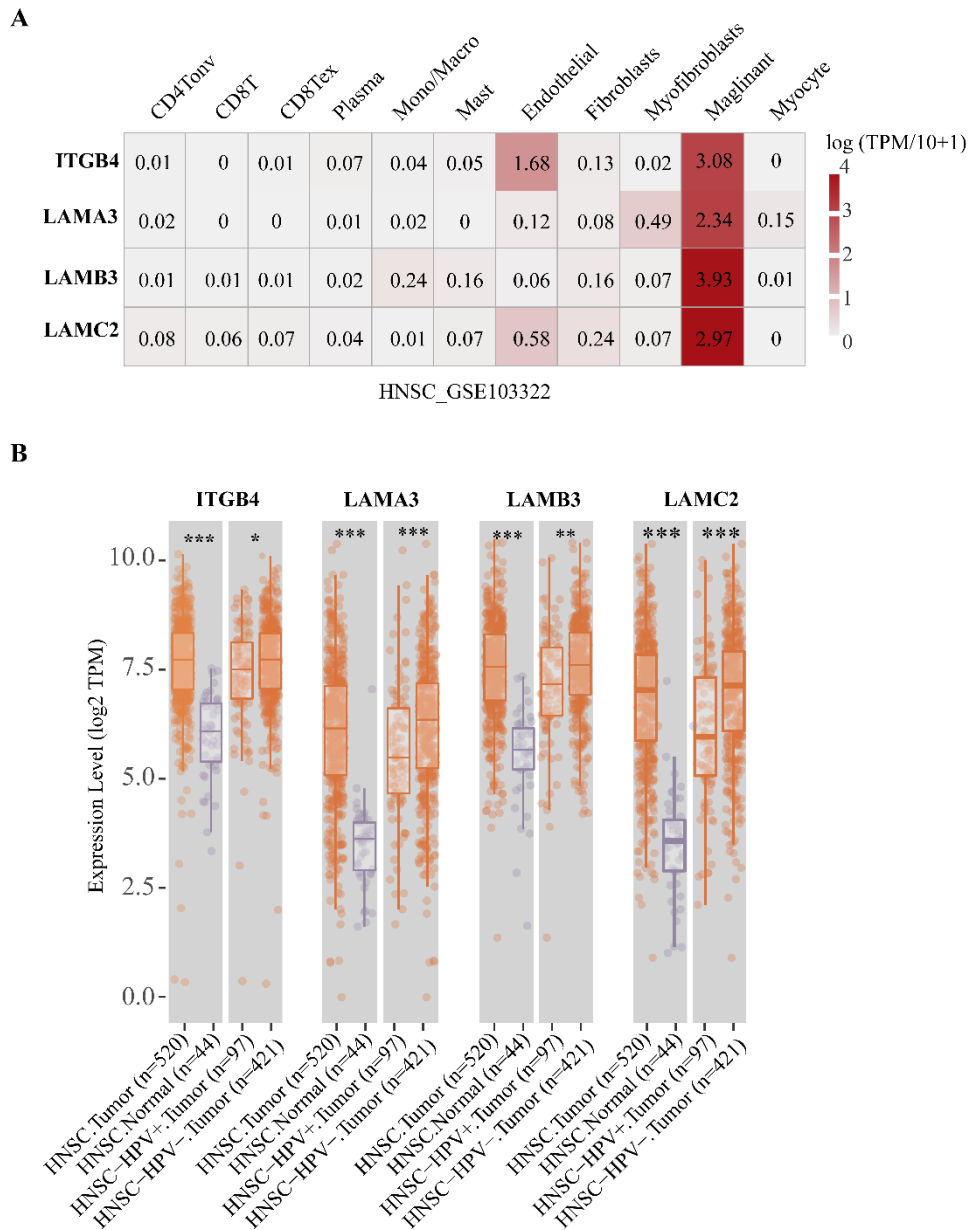


Figure 14 *ITGB4* and laminin 5 gene expression in TCGA cohort and scRNA-seq dataset

(A) TISCH2 online tool was applied for analyzing the expression of *ITGB4*, *LAMA3*, *LAMB3* and *LAMC2* in various cell populations in the GSE103322 scRNA-seq HNSCC dataset. (B) TIMER 2.0 online tool was used to examine the expression differences of *ITGB4*, *LAMA3*, *LAMB3* and *LAMC2* in different tissue types in the TCGA HNSCC cohort. * *p*-value < 0.05 (t-test), *** *p*-value < 0.001 (t-test). All data is presented as the mean values along with SD.

3.2.5 *ITGB4* and *LAMA3* co-expression in HNSCC tumor tissues

To explore co-localization patterns between ITG β 4 and laminin 5, several HNSCC samples with different levels of ITG β 4 expression were selected for further analysis. As shown in the **Fig 15**, colocalization of ITG β 4 and LAMA3 was detected at the basal lamina, and there was also an additional presence of ITG β 4 in the suprabasal cell layers of normal mucosa. Laminin 5 was either not present or exclusively expressed in non-malignant cells in HNSCC tumor samples with low or absent ITG β 4 expression. Interestingly, in ITG β 4-positive HNSCC, ITG β 4 localized differently at the interface between malignant and non-malignant area, the edge of tumor area, or throughout tumor area. Moreover, laminin 5 exhibited co-localization with ITG β 4 exclusively at the interface between the malignant area and stroma, and this co-localization pattern was further confirmed through double immunofluorescence staining in ITG β 4-positive HNSCC. Consistent with IHC staining results, immunofluorescence staining showed that the co-localization of ITG β 4 and laminin 5 was consistently observed at the tumor-stroma interface, regardless of whether ITG β 4 was localized at the tumor margin or throughout the tumor areas (**Fig 16**).

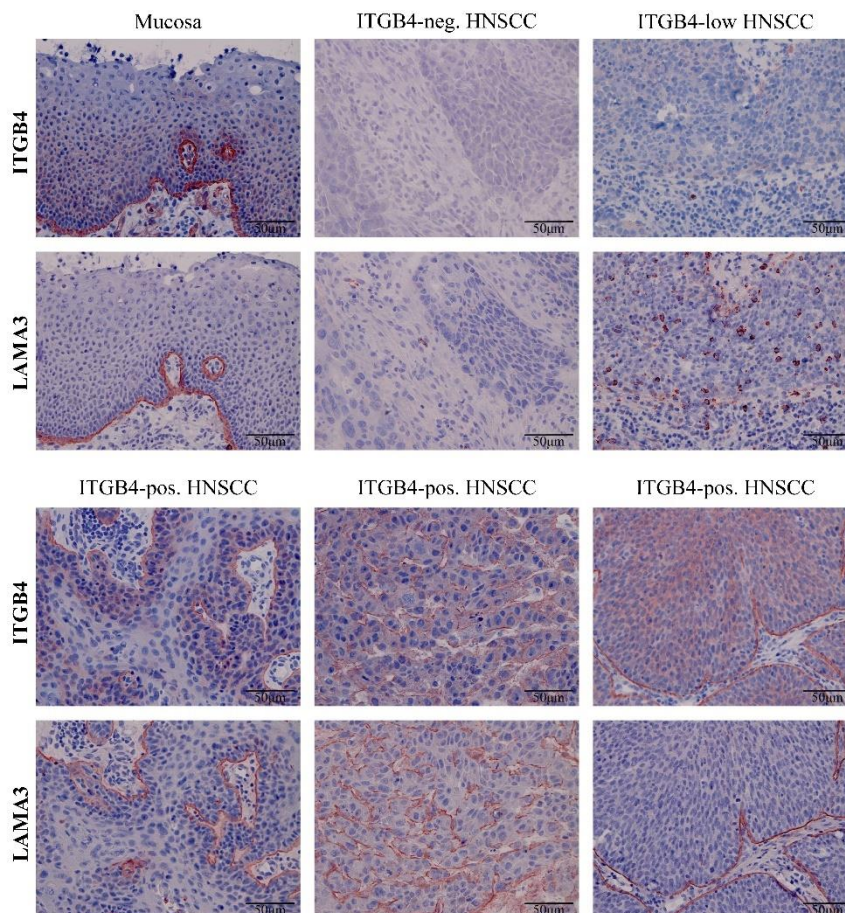


Figure 15 IHC staining of ITG β 4 and LAMA3 in HNSCC tumor tissues

Representative examples of *ITGβ4* and *LAMA3* immunohistochemistry staining in successive sections of both normal mucosa and HNSCC are displayed. Scalebars are indicated for each sample and magnification (100x upper, 200x lower panels).

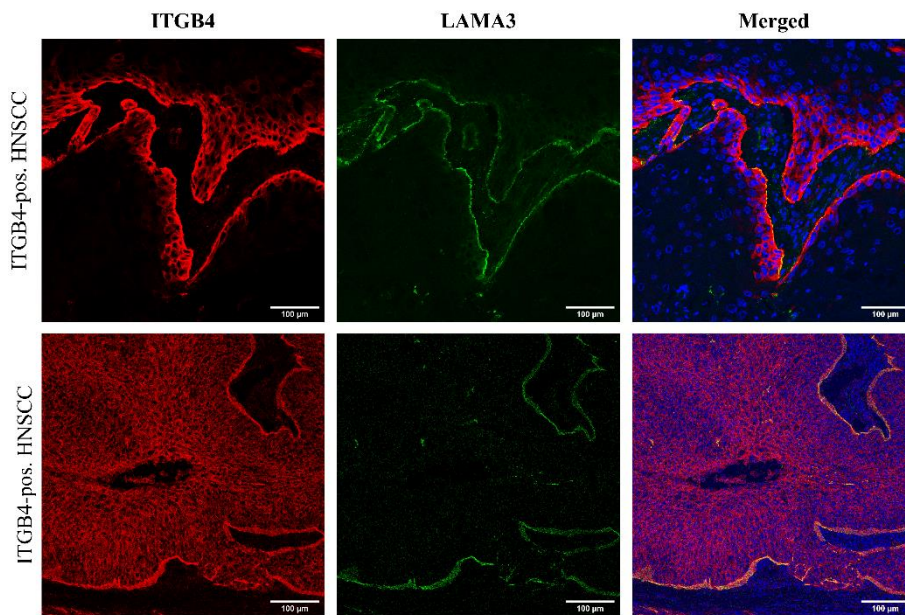


Figure 16 Immunofluorescence staining of *ITGβ4* and *LAMA3* in HNSCC tumor tissue

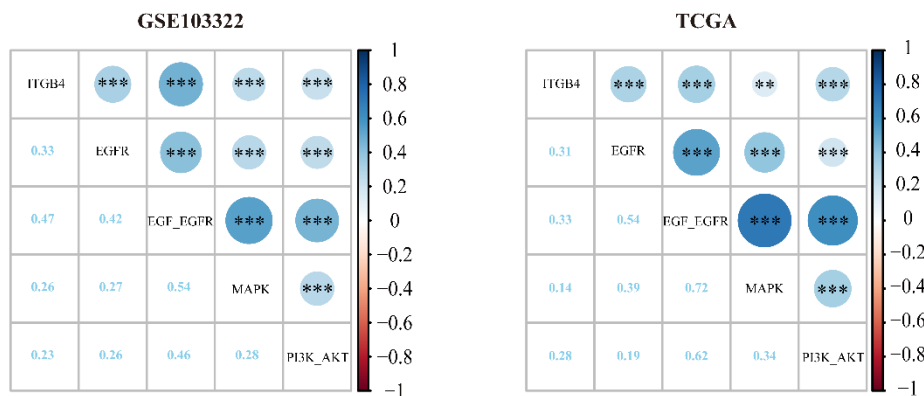
Shown are representative examples of double immunofluorescence staining displaying *ITGβ4* (in red), *LAMA3* (in green), and DAPI (in blue) in HNSCC. All images were captured using confocal laser scanning microscopy and illustrate tumor samples with edge-localized *ITGβ4* expression (upper) and with homogeneous *ITGβ4* expression (lower).

3.3 *ITGβ4* correlates with EGFR activity in malignant HNSCC cells

It has been previously demonstrated by our group that EGFR signaling regulates EMT induction in HNSCC through the MAPK-ERK1/2 axis activation. The correlation between *ITGβ4* expression with *EGFR* expression, EGF-EGFR activation, MAPK-ERK1/2 and PI3K-AKT pathways were analyzed in a cooperative work with Zhengquan Wu. In both scRNA-seq (GSE103322) and TCGA datasets, *ITGβ4* expression was significantly associated with *EGFR* expression, EGF-EGFR activity, MAPK and PI3K-AKT pathways (**Fig 17A**). Among all the correlations examined between *ITGβ4* and *EGFR* expression, EGFR activation, MAPK pathway, and PI3K pathways, it was found

that the correlation with EGFR activity is the strongest. Further validation of EGFR-dependent pathways associated with *ITGB4* induction was performed in HNSCC cells in vitro. Following an 18 h period of serum starvation, FaDu and Kyse30 cells were treated with EGF^{high} alone or co-treatment with Cetuximab, MEK inhibitor or AKT inhibitor for 72 h. After EGF^{high} treatment, *ITGB4* mRNA expression was 5.12-fold and 1.99-fold upregulated in Kyse30 and FaDu cells, respectively (**Fig 17B**). *ITGB4* induction was significantly suppressed by EGF^{high} co-treatment with Cetuximab and MEK inhibitor in both FaDu and Kyse30 cells, whereas no significant effects on *ITGB4* mRNA expression upregulation was observed in EGF^{high} co-treatment with AKT inhibitor. Therefore, upregulation of *ITGB4* is correlated with enhanced EGFR and MAPK signaling pathway activation in HNSCC cells.

A



B

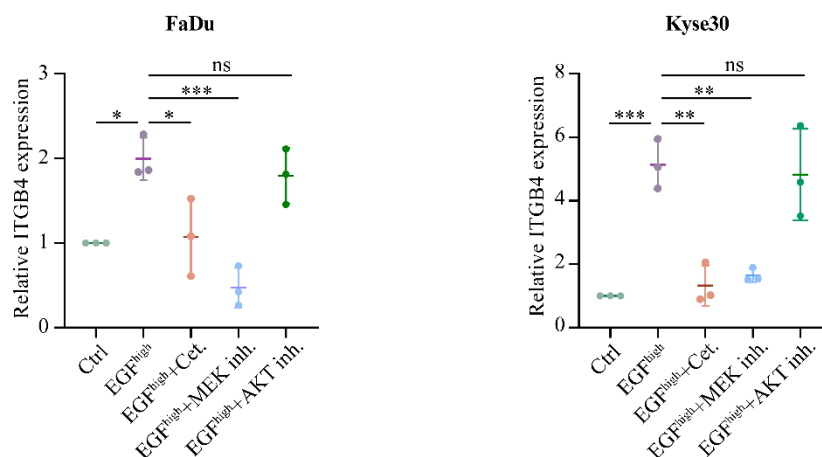


Figure 17 Upregulation of *ITGB4* is associated with enhanced EGFR and MAPK activity

(A) Correlation scores of *ITGB4* and EGFR expression, EGF-EGFR activity, MAPK-ERK1/2 and PI3K-AKT pathways in scRNA-seq (GSE103322) and TCGA datasets. ** *p*-

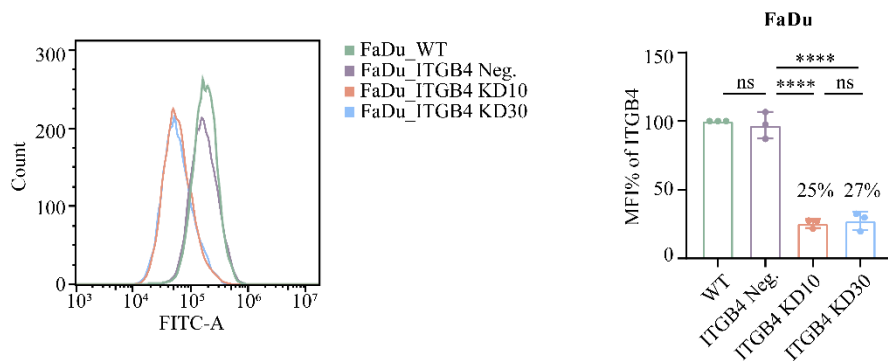
value < 0.01 , *** p -value < 0.001 . (B) mRNA expression of *ITGB4* was measured by qRT-PCR in Kyse30 and FaDu cells after treatment with 50 ng/mL EGF or combinations of EGF with Cetuximab, MEK inhibitor, or AKT inhibitor. Mean values with SD from three independent experiments are shown in scatter dot plots. * ≤ 0.05 ; ** ≤ 0.01 ; *** ≤ 0.001 (One-way ANOVA).

3.4 ITG β 4 promotes migration and invasion in HNSCC

3.4.1 Validation of ITG β 4 knockdown in HNSCC cells

To further explore ITG β 4 functions in migration and invasion in vitro, *ITGB4* knockdown cell lines were generated in FaDu and Kyse30 cell by applying scramble and specific shRNA against *ITGB4* via lentiviral transduction (cooperation with Prof. U. Schumacher, Dr. S. Genduso, UKE, Hamburg, Germany). As shown in the **Fig 18A-B**, scrambled shRNA controls (ITG β 4 Neg) had similar expression of ITG β 4 as wildtype cells, while 73% and 68% reduction in FaDu and 84% and 87% reduction in Kyse30 were observed in *ITGB4*-shRNA transfectants.

A



B

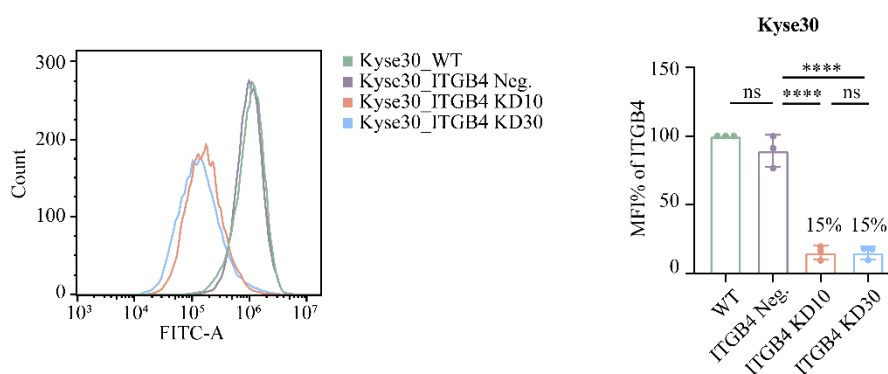


Figure 18 Validation of ITG β 4 knockdown in HNSCC cells

(A-B) Validation of *ITGB4* knockdown was performed using flow cytometry in FaDu and Kyse30 cells (left). *ITGB4* expression level (mean fluorescence intensity, MFI) was determined by quantitative flow cytometry (right) and was presented as the mean values along with SD from a total of three independent experiments ($n = 3$). Ns: not significant, **** p -value < 0.0001 (One-way ANOVA).

3.4.2 Knockdown of *ITGB4* decreases EGFR-mediated 2D migration and invasion in HNSCC cells

Next, *ITGB4*-KD cells were assayed for their migratory and invasive capabilities using a Boyden chamber system without or with Matrigel. In the migration assay, once cells migrate through an 8 μ m-porous membrane from the upper to the lower compartment, they were fixed and stained for quantification. In the invasion assay, to mimic the extracellular matrices encountered by tumor cells during dissemination in vivo, the porous membrane was covered by Matrigel matrix containing Collagen IV, laminin and perlecan. *ITGB4* knockdown in both, FaDu and Kyse cells, showed a significant decrease of EGF-mediated migration (**Fig 19A**) and invasion (**Fig 19B**), when compared with Ctrl cells. Meanwhile, EGF treatment combined with cetuximab in Ctrl and *ITGB4* knockdown cells demonstrated strong inhibition of migration and invasion, providing confirmation of the specificity for EGFR activation.

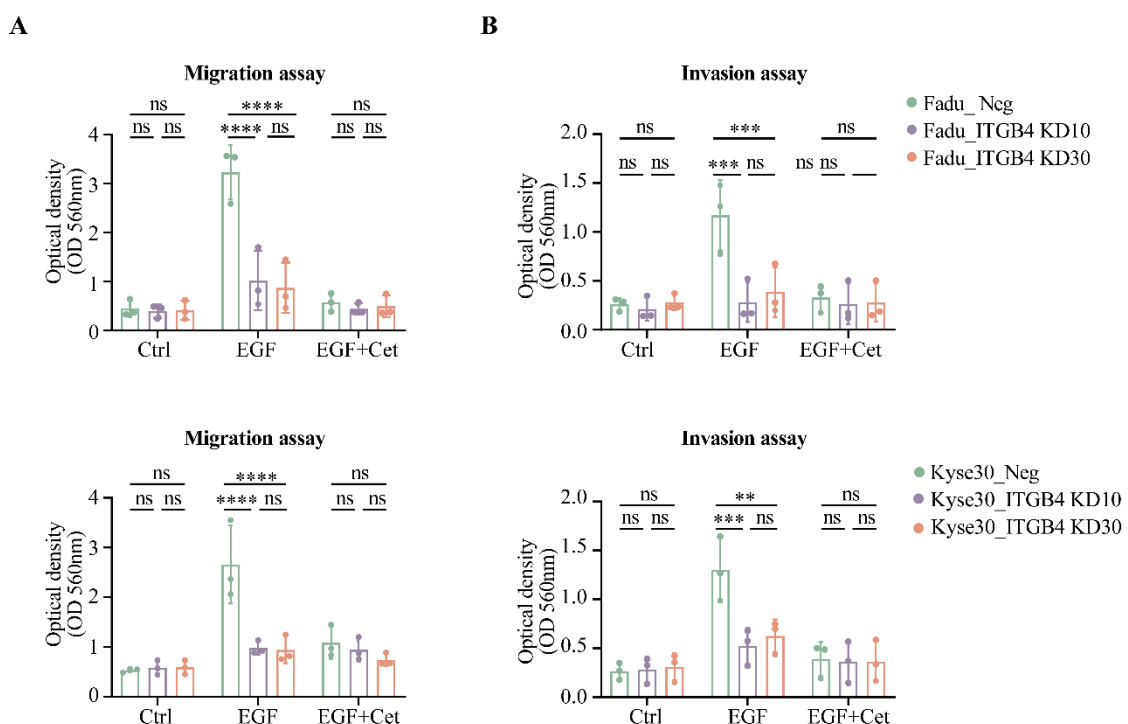


Figure 19 Knockdown of *ITGβ4* decreases *EGFR*-mediated 2D migration and invasion in HNSCC cells

(A-B) Migration and invasion assays were performed under the indicated treatment modalities in FaDu and Kyse30 cells. Optical density (OD) of control (Neg.) and *ITGβ4_KD* cells (KD10 and KD30) of FaDu and Kyse30 were quantified in cells kept untreated (Neg.Ctrl), treated with EGF^{high} , or co-treatment of EGF^{high} and Cetuximab. All data is presented as the mean values along with SD from a total of three independent experiments ($n = 3$). ** p -value < 0.01, *** p -value < 0.001, **** p -value < 0.0001.

Next, a wound healing assay was performed with FaDu and Kyse30 cells to evaluate tumor cell migration in vitro (**Fig 20A-B**). After generating an artificial wound in a cell monolayer, the migratory capacity was quantified by wound closure. It was observed that in comparison to control treatment, EGF^{high} treatment promoted wound closure significantly in both FaDu and Kyse30 control cells, whereas it only induced weak wound closure in *ITGβ4* knockdown cells. Co-treatment of EGF^{high} and cetuximab in all cell lines also completely blocked the EGF-mediated migration in the wound healing assay (**Fig 20C-D**). Thus, *ITGβ4* plays an essential role in *EGFR*-mediated 2D migration and invasion.

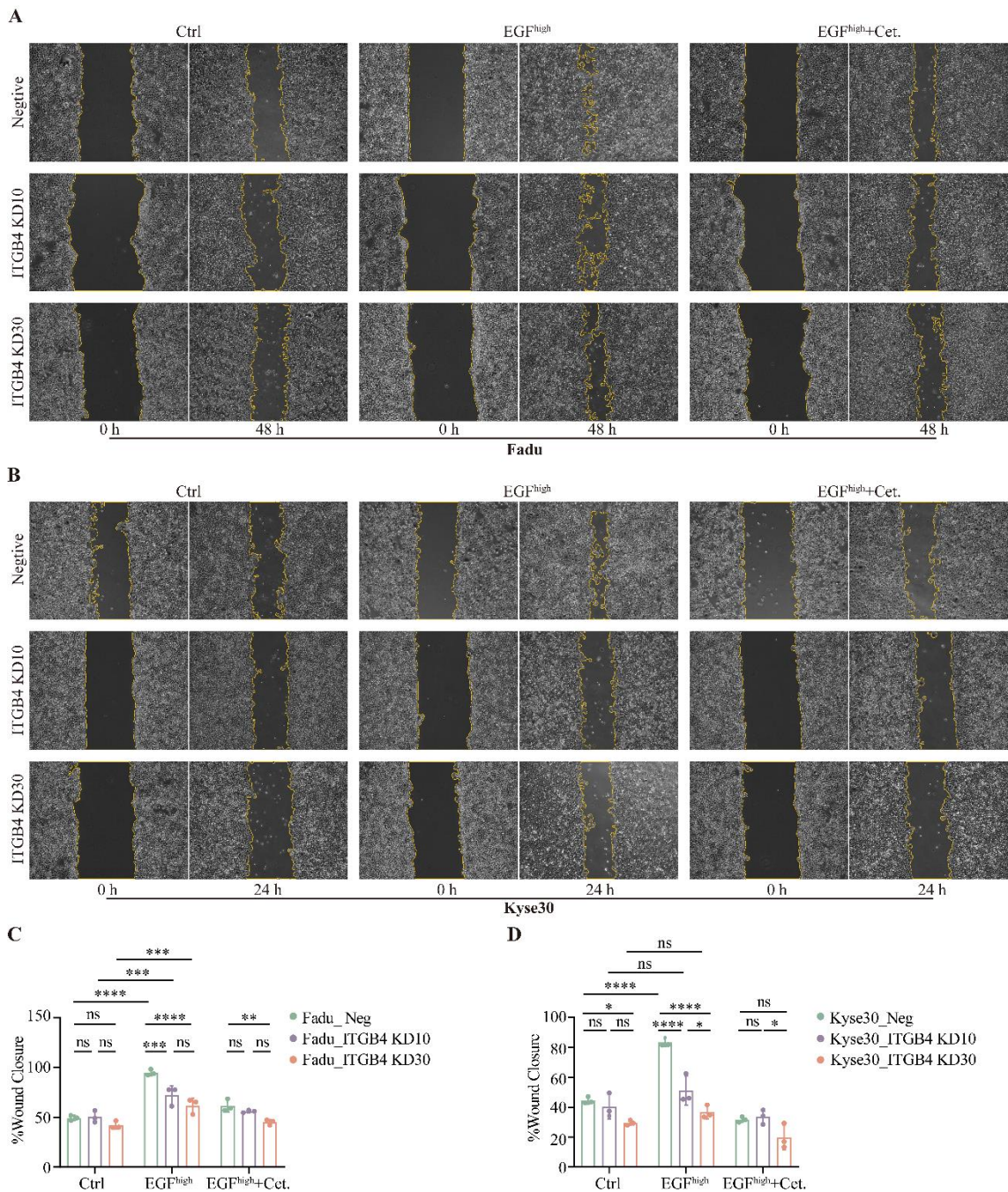


Figure 20 Wound healing capacity of control and ITGβ4-knockdown cell lines

(A-B) Control and ITGβ4-knockdown FaDu and Kyse30 clones were utilized in a wound healing assay. Shown are representative microscopic images of scratches at 0h and 24 h (Kyse30), and at 0h and 48 h (FaDu) from $n = 3$ independent experiments. Scalebars represent 100 μm . (C-D) Quantification of the relative wound closure (%) from A-B and is presented as the mean values with SD from three independent experiments ($n = 3$). Ns: not significant, * < 0.05 , ** p -value < 0.01 , *** p -value < 0.001 , **** p -value < 0.0001 (t-test and One-way ANOVA).

3.4.3 Knockdown of ITG β 4 decreases EGFR-mediated 3D invasion in HNSCC cells

To further assess the functional role of ITG β 4 in EGFR-mediated invasion, a 3D spheroid model in Matrigel was performed. FaDu control cells and *ITG β 4* knockdown cells were plated in 96-well low-attachment plates for spheroids generation, then formed spheroids were embedded in Matrigel before adding treatment in the supernatant. The morphology pictures in **Fig 21A** revealed that compared with the negative control group, EGF^{high} treatment induced significant invasion in FaDu control cells, with many cells spreading from the spheroid into the adjacent Matrigel matrix. This EGF-induced local invasion was strongly inhibited by co-treatment with Cetuximab. However, compared with FaDu control cells, EGF^{high} treatment induced invasion was significantly reduced in FaDu *ITG β 4* knockdown cells and was efficiently blocked by Cetuximab treatment, too. The invasive area and invasive distance in the 3D model were quantified as described in the Method part using the outer area and the mean invasive distance of minimum ten cells per spheroid. Quantification confirmed that EGF^{high} resulted in strongly enhanced invasive area and invasive distance in FaDu control cells, which was significantly decreased in *ITG β 4* knockdown cells (**Fig 21B**). Notably, the number of invasive cells within the designated invasive region were also greatly reduced as visualized for *ITG β 4* knockdown cells. Co-treatment with Cetuximab efficiently inhibited EGFR-mediated invasion in FaDu control cells and *ITG β 4* knockdown cells. Consequently, the expression of ITG β 4 enhances EGFR-mediated 3D invasion.

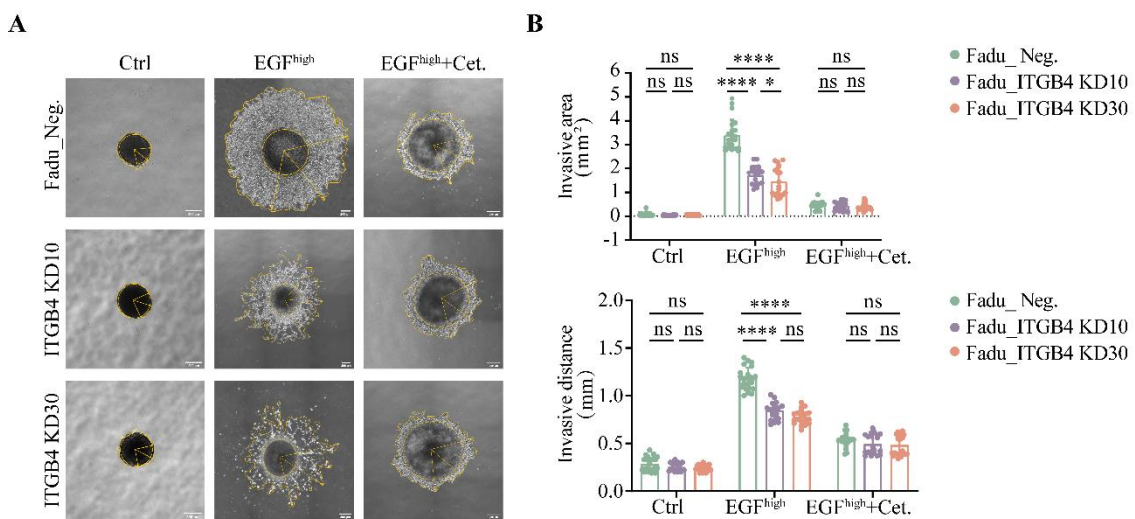


Figure 21 Knockdown of ITG β 4 decreases EGFR-mediated 3D local invasion in HNSCC cells

(A) Spheroids of FaDu control (Neg.) and ITG β 4_KD cells (KD10 and KD30) were cultivated in Matrigel (1 mg/ml). These spheroids were subjected to three different treatments: untreated (Neg.Ctrl), EGF^{high}, or co-treatment of EGF^{high} and Cetuximab (10 μ g/mL). Representative images with multiple spheroids are shown. (B) Quantification of the invasive area and invasive distance from A and is presented as the mean values along with SD from a total of three independent experiments ($n = 3$). Yellow circumference and lines indicate the invasive area and locally invasive cells. Ns: not significant, * < 0.05 , ** p -value < 0.01 , *** p -value < 0.001 , **** p -value < 0.0001 (t-test and One-way ANOVA).

3.4.4 Antagonizing ITG β 4 inhibits local invasion in HNSCC cells

To better understand the role of ITG β 4 in migration and invasion mediated by EGFR activation, ITG β 4 antagonist antibody ASC8 was investigated in 2D and 3D function models. ASC8 antagonizes the interaction of ITG β 4 with its natural ligand laminin 5, which is present in Matrigel and additionally up-regulated upon EGF^{high} treatment. Firstly, in 2D migration and invasion assays without or with Matrigel coating in a Boyden chamber system, EGF^{high} treatment significantly promoted migration and invasion in FaDu and Kyse30 wildtype cells. These effects were effectively counteracted by concurrent treatment with Cetuximab. Compared with EGF^{high} treatment alone, ASC8 co-treatment showed no significant inhibitory effect on migration in FaDu and Kyse30 cells, whereas it blocked 2D invasion similarly to Cetuximab (**Fig 22A-B**).

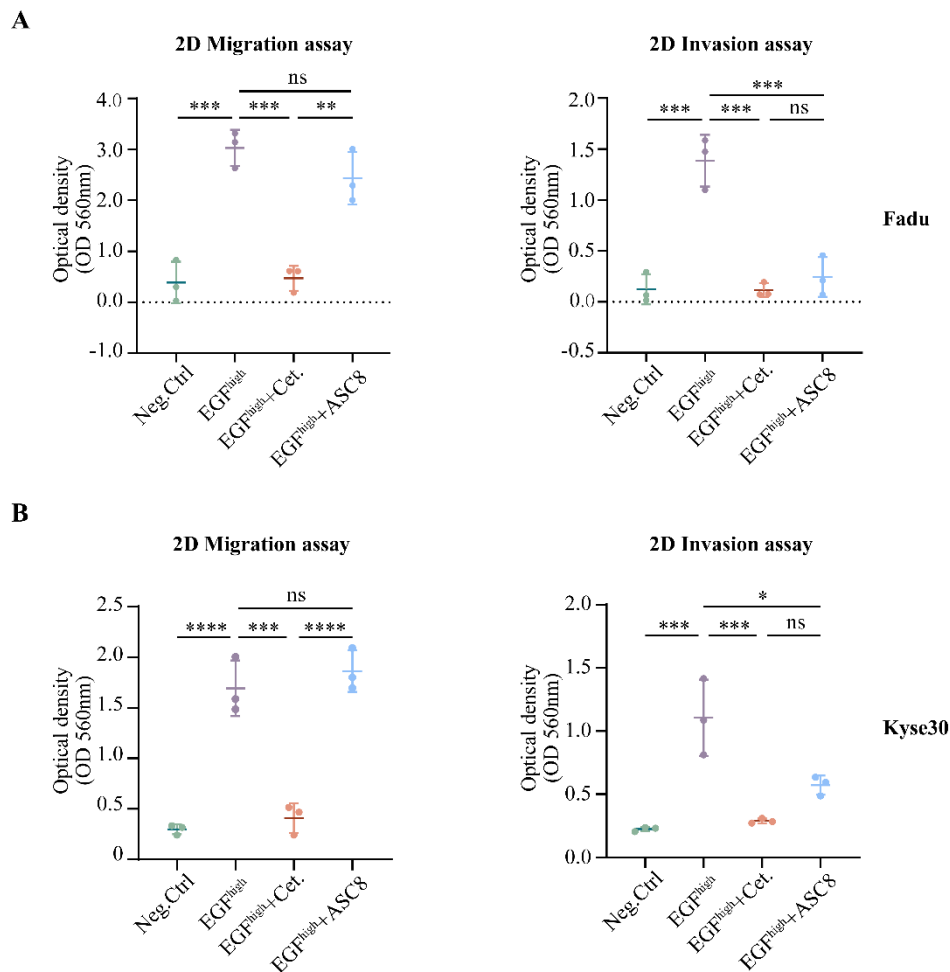


Figure 22 Antagonizing *ITGβ4* inhibits *EGFR*-mediated 2D migration and invasion in HNSCC cells

(A-B) Optical density (OD) of control (Neg.) and *ITGβ4*_KD cells (KD10 and KD30) of *Fadu* and *Kyse30* either kept in serum-free medium (Neg.Ctrl), treated with *EGF*^{high}, or *EGF*^{high} co-treated with either Cetuximab or *ITGβ4* antagonist antibody ASC8 are shown as the mean values along with SD ($n = 3$ independent experiments). Ns: not significant, * < 0.05 , ** p -value < 0.01 , *** p -value < 0.001 .

Secondly, to further address the effect of the ASC8 antibody on local invasion, a 3D spheroid model was performed with FaDu wildtype cells. After embedding FaDu spheroids in Matrigel, spheroids were treated in different treatments including serum-free condition (negative control), *EGF*^{high}, *EGF*^{high} co-treatment with Cetuximab, ASC8, or anti-GFP antibody (as a control). The morphology pictures showed *EGF*^{high} treatment induced local invasion into Matrigel, a phenomenon that was effectively prevented by co-administration of Cetuximab. ASC8 antibody was also effective in inhibiting *EGFR*-

Previous data in this thesis have revealed that *ITGβ4* expression is essential in EGFR-mediated migration and invasion in HNSCC. It has been previously demonstrated that the leading edge of tumors, comprising layers of tumor cells at the tumor border, holds prognostic significance in clinical outcomes and could play a role in mediating tumor invasion and metastasis (Arora et al., 2023; Masugi et al., 2015; Sharma et al., 2013). Thus, it was of interest to examine the expression of *ITGβ4* and its ligand laminin 5 at the leading edge and the core of HNSCC. Arora *et al.* have characterized tumor core (TC) and leading edge (LE) in HPV-negative oral squamous cell carcinoma (OSCC) by analyzing distinct transcriptional profiles, surrounding cellular compositions, and ligand-receptor interactions upon 10x Genomics Visium spatial transcriptomic analysis. An online tool was provided for exploring TC and LE biology and interactive spatial mapping (http://www.pboselab.ca/spatial_OSCC/). *EGFR*, *ITGβ4*, *LAMA3*, *LAMB3* and *LAMC2* genes expression in TC and LE were explored using this online tool. In **Fig 24A-B**, the localization information of TC (blue), LE (red) and transitory region (yellow) is depicted for three representative tumor samples, along with a visualization of gene expression intensities in TC and LE areas. Quantification analysis of all tumor samples (n=12) demonstrated that EGFR showed a similar expression pattern between TC and LE, whereas LC was characterized by a stronger expression of *ITGβ4* and genes encoding laminin 5 including *LAMA3*, *LAMB3* and *LAMC2*. when compared with TC (**Fig 24C**). This analysis suggested that *ITGβ4* and genes encoding its ligand laminin 5 are more strongly expressed at the tumor leading edge.

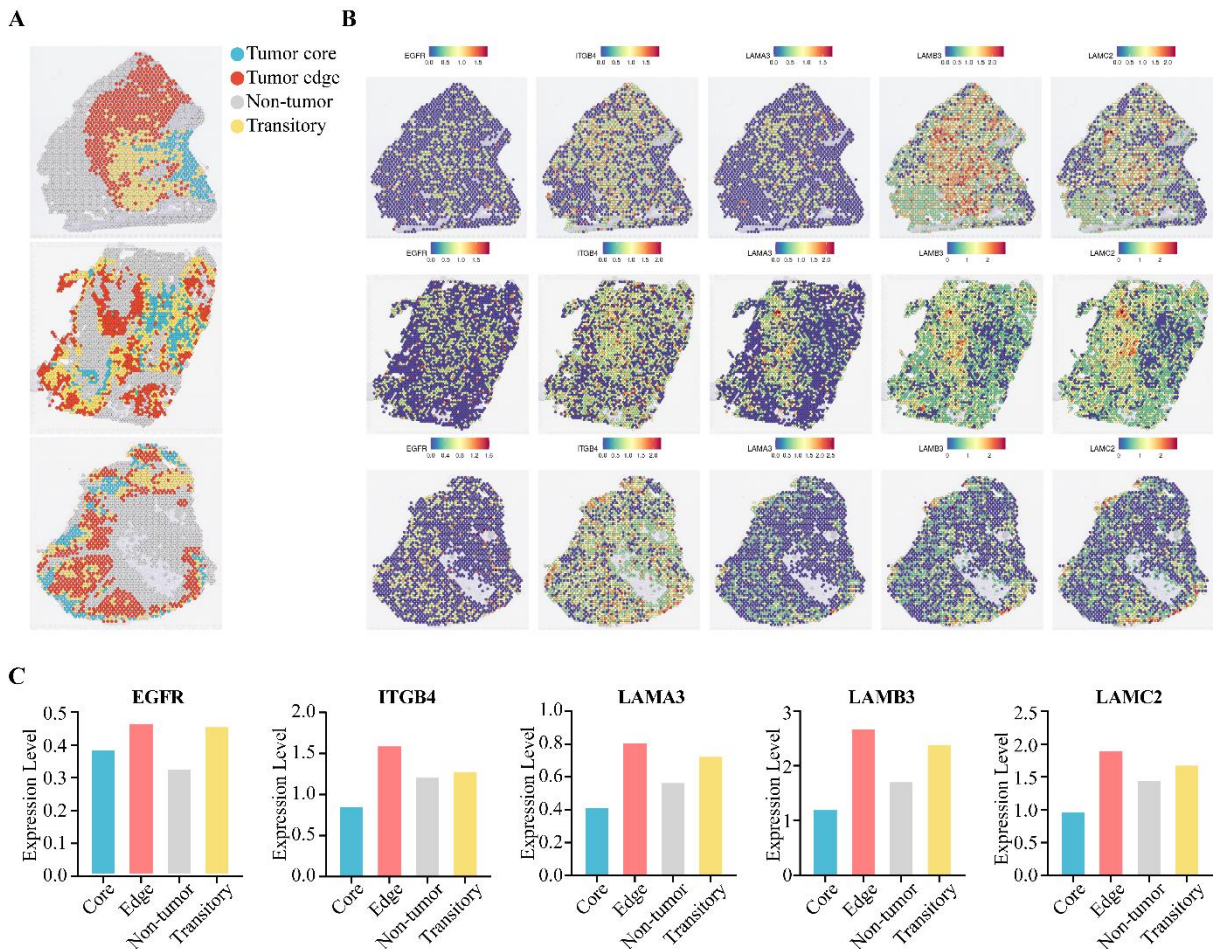


Figure 24 *ITG β 4* and laminin 5 genes are upregulated in the leading edge in spatial transcriptomic analysis of OSCC

(A) Representative examples of $n = 3$ OSCC spatial transcriptome images with tumor regions marked with the indicated colors in the publicspatial transcriptomic dataset GSE208253. (B) Spatial expression patterns of the five genes *EGFR*, *ITG β 4*, *LAMA3*, *LAMB3*, *LAMC2* are displayed in the representative spatial transcriptome image from (A). (C) Differences in mean expression levels of *EGFR*, *ITG β 4*, *LAMA3*, *LAMB3* and *LAMC2* in the indicated spatial regions in OSCC samples ($n=12$).

3.5.2 *ITG β 4* availability in the leading edge of invasion in EGF-treated spheroids

To further validate the availability of *ITG β 4* in locally invasive tumor cells as a potential target for therapeutic intervention, a 3D spheroid model was applied in Matrigel. FaDu spheroids were cultured in serum-free condition as negative control and EGF^{high} treatment

for 24 h. The initial invasion was observed after short-time treatment and outer layers of invasive cells were regarded as locally invading tumor cells potentially representing leading edges of tumor invasion. The immunofluorescence staining of ITG β 4 and the proliferation marker Ki67 revealed that ITG β 4 was only weakly expressed in outermost cell layers of serum-free-treated spheroids, whereas strong expression of ITG β 4 and decreased expression of Ki67 were observed at the leading edge of EGF^{high} treatment spheroids (**Fig 25**). Therefore, ITG β 4 is strongly expressed in the leading edge and may be available as a target in local invasion.

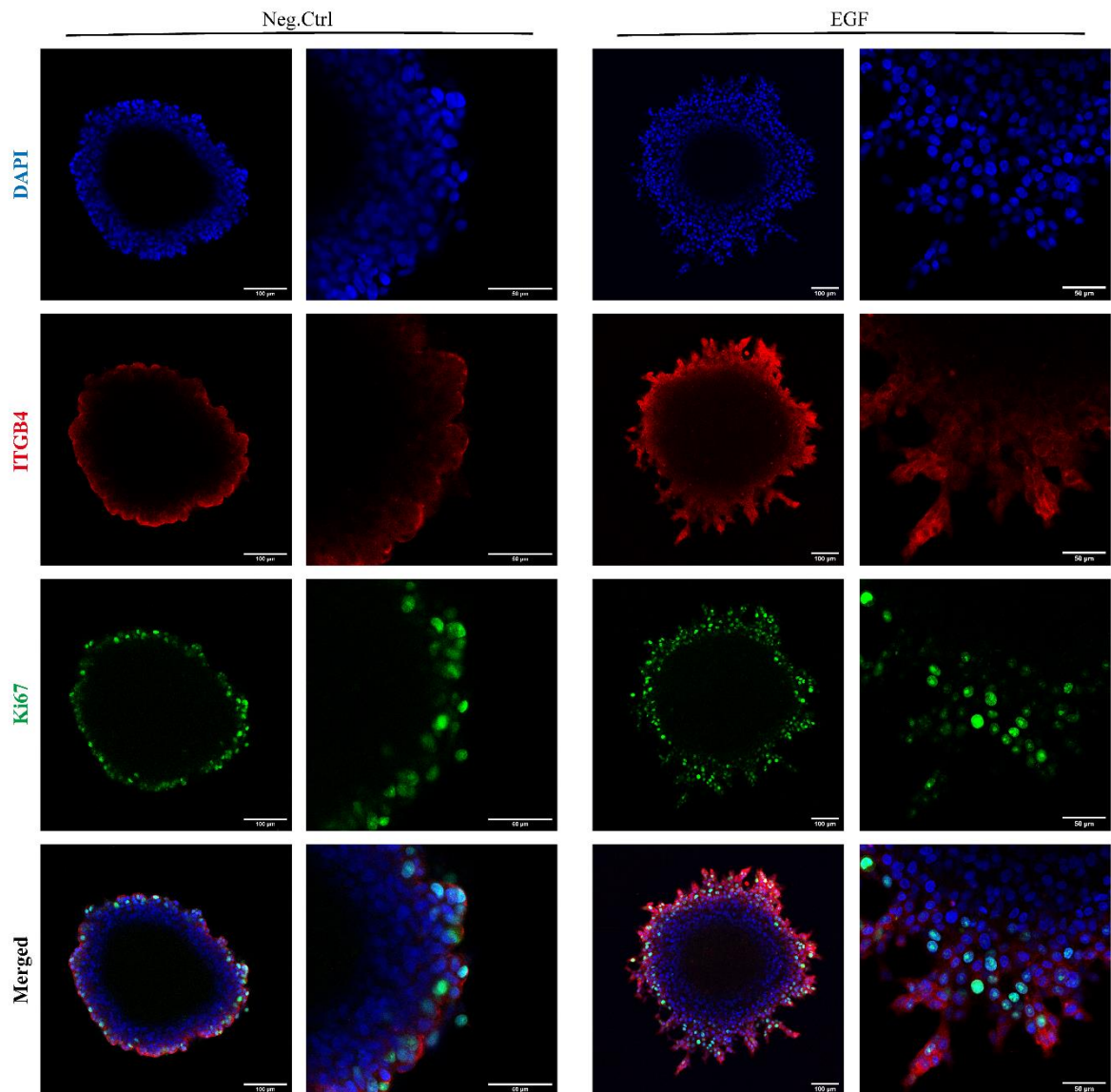


Figure 25 Immunofluorescence staining of ITG β 4 and Ki67 in FaDu spheroids

Shown are representative immunofluorescence confocal images displaying ITG β 4 (Red), Ki67 (Green), and nuclei (Blue) in the outer cells of both control and high EGF-treated

FaDu spheroids. Additionally, composite images of the entire spheroids are also presented.

3.5.3 Edge localization of ITG β 4 is associated with stronger tumor budding intensity

It has been reported that tumor budding, characterized by single malignant cells or small groups composed of fewer than five tumor cells, which have detached from the base or leading edge of the tumor mass, is a potential pan-cancer prognostic factor including primary HNSCC. As observed in **Fig 26A**, ITG β 4 can localize preferentially at the interface between tumor and non-tumor area, *i.e.* the edge of tumor area, or homogeneously throughout the tumor area. Based on this observation, patients were further grouped into “ITG β 4-edge” and “ITG β 4-homogenous” groups. 31.1% were categorized in the “ITG β 4-edge” group and 68.9% in the “ITG β 4-homogenous” group, among all 106 tumor samples of the LMU cohort (**Fig 26B**). Two experienced scientists/pathologists, blinded for the ITG β 4 expression patterns and clinical outcomes, assessed tumor budding intensities which was classified as negative, weak, intermediated, and strong (**Fig 26C**). The ITG β 4-edge group was significantly associated with more positive tumor budding (90.9%) and stronger tumor budding intensity when compared with the ITG β 4-homogeneous group (**Fig 26D-E**). Hence, the significant association of ITG β 4's edge localization with increased tumor budding intensity has been observed.

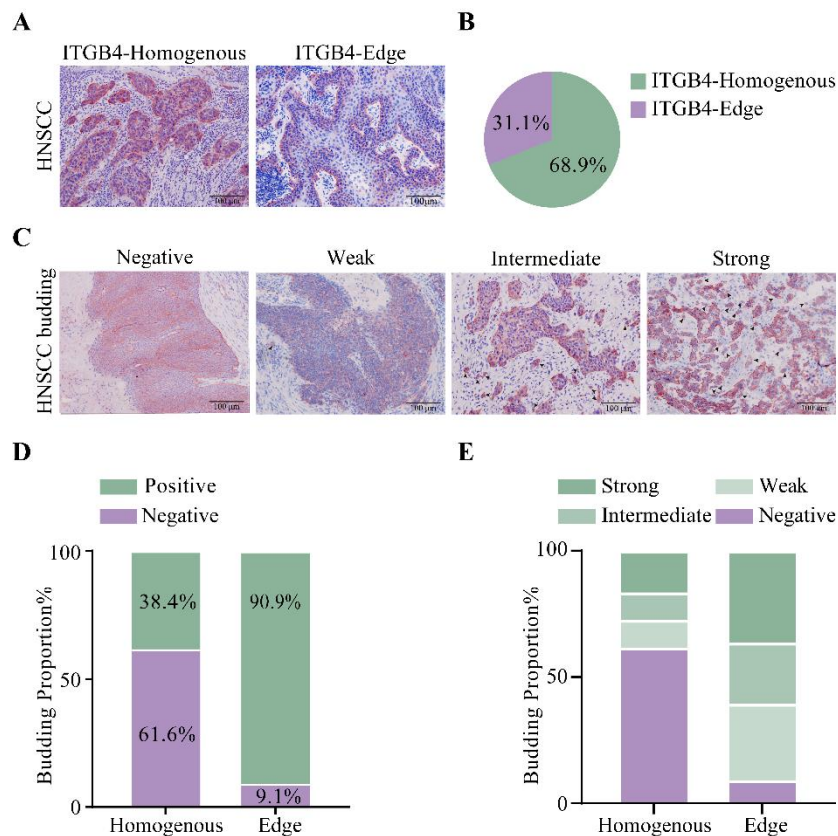


Figure 26 Edge localization of ITGβ4 is associated with stronger intensity of tumor budding in HNSCC

(A) Representative examples of homogeneous and edge localization of ITGβ4 within HNSCC tumor tissue are shown. (B) Distribution of homogeneous and edge localization of ITGβ4 within 106 HNSCC samples. (C) Different levels of budding intensities can be observed in HNSCC samples stained with ITGβ4, varying from no to weak, moderate, and strong budding. The tissues are specifically stained to highlight ITGβ4 in red, with tumor budding indicated by arrowheads. Scalebars represent 100 μm. (D-E) Proportions of HNSCC budding intensity are illustrated exhibiting either homogeneous or edge localization of ITGβ4, comprising a total of 106 cases.

3.6 Laminin 5-ITGβ4 promotes EGFR-mediated local invasion

To better understand how the interaction of ITGβ4 and laminin 5 impacts on local invasion mediated by EGFR activity, a 3D spheroid model in Collagen I without or with additional laminin 5 was performed in HNSCC cells. FaDu or Cal27 spheroids were embedded in Collagen with different concentration of laminin 5 at 0, 0.1, 1, and 10

$\mu\text{g/mL}$. Local invasion was performed in serum-free medium and spheroids were cultured in serum-free medium, serving as negative control, or were treated with EGF^{high} (**Fig 27A**). As shown in **Fig 27B**, induction of local invasion was observed in neither FaDu nor Cal27 spheroids embedded in Collagen with $10 \mu\text{g/mL}$ of laminin 5 in the absence of EGF^{high} treatment. However, laminin 5 supplementation in Collagen greatly enhanced local invasion after EGF^{high} treatment in FaDu and Cal27 spheroids. Measurement of invasive area (IA) and invasive distance (ID) (**Fig 27C**) revealed a lack of local invasion induction in the presence of laminin 5 only, which was similar to the negative control group in the absence of EGF^{high} treatment. In the presence of EGF^{high} treatment, laminin 5 supplementation in Collagen significantly enhanced IA and ID in both FaDu and Cal27 cells compare to EGF^{high} treatment alone. The effect was accentuated with increasing dose of laminin 5 and it was strongest at the highest concentration ($10 \mu\text{g/mL}$), showing 3.21-fold and 2.30-fold increase of IA, and 1.74-fold and 1.61-fold increase of ID in FaDu and Cal27, respectively. Hence, as the main ligand of $\text{ITG}\beta 4$, laminin 5 shows a dose-dependent effect on promotion of EGFR-mediated local invasion in HNSCC.

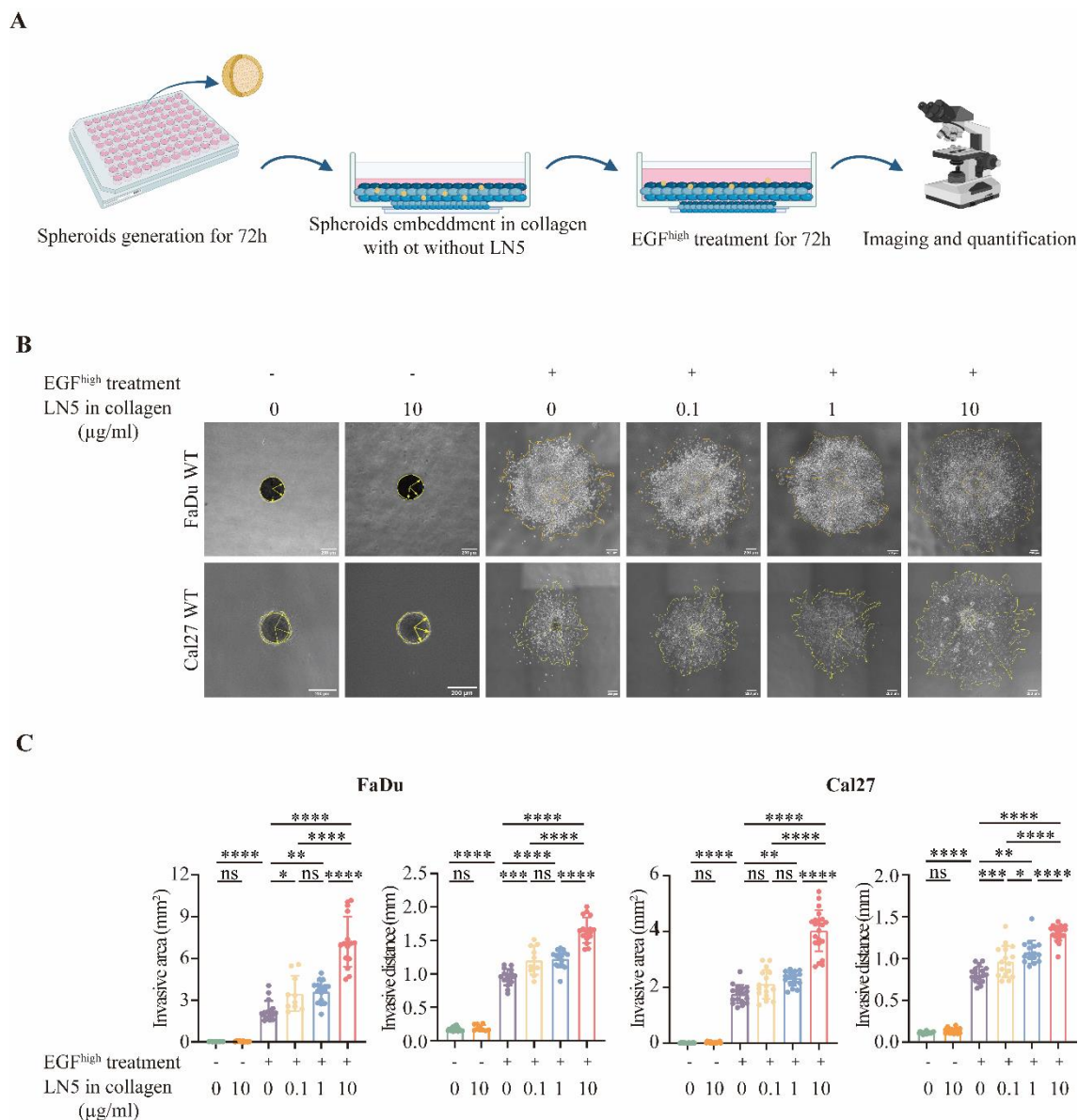


Figure 27 Laminin 5 promotes EGF-mediated local invasion in HNSCC

(A) Flow chart detailing the experimental procedure for determining the role of laminin 5 in EGF-mediated 3D invasion. (B) FaDu wild type (WT) and Cal27 wild type (WT) spheroids were cultured in Collagen I supplemented with different concentration of laminin 5 (ranging from 0-10 μg/mL). Spheroids were treated in serum-free as control or high-dose of EGF (9 nM). Shown are representative images from three independent experiments (n=3). (C) Measurement of the invasive area and invasive distance from (B) and are presented as the mean values along with SD from a total of three independent experiments (n = 3). Ns: not significant, * < 0.05, ** p-value < 0.01, *** p-value < 0.001, **** p-value < 0.0001 (One-way ANOVA).

3.7 CD73 expression is upregulated via the EGFR-MAPK axis in HNSCC

Previously, we identified an EGFR-mediated EMT signature containing 181 genes in HNSCC, including *CD73/NT5E* (Schinke et al., 2022). CD73 is a membrane-tethered 5'-ectonucleotidase that is overexpressed in various types of tumors and hydrolyzes extracellular AMP to ADO. ADO accumulates in the TME and exerts functions related to immunosuppression and regulation of EMT. We hereafter focused on exploring the function of CD73 in local invasion mediated by EGFR activation in HNSCC, assessing it as a potential druggable target in HNSCC.

Compared with untreated ctrl samples, EGF^{high} treatment for 72 h in FaDu and Kyse30 cells resulted in a significant upregulation of *CD73* expression with log₂fc of 3.2 ± 0.69 and 1.73 ± 0.38 , respectively (**Fig 28A**). To further validate upregulation of CD73 induced by EGF^{high} treatment, CD73 expression at protein level was exterminated in independent experiments. After serum starvation for 18 h, FaDu and Kyse30 were cultured in serum-free medium as negative control, EGF^{high} treatment or co-treatment with Cetuximab. CD73 expression at the plasma membrane was tested using flow cytometry following specific staining. It was observed that compared with negative control, EGF^{high} treatment enhanced CD73 expression in FaDu and Kyse30 cells by 9.06-fold and 2.76-fold, respectively (**Fig 28B**), which is similar to the transcriptomic analysis. Upregulation of CD73 expression after EGFR activation was further significantly blocked by co-treatment with Cetuximab, which indicated that CD73 upregulation is dependent upon EGFR signaling pathway.

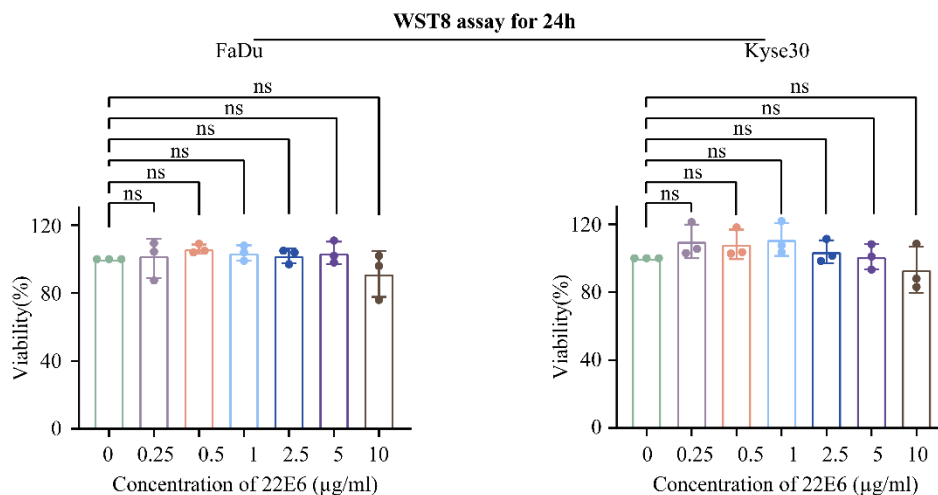
(A) The correlation between CD73 expression level and activation of EGF-EGFR pathway, EMT, Patial-EMT, EGFR-mediated EMT, MAPK pathway and PI3K-AKT pathway in GSE103322, TCGA and FHCRC cohorts is shown. (B) Flow cytometry was performed to evaluate the cell surface expression of CD73 in FaDu and Kyse30 cells following treatment with various conditions: Neg.Ctrl (serum-free medium), EGF^{low} (1.8 nM), EGF^{high} (9 nM), and a combination of EGF^{high} with either a MEK inhibitor AZD6244 (0.1 μM) or an AKT inhibitor MK2206 (0.1 μM) for 72 h. The left panel displays representative histograms obtained from three separate experiments (n=3). The MFI of CD73 from different treatment groups in FaDu and Kyse30 cells (right panel, were measured and are presented as the mean values along with SD from a total of three independent experiments (n = 3). Ns: not significant, * < 0.05, ** p-value < 0.01 (t-test and One-way ANOVA).

3.8 Functional role of CD73 in EGFR-mediated migration and invasion in HNSCC

3.8.1 CD73 blocking does not impacts on EGFR-EMT induction

WST8 assay was firstly conducted to test potential cellular cytotoxicity of 22E6 with different concentrations in both FaDu and Kyse30. The analysis showed that 22E6 treatment did not present any cellular cytotoxicity at concentrations up to 10 μg/mL (**Fig 30**). To examine effects of CD73 blocking on EGFR-mediated EMT, EGF^{high} treatment combined with IgG as control or 22E6 was utilized to treat FaDu cells for 72 h, and the evaluation of both morphologic and molecular markers of EMT was further conducted. As shown in the **Fig 31A**, an impact of CD73 blockade on morphologic changes after EGF-induced EMT was not observable. The presence of increased spindle-shape and the lack of cell-cell adhesion were still evident even after EGF^{high} co-treatment with 22E6. E-cadherin mRNA expressions were not altered following EGF^{high} treatment combined with IgG as control or 22E6, compared with the serum-free treated control group (**Fig 31B**). The expression of EMT markers N-cadherin, TWIST1, and vimentin, were significantly enhanced in both EGF^{high} treatment combined with IgG as control or 22E6 antibody, suggesting CD73 may not serve as a regulator in EGFR-mediated EMT in HNSCC.

A



B

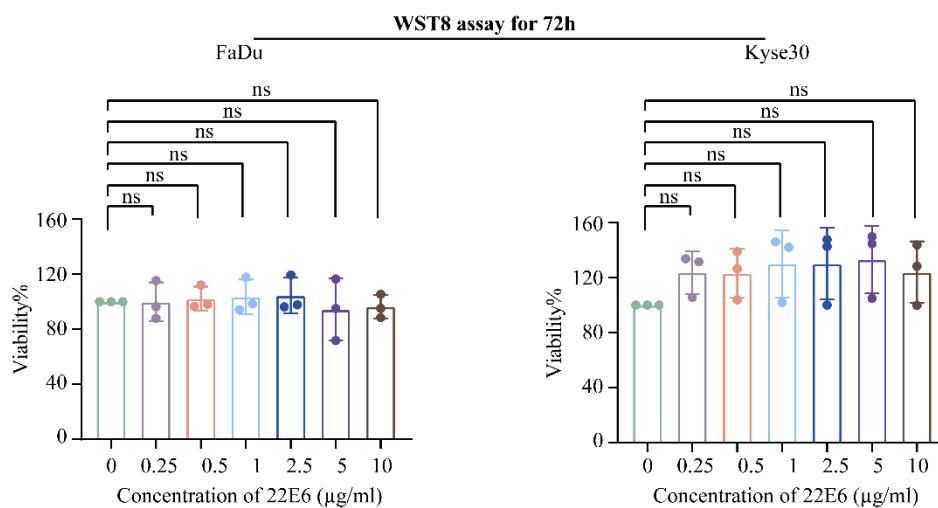


Figure 30 WST8 assay for 22E6 treatment in FaDu and Kyse30 cells

Cell viability was assessed in FaDu and Kyse30 cells treated with different concentration of 22E6 antibody (range from 0 to 10 µg/mL) for 24 h (A) and 72 h (B). Data shown represent means with SD from $n = 3$ independent experiments. Ns: not significant (One-way ANOVA)

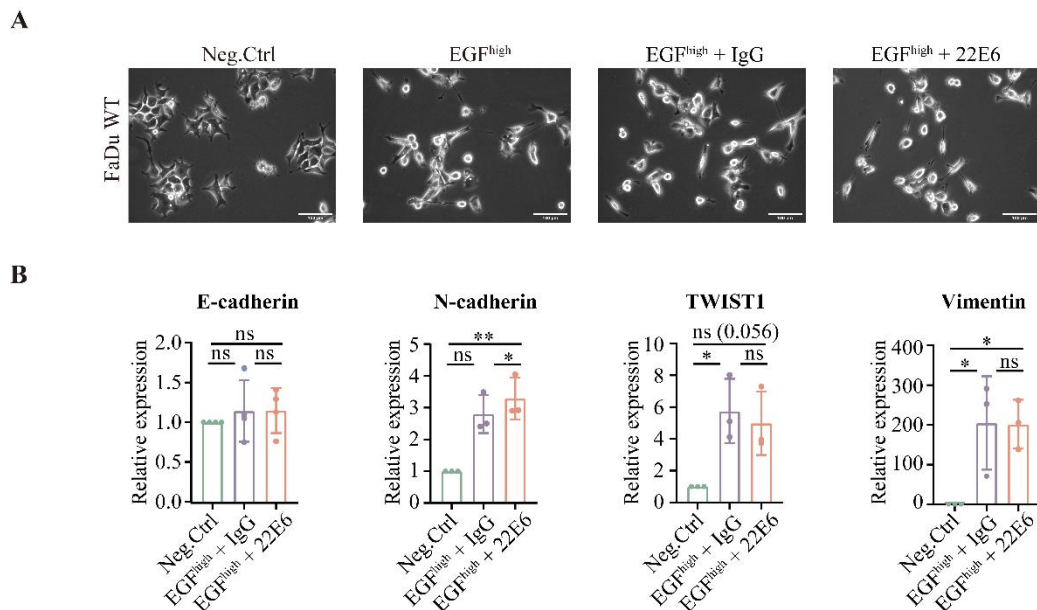


Figure 31 CD73 blocking impacted on EGFR-EMT induction

(A) Microscopic images illustrating the morphology of FaDu cells subjected to the indicated treatments including serum-free medium (Neg.Ctrl), EGF^{high} , EGF^{high} co-treated with either IgG or CD73-antagonizing antibody 22E6. (B) Quantitative RT-PCR (qRT-PCR) analysis of expression of E-cadherin, N-cadherin, TWIST1 and Vimentin in FaDu cell line upon different treatments from $n = 3$ independent experiments. Ns: not significant, * p -value < 0.05 , ** p -value < 0.01 (One-way ANOVA).

3.8.2 Inhibition of CD73 impacts on EGFR-mediated 2D migration and invasion

To investigate the functional role of CD73 in EGFR-mediated migration and invasion, 2D migration and invasion assay in a Boyden chamber system were performed and antagonizing CD73 antibody 22E6 was applied to inhibit the enzymatic activity of CD73 in FaDu and Kyse30 cells. 2D migration and invasion assay showed that both functions were induced by EGF^{high} treatment in both FaDu and Kyse30 cells, which were suppressed by co-treatment of EGF^{high} and Cetuximab. Compared with EGF^{high} combined with isotype control antibody treatment, treatment with the 22E6 antibody at a concentration of 5 μ g/mL suppressed EGFR-mediated migration and invasion (**Fig 32A-B**). The quantification of migrated cells and invasive cells confirmed a significant induction of EGFR-mediated migration and invasion in FaDu and Kyse30 cells. Moreover, Cetuximab and 22E6 antibody treatment reduced EGFR-mediated migration by 75% and 68.4% in FaDu cells, and by 64.5% and 43% in Kyse30, respectively (**Fig 32C**). Hence, blocking the enzymatic

activity of CD73 by 22E6 antibody can significantly suppress EGFR-mediated 2D migration and invasion in HNSCC cells.

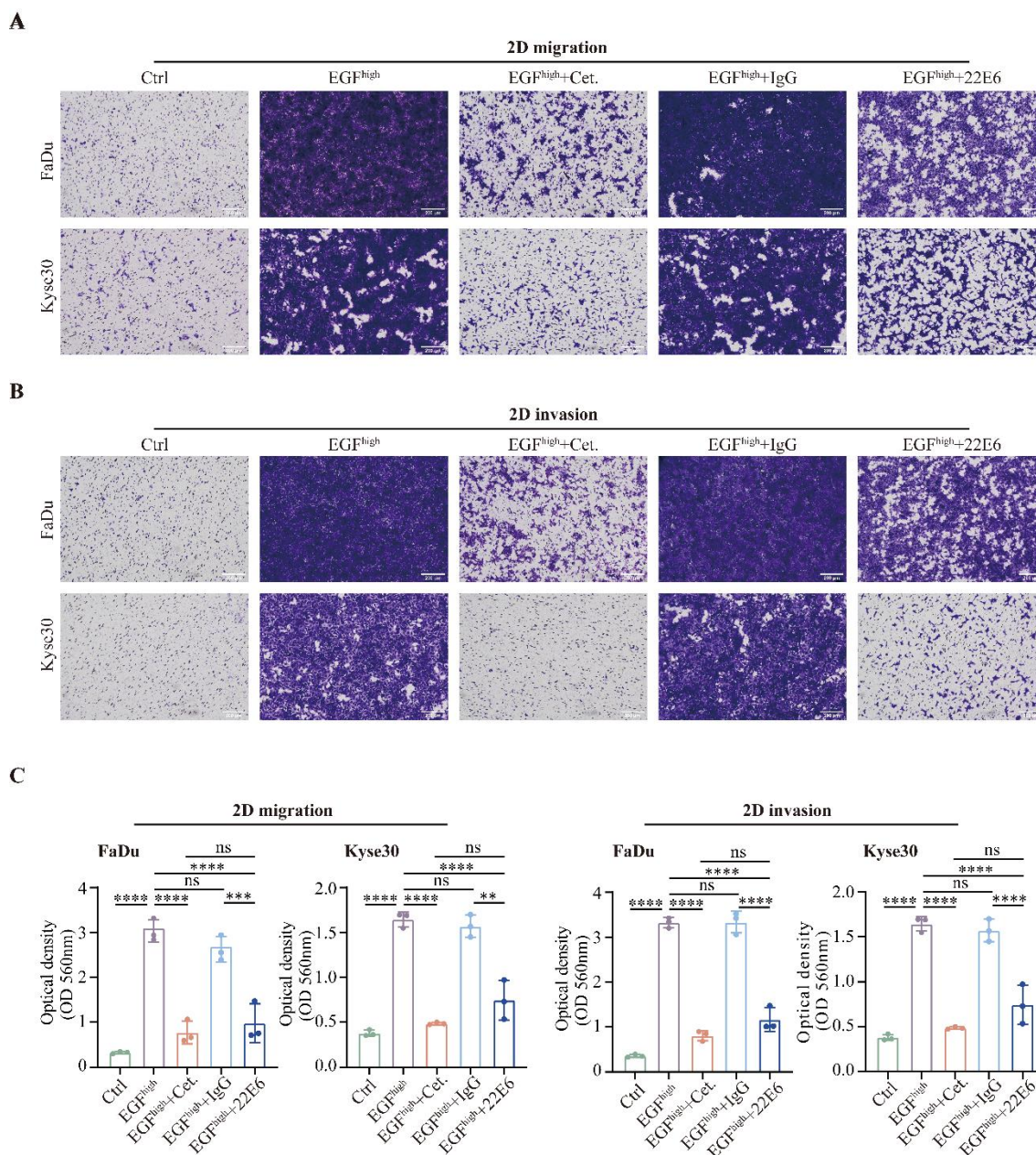


Figure 32 Functional role of CD73 in EGFR-mediated 2D migration and invasion in HNSCC

(A-B) Representative images of transwell experiments for FaDu and Kyse30 that remained untreated (Ctrl), or were treated with EGF^{high} , EGF^{high} co-treated with either Cetuximab, IgG as isotype control or antagonizing CD73 antibody 22E6. (C) The optical density (OD) of migrated and invaded stained FaDu and Kyse30 cells in different treatment conditions was measured from $n = 3$ independent experiments. Shown are mean values with SD. Ns: not significant, $* < 0.05$, $**** p\text{-value} < 0.0001$ (One-way ANOVA).

3.8.3 Blocking CD73 represses EGFR-mediated local invasion

To better understand effects of blocking CD73 in EGFR-mediated local invasion, a 3D spheroid model in Matrigel was further performed with FaDu cells. FaDu cell spheroids were embedded in Matrigel and subjected to high-dose of EGF or combined with either Cetuximab or 22E6 antibody. Local invasion into Matrigel was strongly induced in EGF^{high} treatment, which was suppressed by co-treatment with Cetuximab, confirming the specificity for EGFR activation. Moreover, compared with EGF^{high} combined with isotype control IgG treatment, 22E6 antibody treatment showed a strong inhibitory effect on EGFR-mediated local invasion (**Fig 33A**). The quantification of invasive area and invasive distance (**Fig 33B**) showed that EGF^{high} promoted a significant induction of the invasive area and invasion distance. Co-treatment with Cetuximab suppressed 95% of the invasive area and 61.4% of the invasive distance. Antagonizing CD73 by 22E6 antibody also blocked invasive area by 52.3% and invasive distance by 27.9% in EGFR-mediated local invasion.

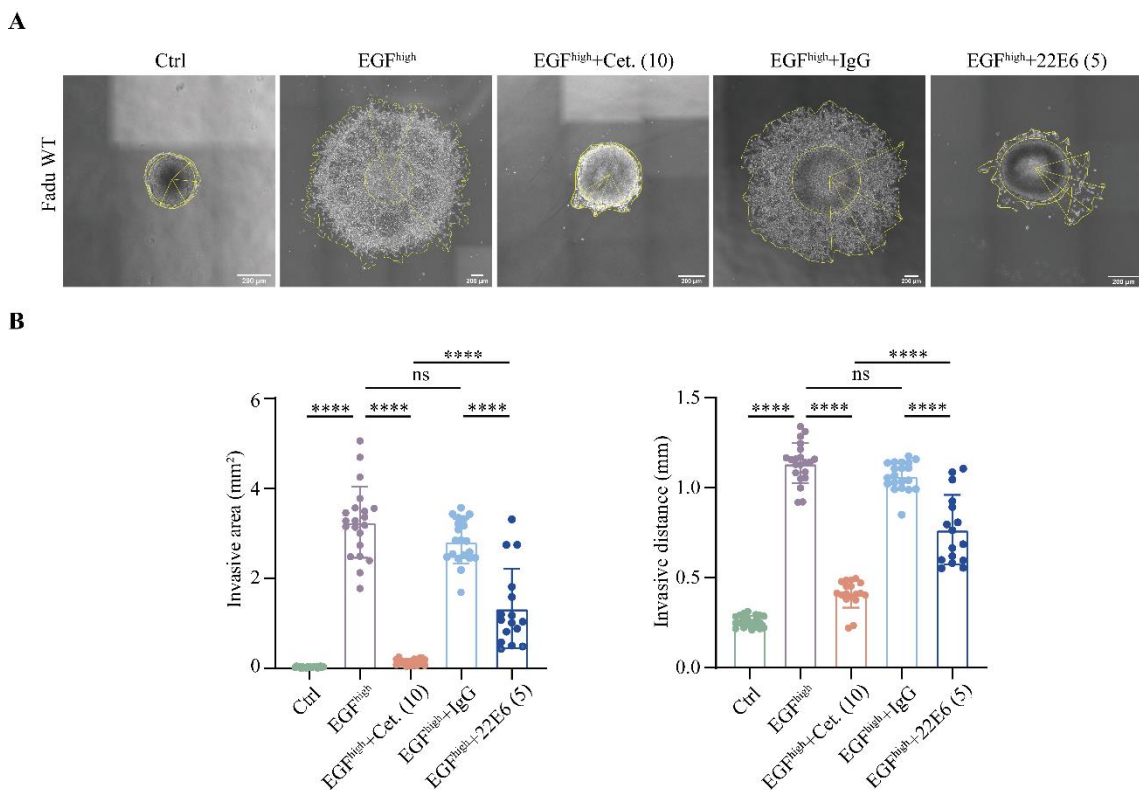


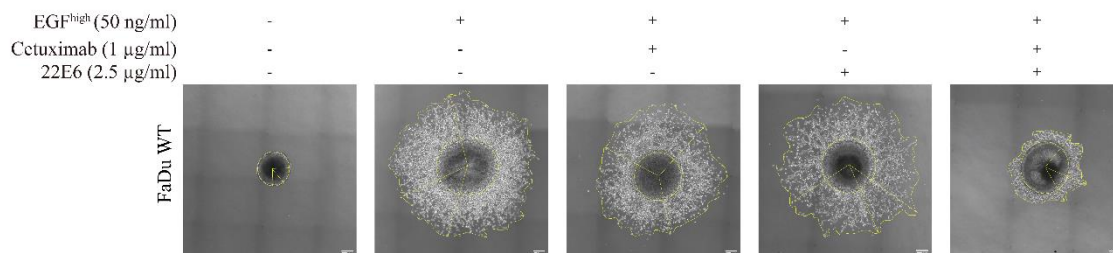
Figure 33 Antagonizing CD73 suppresses EGFR-mediated 3D invasion in HNSCC cell

(A) Representative images of 3D FaDu spheroid model in Matrigel either untreated (Ctrl), or treated with EGF^{high}, EGF^{high} with Cetuximab, and combinations of EGF^{high} and either IgG as isotype control or antagonizing CD73 antibody 22E6 (B) Quantification

*of the invasive area and invasive distance from (A) (n = 3 independent experiments). Shown are mean values with SD. Ns: not significant, **** p-value < 0.0001 (One-way ANOVA).*

Next, combinations of low-dose of cetuximab and 22E6 were further assessed in the suppression of EGFR-mediated local invasion. Treatment with 1 µg/mL cetuximab or 2.5 µg/mL 22E6 individually in spheroids were ineffective regarding EGFR-mediated local invasion, whereas co-treatment of Cetuximab and 22E6 antibody at low concentrations significantly inhibited invasive area by 80.6% and invasive distance by 46% (**Fig 34A-B**). This observation led us to delve deeper into investigating the effective IC₅₀ value of Cetuximab in combination with 22E6 in suppressing local invasion mediated by EGFR activation. Spheroids were embedded in Matrigel and treated with EGF^{high} treatment as positive control, EGF^{high} combined with Cetuximab in a concentration range of 0.5 to 10 µg/mL, either alone or combined with 22E6 antibody at a non-effective concentration of 2.5 µg/mL (**Fig 35A**). It was observed that Cetuximab at concentrations below 2.5 µg/mL did not substantially inhibit EGFR-mediated local invasion, whereas inhibitory effects started at a concentration of 2.5 µg/mL and achieved maximum suppression at 10 µg/mL (**Fig 35B**). However, co-treatment with 22E6 antibody efficiently blocked invasive area starting at the lowest concentration of Cetuximab at 0.5 µg/mL. Calculation of functional IC₅₀ of Cetuximab showed that co-treatment with 22E6 antibody decreased the functional IC₅₀ from 3.0 µg/mL to 0.71 µg/mL (**Fig 35C**). Thus, blocking CD73 represses EGFR-EMT-mediated local invasion and co-treatment of Cetuximab and 22E6 antibody has combinatorial effects on inhibition of it in HNSCC.

A



B

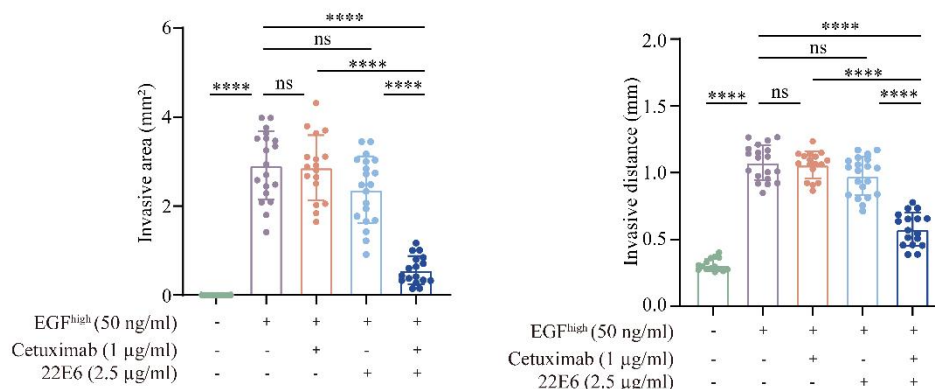


Figure 34 Co-treatment of low-dose of cetuximab and 22E6 impacts on EGFR-mediated local invasion

(A) Representative images of 3D FaDu spheroid model in Matrigel either untreated (Ctrl), or treated with EGF^{high} (9 nM), EGF^{high} co-treated with either cetuximab (1 μg/mL) or 22E6 (2.5 μg/mL) individually, and EGF^{high} co-treated with both cetuximab and 22E6. (B) Quantification of the invasive area and invasive distance from $n = 3$ independent experiments. Shown are mean values with SD. Ns: not significant, **** p -value < 0.0001 (One-way ANOVA).

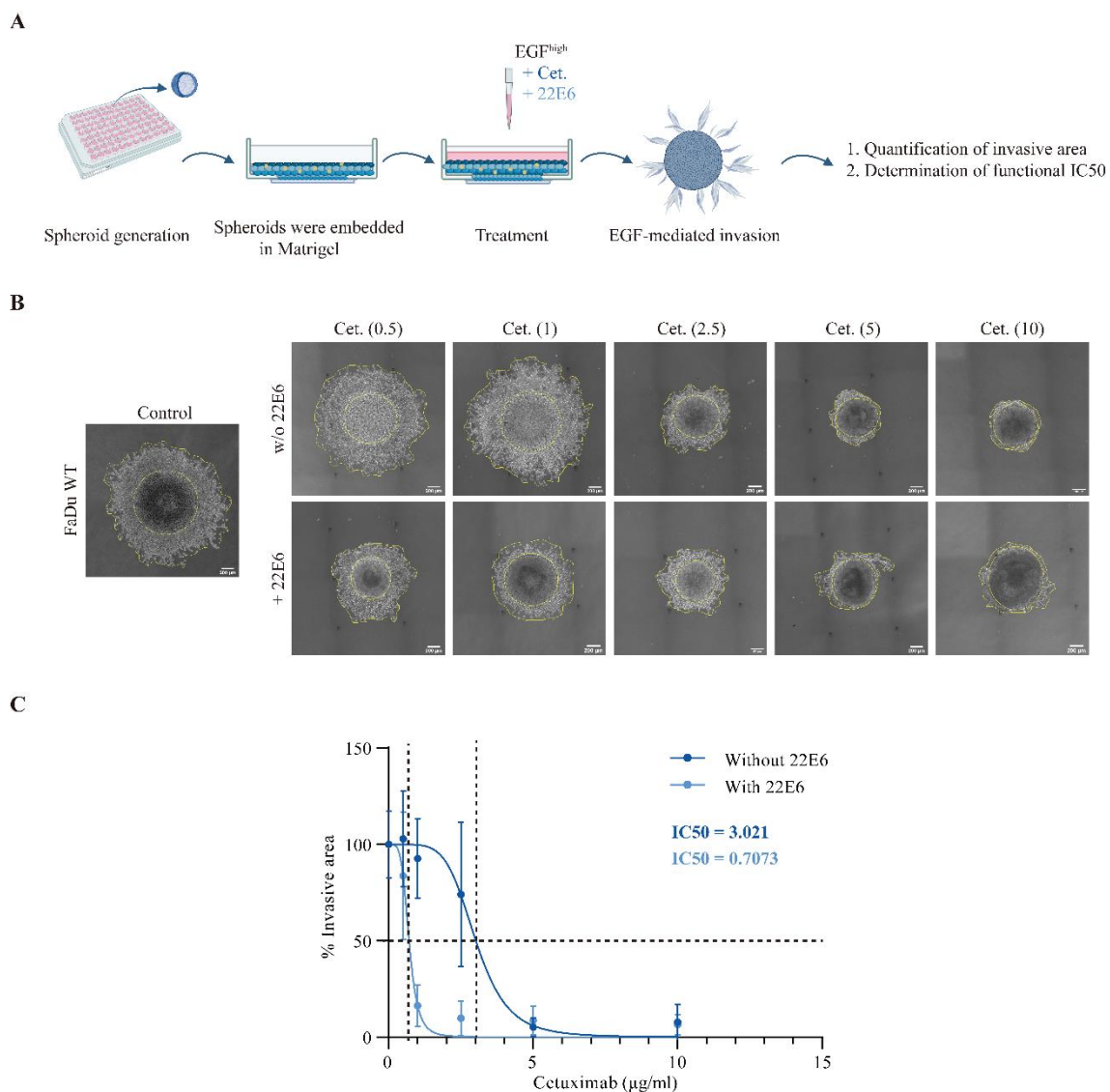


Figure 35 Assessment of functional IC₅₀ values of Cetuximab in the absence and presence of 22E6

(A) Flow chart of the experimental procedure to assess functional IC₅₀ values of Cetuximab in the absence and presence of 22E6 antibody. (B) Representative images of 3D spheroid model in Matrigel of FaDu cells treated with EGF^{high} alone, or EGF^{high} combined with Cetuximab varying from 0.5 to 10 µg/mL, either alone or alongside the 22E6 antibody at a non-effective concentration of 2.5 µg/mL. (C) Dose-response curve of EGFR-mediated invasion area as a function of cetuximab concentration with or without supplementary 22E6 antibody. Functional IC₅₀ values for the inhibition of EGFR-mediated invasion by cetuximab are shown as the mean values with SD from a total of three independent experiments ($n = 3$).

3.9 CD73 serves an effector of EGFR-mediated EMT

Based on all observations, we hypothesize that CD73 may serve as either an effector or a regulator of EGFR-mediated EMT in HNSCC. Activation of EGF-EGFR signaling could potentially stimulate the transcription of *CD73*, potentially playing a crucial role in enhancing proliferation and metabolism and/or inducing EGFR-EMT program. In addition, CD73 might also serve as a gene target for EGFR-EMT and may represent an effector of local invasion in HNSCC.

3.9.1 Proliferation-independent effect of CD73 inhibition on EGFR-mediated local invasion

To explore if CD73 may be a proliferation/metabolism regulator in EGFR-mediated EMT, FaDu cells were subjected to mitomycin C (MMC) in a 3D spheroid model. IC₅₀ of MMC treatment for 24 h, 48 h and 72 h were initially measured in FaDu cells and IC₅₀ at 72 h (0.02 µg/mL) was defined as the final working concentration of MMC treatment in 3D spheroids (**Fig 36A-B**). It showed that administering MMC caused a reduction in both cell survival and the extent of EGFR-mediated local invasion (**Fig 36C**). However, blocking CD73 activity with 22E6 still significantly suppressed EGFR-mediated local invasion by 72%, which implied that the effect of CD73 inhibition on EGFR-mediated local invasion is proliferation-independent in HNSCC.

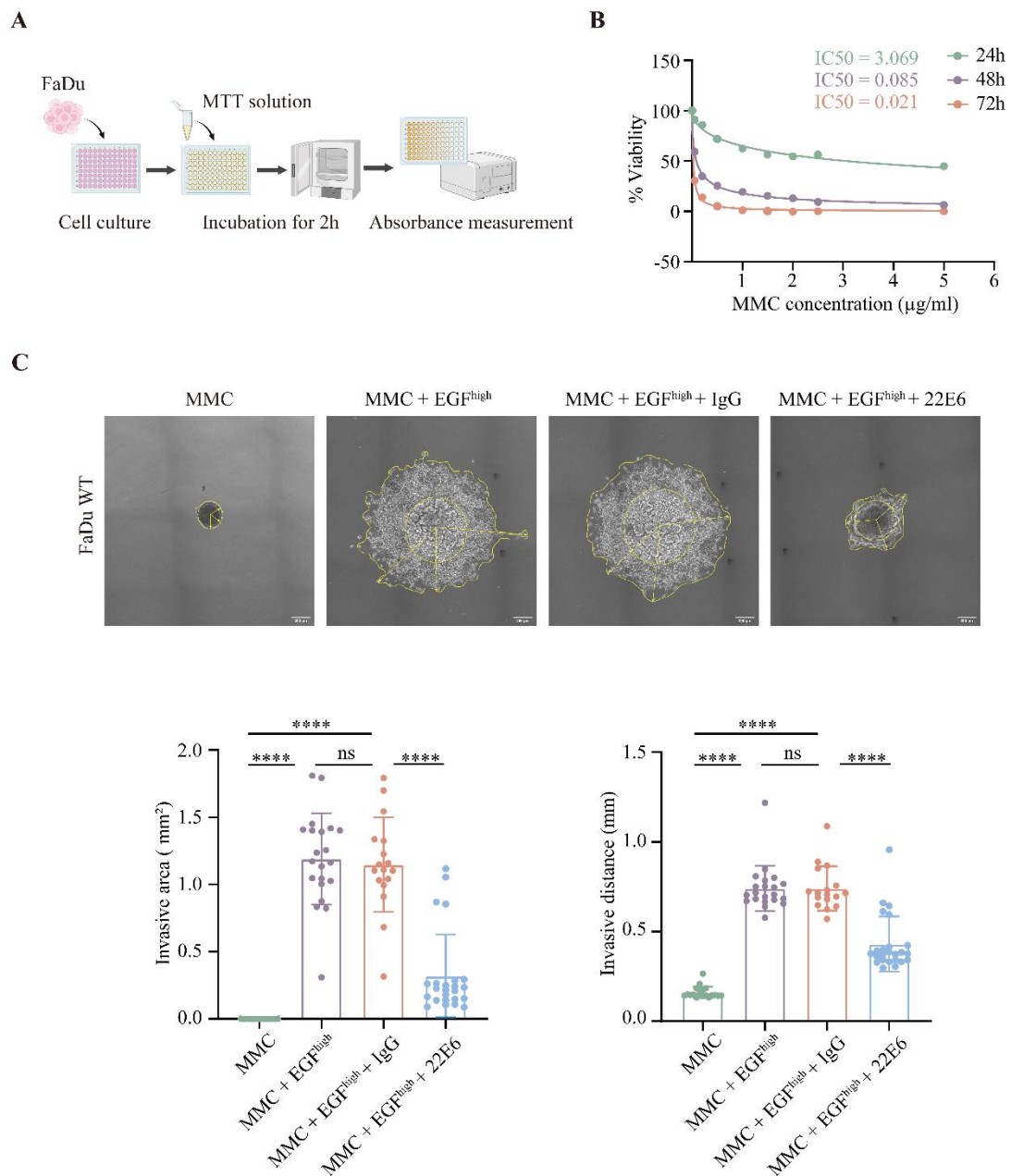


Figure 36 Proliferation-independent effects of CD73 inhibition on EGFR-mediated local invasion

(A) Flow chart illustrating the experimental procedure for examining the impact of various mitomycin C (MMC) concentrations on FaDu cell proliferation. (B) Determination of the IC₅₀ values of MMC on FaDu cell proliferation at different treatment timepoints. (C) Representative images of 3D spheroid model in Matrigel for FaDu treated with MMC (0.02 µg/mL) alone or combined with indicated compounds including high-dose of EGF (9 nM), IgG (5 µg/mL), or antagonizing CD73 antibody 22E6 (5 µg/mL) (upper panel). Quantification of the invasive area and invasive distance was presented as mean values with SD from a total of three independent experiments ($n = 3$) (lower panel). Ns: not significant, **** p -value < 0.0001 (One-way ANOVA).

3.9.2 Functional characterization of CD73 on EGFR-EMT-mediated local invasion

Since CD73 blockade significantly repressed EGFR-mediated local invasion in HNSCC cells, further research was conducted to understand how CD73 specifically influences local invasion. Firstly, loss- and gain-of-function of *CD73* in FaDu cells were performed upon stable transfection. *CD73* was knocked down by 98.5% in FaDu (CD73-KD) using specific shRNA encoding plasmids (**Fig 37A**) and was successfully re-gained (KD-OE) upon transfection with a CD73 expression plasmid in CD73-KD cells (**Fig 37B**). CD73 was further over-expressed in FaDu WT cells by transfection with a CD73 expression plasmid and CD73 expression was enhanced 13.4-fold when compared to cells that were transfected with a control vector (**Fig 37C**).

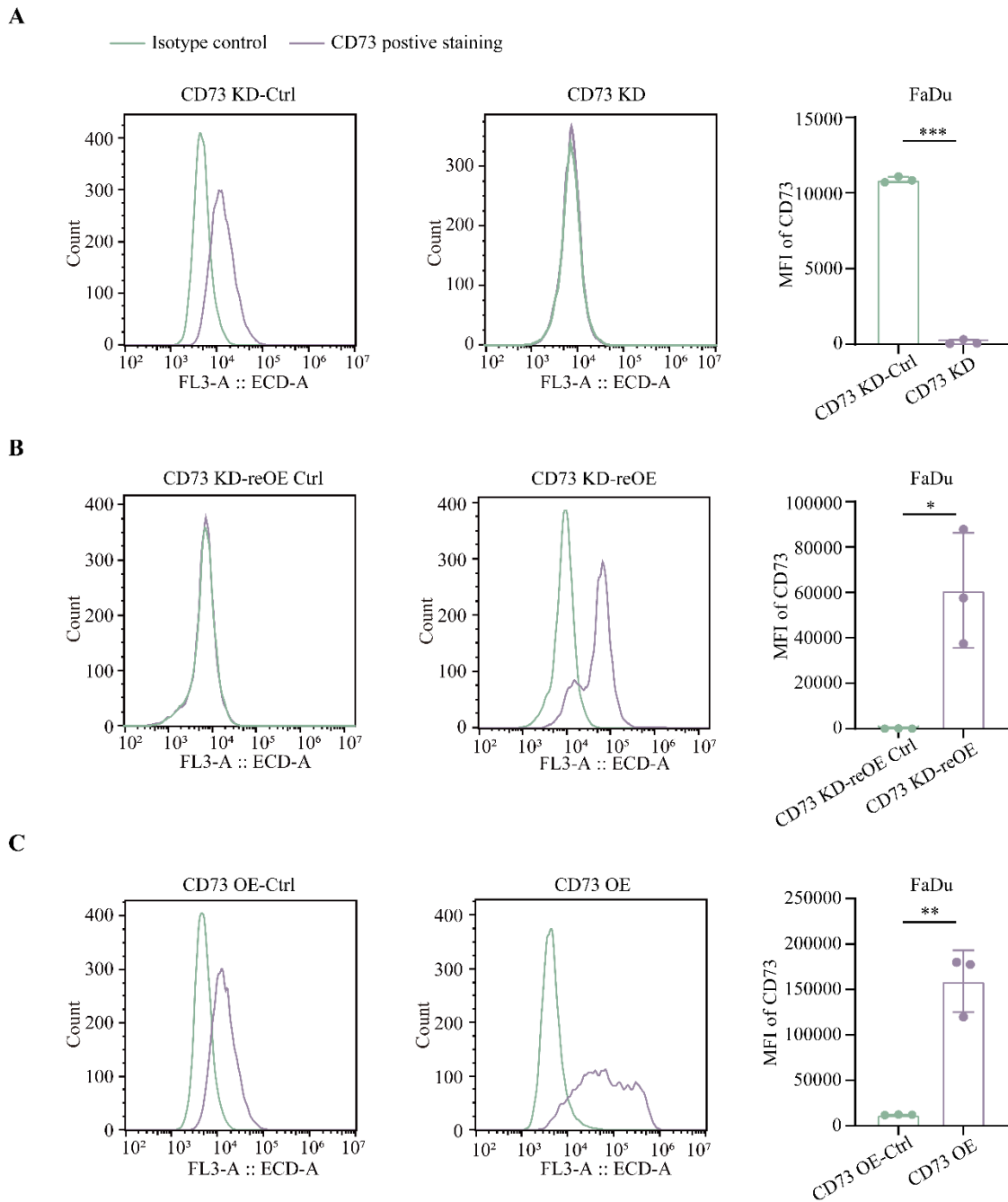
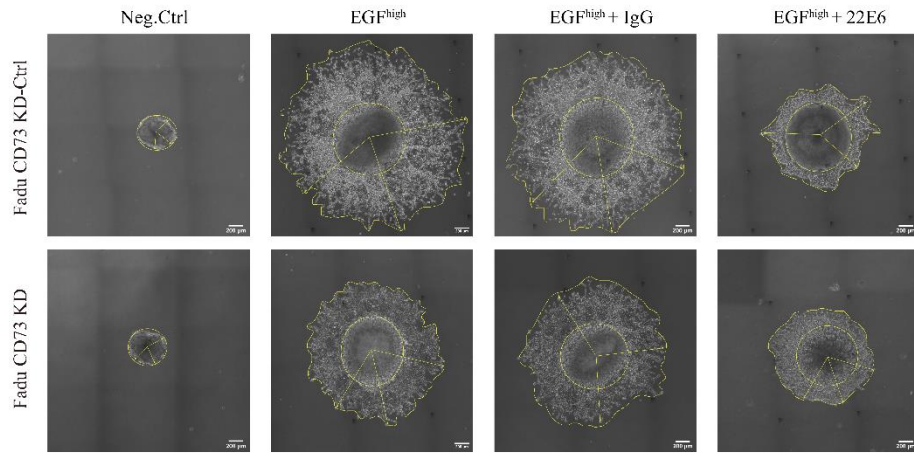


Figure 37 CD73 knockdown and overexpression in FaDu cells

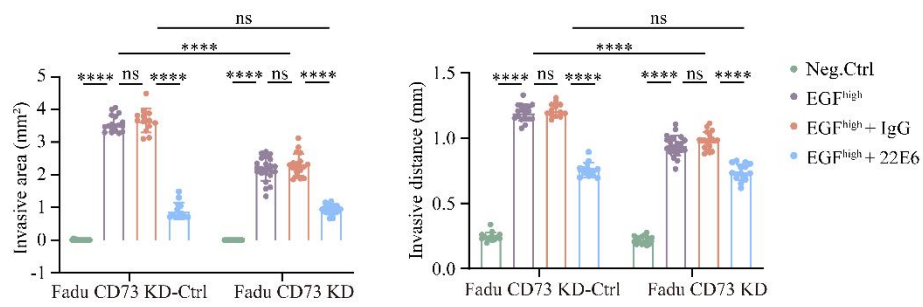
Flow cytometry was conducted to assess the CD73 expression at cell surface in (A) FaDu CD73 control (CD73 KD-Ctrl) and knock-down (CD73 KD) cells; (B) FaDu CD73 knock-down control (CD73 KD-reOE Ctrl) and re-gain in knock-down (CD73 KD-reOE) cells. (C) FaDu CD73 control (CD73 OE-Ctrl) and CD73 over-expression (CD73 OE) cells. Mean fluorescence intensity (MFI) of CD73 was measured and presented with SD from $n=3$ independent experiments. * p -value < 0.05 , ** p -value < 0.01 , *** p -value < 0.001 (t -test).

In a 3D spheroid model in Matrigel, EGFR-mediated local invasion of FaDu CD73-KD cells was significantly decreased compared with control cells, confirming a role of CD73 in this process. In FaDu control cells and CD73-KD cells, blocking CD73 upon 22E6 treatment showed comparable inhibitory effects on EGFR-mediated local invasion (**Fig 38A-B**). It was further observed that under EGF^{high} treatment, CD73 expression on the surface of FaDu CD73-KD cells was re-expressed at a level like that of FaDu control cells under serum-free treatment (**Fig 38C-D**). Hence, EGF-EGFR activation partially rescued the effect of knock-down of CD73 expression, providing a target molecule for CD73 blockade. These findings indicated that 22E6 continued to maintain its inhibitory impact on EGFR-mediated local invasion in FaDu CD73-KD cells. In addition, EGFR-mediated local invasion was mildly promoted by overexpression of CD73 in FaDu (CD73-OE) compared with FaDu Ctrl cells (**Fig 39A**). Restoration of CD73 in FaDu CD73-KD cells further rescued EGFR-mediated local invasion to the level of FaDu WT cells (**Fig 39B**). In summary, we can conclude that CD73 serves as an active effector of EGFR-EMT-mediated local invasion, instead of serving as a regulator of EGFR-mediated EMT.

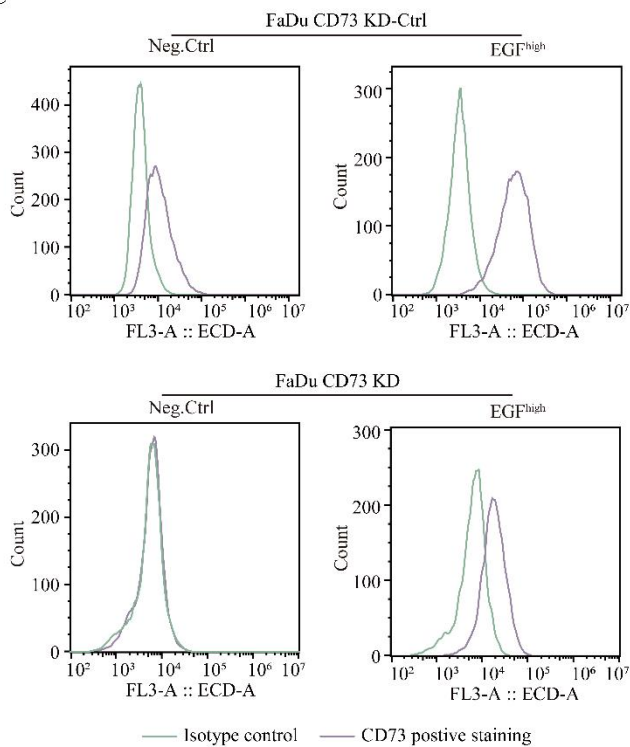
A



B



C



D

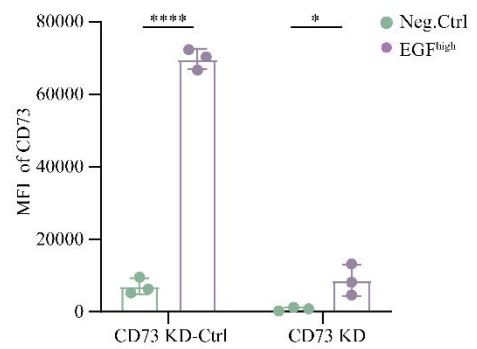


Figure 38 CD73 knock-down inhibits EGFR-mediated 3D invasion in HNSCC cells

(A) Spheroids of FaDu control (CD73 KD-Ctrl) and CD73 knock-down (CD73 KD) were embedded in Matrigel and subjected to various treatment in serum-free condition for 72h: EGF (50 ng/mL), IgG antibody (5 μ g/mL), antagonizing anti-CD73 monoclonal antibody 22E6 (5 μ g/mL). Yellow outlines and arrow lines are used to quantify the invasive area and invasive distance. (B) Quantification of the invasive area and invasive distance from (A) in $n=3$ independent experiments. Shown are mean values with SD. Ns: not significant, **** p -value < 0.0001 (Two-way ANOVA). (C-D) CD73 expression was analyzed by flow cytometry using specific antibodies (CD73) or isotype control antibody (iso) in control (CD73 KD-Ctrl) and CD73 knockdown (CD73 KD) FaDu cells. Cells were cultured under serum-free conditions (Neg.Ctrl) and kept untreated or further treated with EGF^{high} (9 nM). Displayed are typical histograms for each cell line, illustrating both isotype control and positive staining for CD73. Standardized MFI of CD73 staining at cell surface are shown as means with SD from $n = 3$ independent experiments. * $p < 0.05$, **** $p < 0.0001$, (Two-way ANOVA).

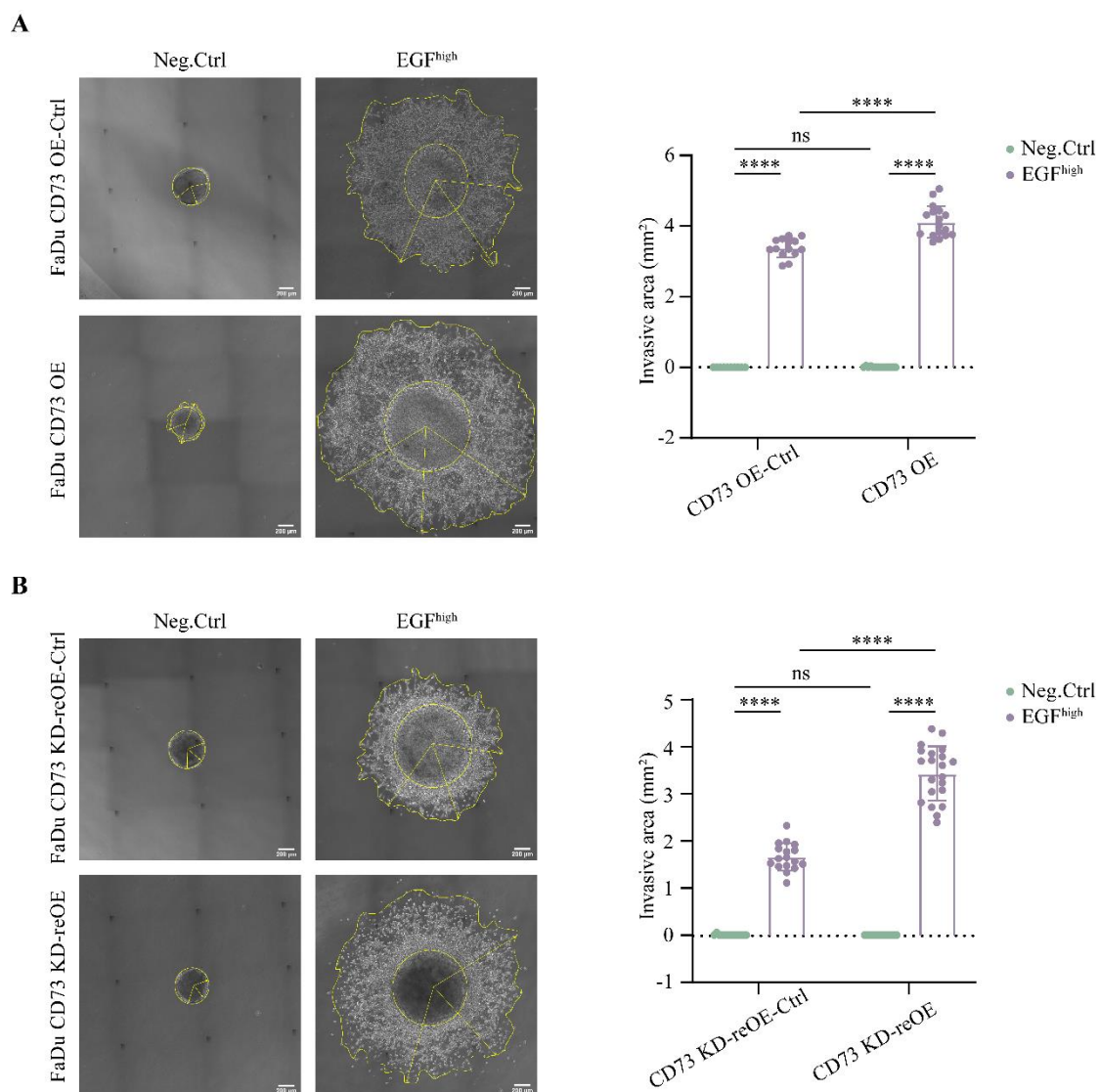


Figure 39 *CD73 over-expression promotes EGFR-mediated 3D invasion in HNSCC cell*

Representative images of a 3D spheroid model in Matrigel of (A) FaDu CD73 OE-Ctrl and CD73 OE cells and (B) FaDu CD73 KD-reOE Ctrl and CD73 KD-reOE cells upon treatments of serum-free medium (Neg.Ctrl) and EGF^{high} (9 nM) for 72 h (left panel). Quantification of the invasive area of the previously described treatment groups was measured from $n=3$ independent experiments (right panel). Shown are mean values with SD. Ns: not significant, **** p -value < 0.0001 (Two-way ANOVA).

3.10 CD73 is highly expressed in budding cells in HNSCC

According to the assessment of the role of CD73 in EGFR-EMT-mediated local invasion in vitro, we proceeded to analyze the expression of CD73 in paired normal mucosa and

tumor samples obtained from patients with HPV-negative HNSCC in LMU cohort (n=20). The demographics of 10 patients each from the non-budding and budding HNSCC groups are displayed in **Table 3**. Statistical analysis showed that there were no significant variations in tumor sizes or pathological/clinical parameters between non-budding and budding samples, mitigating any potential influence of these parameters on budding. **Fig 40 A** illustrates representative IHC staining of CD73 in paired normal mucosa and HNSCC tumor tissues with non-budding and budding at 100× and 200× magnifications, respectively. In the quantification of CD73 IHC staining, tumor samples exhibited notably higher CD73 expression, showing a mean value of 60.53, in contrast to 13.19 observed in normal mucosal tissue (**Fig 40B**). In the comparison of CD73 expression between non-budding and budding HNSCC, we observed a 8.10-fold stronger expression of CD73 in budding than in non-budding tumors (**Fig 40C**). Consequently, there was a strong correlation between CD73 expression and tumor budding in HNSCC samples, with budding cells displaying strong CD73 expression. Moreover, overall survival (OS) analysis showed no significant association with *CD73* expression in HPV-negative HNSCC patients in TCGA and GSE65858 cohorts. Only in the cohort of oral carcinomas from the Fred Hutchinson Cancer Research Center (FHCRC), strong *CD73* expression was significantly linked with poorer OS in patients.

Table 3. Clinical parameters budding-negative and budding positive HNSCC

Clinical parameters	Budding (n=10)	Non-budding (n=10)	p-value
Gender			
Female	2	3	1
Male	8	7	
Adjuvant treatment			
Yes	8	6	0.476
No	2	3	
Unknown	0	1	
T-stage			
T1	1	2	0.761
T2	3	3	
T3	5	3	
T4a	1	2	
N-stage			
N0	3	0	0.267
N1	2	2	

N2	3	3	
N3	2	3	
Nx	0	2	
N-Status			
N+	7	8	0.356
N-	3	1	
Unknown	0	1	
Localization			
Hypopharynx	1	1	0.145
Oral	3	1	
Oropharynx	6	4	
larynx	0	4	
Grading			
G2	2	0	0.217
G3	8	9	
Unknown	0	1	
Lymphovascular			
Yes	4	5	1
No	6	5	
Angioinvasion			
No			1
Perineural invasion			
Yes			0.143
No	5	1	
ENE			
ENE+			0.584
ENE-	3	3	
Unknown	6	7	
Smoking status			
Current			0.301
Former	4	6	
Never	6	3	
CD73_Tumor			
High (score >17.5)			0.002
Low (score ≤17.5)	9	1	
	1	9	

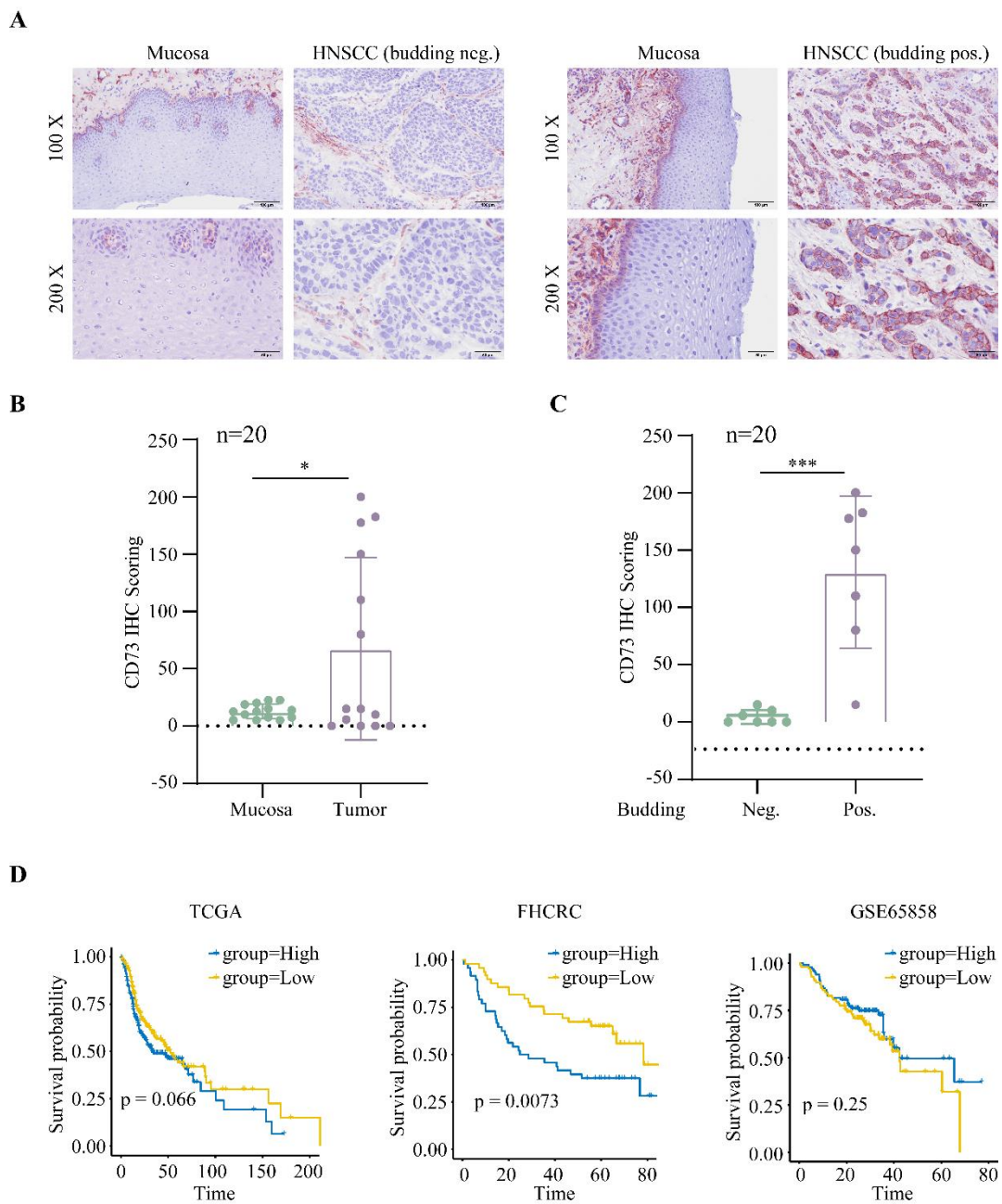


Figure 40 CD73 is associated with budding in HNSCC

(A) Representative IHC staining images of CD73 in both normal mucosa and HNSCC from tumors classified as budding-negative and budding-positive, presented at two different magnifications. (B) Quantification of CD73 IHC scores in a set of 20 paired samples, comprising normal mucosa and primary HNSCC (left), and in budding-negative and budding-positive HNSCC, with each group consisting of 10 samples. Shown as mean value with SD. (D) Overall survival analysis of CD73 expression in TCGA, FHCRC and GSE65858 cohorts. * p -value < 0.05, *** p -value < 0.001 (t-test).

3.11 CD73 expression as a predictive marker of Cetuximab response

EGFR_EMT_signature genes functionally involved in tumor progression may further serve as surrogate markers for patient responses to Cetuximab treatment in HNSCC. Given that *CD73* is such a functional differentially expressed gene (DEG) in the EGFR_EMT_signature, we hypothesized that *CD73* expression might predict cetuximab response in HNSCC patients. In a cooperative work with Zhengquan Wu, *CD73* expression was assessed using the GSE84713 data set containing gene expression data from 28 HNSCC patient-derived xenografts, with 26 out of 28 being HPV-negative and dependent on Cetuximab treatment. In this dataset, 28 PDX were clustered into Cetuximab non-responder and responder groups according to the measurement of tumor volume after Cetuximab therapy. When compared with Cetuximab non-responder group, PDX in the Cetuximab responder group had a significantly increased *CD73* expression. The area under the ROC curve (AUC) for specificity and sensitivity of *CD73* expression in distinguishing Cetuximab responder from non-responder patients had a value of 0.734 (**Fig 41A**).

Secondly, analysis of *CD73* expression was conducted using the GSE65021 dataset, which includes information from 40 patients with advanced recurrent/metastatic HNSCC (R/M-HNSCC), each treated with a regimen based on Cetuximab therapy. Based on therapy response, 14 patients with a long progression-free survival (PFS) of more than 19 months (long PFS) and 26 patients with a short PFS of less than three months (short PFS) were selected. Patients with long PFS exhibited notably stronger expression of *CD73* compared to those with short PFS. The AUC (area under the curve) value for discriminating patients with long PFS to short PFS was 0.810 (**Fig 41B**). A multivariate linear regression model was employed, incorporating *CD73* expression and clinical factors such as age, gender, tumor grade/stage, and radiotherapy, to calculate the odds ratio for predicting patients belonging to the short or long PFS group. This analysis revealed that patients with low *CD73* expression had significantly higher risk of shortened PFS, whereas all other clinical parameters were not significantly correlated with PFS prediction (**Fig 41C**). Therefore, *CD73* is a promising candidate predictor of Cetuximab response in HNSCC.

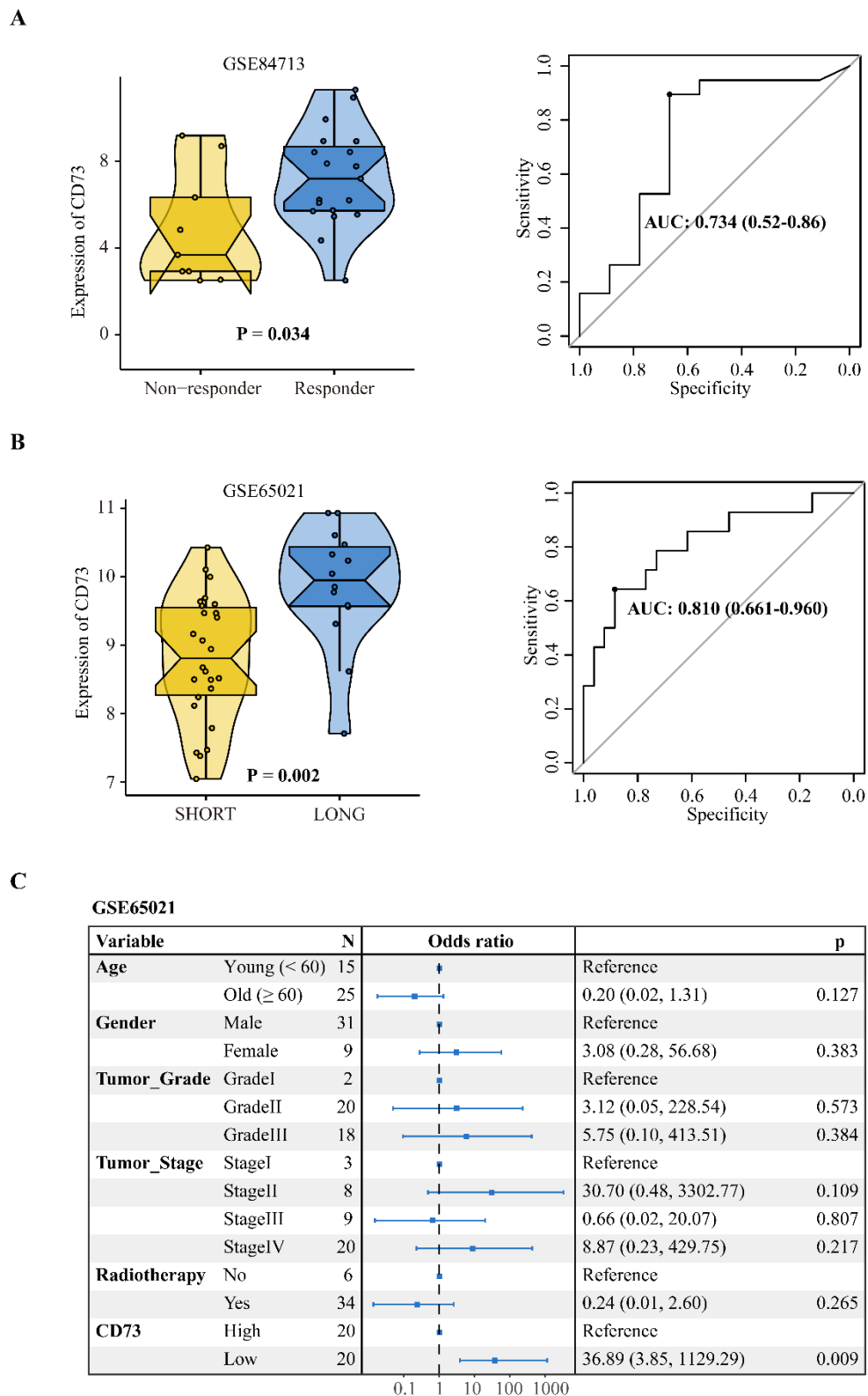


Figure 41 CD73 expression as predictive biomarker of Cetuximab response in HNSCC

(A) The analysis of CD73 mRNA expression in PDX models of HNSCC from the GSE84713 dataset, which are either non-responsive or responsive to Cetuximab, is presented in violin plots featuring individual data points and median values (left panel). Re-

ceiver operating characteristics of CD73 expression to differentiate Cetuximab non-responders from responder patients xenotransplantation (PDX) models (right panel). (B) CD73 mRNA expression in patients with short PFS (< 3 months) and long PFS (> 19 months) is displayed in the GSE65021 dataset as violin plot, including individual data points and median values (left panel). Analysis of receiver operating characteristics to evaluate the specificity and sensitivity of CD73 expression in distinguishing between short and long PFS is shown (right panel). (C) A multivariate linear regression model incorporating CD73 expression and clinical parameters such as age, gender, tumor grade, tumor stage, and radiotherapy was used to analyze the odds ratio for predicting short versus long PFS. The Forest plot includes all variables, encompassing each reference, odds ratio, number of patients (N), 95% confidence interval (CI), and p-value, with CD73 being categorized based on median expression.

4. Discussion

HNSCC are highly malignant tumors, frequently exhibiting advanced stages entailed by recurrences and metastasis, and therefore HNSCC continue to be a significant unresolved challenge in clinical treatment (Johnson et al., 2020). Genomic and transcriptomic analyses based on tumor bulk or single cancer cells in HNSCC have yielded insightful data regarding inter- and intra-tumor heterogeneity (Cancer Genome Atlas., 2015; Stransky et al., 2011). EMT serves as a principal contributor to tumor heterogeneity and is associated with the initiation, progression, metastasis, and therapeutic resistance in HNSCC (Puram et al., 2017, 2018, 2023; Schinke et al., 2022). Tumor cells located at the tumor-stroma interface are more susceptible to be induced into pEMT or EMT due to interactions with CAFs in the TME and could potentially detach from the tumor mass to generate tumor buds as a source of local invasion, recurrences, and therapeutic resistance. In HNSCC, EGFR signaling pathway activation plays a central role in the regulation of EMT, tumor progression and metastasis formation. Since EGFR targeting monoclonal antibody Cetuximab is approved for treating advanced and recurrent HNSCC, investigating the relationship between EGFR-mediated EMT and tumor progression becomes particularly interesting.

Our group conducted a transcriptomic mapping associated with EGFR-mediated EMT in HNSCC and identified an EGFR-mediated EMT signature (n=171), which characterized molecular alterations in cell-cell adhesion, cell-matrix interaction, and the development of tumor leading edges. These changes are typical hallmarks of EMT and are correlated with enhanced migration, invasion, and treatment resistance. EGFR-mediated EMT described by our group also presented a similar yet not identical ability of defining cells in an EMT state to MSigDB EMT hallmark and the pEMT gene signature in HNSCC. Interestingly, among these 171 genes, only a few genes (**Table 1**) are overlapped with the EMT hallmark and pEMT gene signatures, suggesting that EGFR-mediated EMT constitutes a unique meta-framework of EMT in HNSCC (Schinke et al., 2022). However, the molecular mechanism of EGFR-mediated EMT and invasion in HNSCC remains insufficiently understood and exploring potential therapeutic targets and biomarkers for predicting response to EGFR-targeted therapy is in great demand.

4.1 Functional characterization of ITG β 4 and CD73 in EGFR-mediated EMT in HNSCC

4.1.1 ITG β 4 binding to laminin 5 promotes EGFR-mediated local invasion in HNSCC

Our group developed a multivariate Cox proportional hazard regression model, featuring a 5-gene prognostic signature, based on EGFR-mediated EMT signature genes that showed a significant correlation with reduced OS in the TCGA-HNSCC cohort (Schinke et al., 2022). The risk score computed from this identified 5-gene signature was confirmed to be significantly associated with OS in the validation HNSCC cohorts of MDACC and FHCRC. In this thesis, *ITG β 4*, one component of the 5-gene signature, was evaluated for its function in EGFR-mediated local invasion in HNSCC.

ITG β 4 binding to its ligand laminin 5, encoded by the *LAMA3*, *LAMB3* and *LAMC2* genes, is critical for maintenance of the structural integrity of epithelial cells (Gil et al., 1994; Nievers et al., 2000). During tumor progression, ITG β 4 is involved in the regulation of EMT, migration and invasion in some cancers such as gastric cancer, non-small cell lung cancer, and breast cancer (Gan et al., 2018; Vuoriluoto et al., 2011; P. Wu et al., 2019). In the present thesis, ITG β 4 was found to be upregulated at both mRNA and protein levels in HNSCC cells after EGF-induced EMT (**Fig 9,12**), and in primary tumors and lymph node metastasis (**Fig 13**). In line with these findings, it was observed that *ITG β 4* expression was overexpressed in malignant single cells and in primary tumors in TCGA cohort, a finding that was independent of the HPV infection status of the patient (**Fig 14**). In the process of EGFR-mediated EMT, it has been documented that MAPK/ERK pathway is considered as a major driver (Lu et al., 2020; Sheng et al., 2017; Schinke et al., 2022; Pan et al., 2018). Correlation analysis revealed that *ITG β 4* expression was positively associated with EGFR activation and MAPK signaling pathway in both, the HNSCC-TCGA cohort and the scRNA sequencing dataset published by Puram et al. (Pan et al., 2018). A direct induction of *ITG β 4* via the EGF-EGFR-MAPK axis was further corroborated in HNSCC cells in vitro in this thesis (**Fig 17**). Thus, ITG β 4 is a confirmed target of EGFR-mediated EMT in HNSCC.

In previous studies, it has been demonstrated that the overexpression of ITG β 4 is significantly associated with advanced tumor grade and poorer OS, and considered to be a potential prognostic biomarker in pancreatic cancer (Masugi et al., 2015). In in vivo

experiments, ITG β 4 was found to be upregulated in prostate cancer, influencing tumor growth by modifying the local immune environment (Genduso et al., 2023). In TNBC, ITG β 4 activates small GTPase RAC1, confers DNA damage-associated drug resistance, and was significantly correlated with decreased relapse-free OS following chemotherapy (Fang et al., 2023). In HNSCC, we determined that ITG β 4 is a crucial effector of migration and invasion mediated by EGFR activation using loss-of-function approaches in 2D and 3D models (**Fig 19-21**). In addition, blocking ITG β 4 binding to laminin 5 with ASC8 antibody significantly suppressed EGFR-mediated local invasion (**Fig 22-23**), whereas supplement of laminin 5 enhanced EGFR-mediated invasion in HNSCC (**Fig 27**). This suggested that interaction between ITG β 4 and laminin 5 plays a crucial role in the regulation of EGFR-mediated local invasion and ITG β 4 could serve as a potential therapeutic target in HNSCC.

Laminin 5, serving as a ligand for ITG β 4, is an essential part of the basement membrane, a specialized structure within the extracellular matrix that offers structural support to epithelial tissues (Aumailley et al., 2003; Miyazaki, 2006). Under physiological conditions, ITG β 4 binds to laminin 5 to anchor epithelial cells to the basal membrane, maintaining tissue structure and integrity. Moreover, laminin 5 is also involved in cell differentiation and migration through activation of signaling pathways (Kirtonia et al., 2022; B. P. Nguyen et al., 2000; H. Zhang et al., 2019; Yan Zhang et al., 2020). However, the functions of ITG β 4 and laminin 5 in tumor migration and invasion are multifaceted. ITG β 4 interacts with laminin 5 to foster detachment of cancer cells, and facilitating immune evasion and angiogenesis capabilities, contributing to the development of new blood vessels in the TME (Y. Gao et al., 2021; Lin et al., 2007). Hence, laminin 5 can provide a framework for ITG β 4's binding, consequently activating integrin-dependent intracellular signaling and facilitating tumor EMT, migration and invasion.

In our study, we found that together with *ITG β 4*, genes encoding laminin 5 including *LAMA3*, *LAMB3* and *LAMC2* were overexpressed in HNSCC single malignant cells and in primary tumors in the TCGA HNSCC cohort. In parallel, we determined in the transcriptomic analysis that all three laminin 5 genes were upregulated after EGF-induced EMT (**Fig 11**). This suggested a coordinated induction of the ITG β 4-laminin 5-axis in EGFR-mediated EMT in HNSCC. Interestingly, we observed the co-localization of ITG β 4 and LAMA3 expression at the tumor-stroma interface in HNSCC, whereas LAMA3 expression was absent in ITG β 4-negative tumor tissues (**Fig 15-16**), suggesting a co-dependence of ITG β 4 and laminin 5 expressions in HNSCC. In the spatial

transcriptomic analysis of OSCC (Arora et al., 2023), the characteristic map of “tumor core” and “tumor edge” revealed that *ITGβ4* and its ligand laminin 5 genes were upregulated at the edge of tumor, when compared with the tumor core area (**Fig 24**). The leading edge, defined by malignant cell layers at the border of tumors, has been previously recognized for its prognostic significance in clinical classification and might facilitate invasion and metastasis in cancers including HNSCC (Anguiano et al., 2020; Chowdhury et al., 2019; Y. M. Liu et al., 2023; Wolfe et al., 2020). EMT is essential in the initiating steps of metastasis formation, and contributes to forming buds that might be the source of local invasion and recurrence (Enderle-Ammour et al., 2017; Grigore et al., 2016; Jensen et al., 2015). Puram *et al.* described cells characterized by a pEMT signature localized at the leading edge of HNSCC primary tumors, and laminin 5 genes are part of pEMT signature genes in HNSCC (Puram et al., 2017). Hence, our study further demonstrated that *ITGβ4* was strongly expressed at the leading invasive cells in the EGFR-mediated invasion (**Fig 25**). Alongside elevated expression of *ITGβ4*, *Ki67*, a proliferation marker, exhibited a decrease in early invading cells. These results are consistent with common features of EMT, such as the increased presence of cellular components associated with focal adhesion and cell leading edge, along with the suppression of cell cycle and DNA replication in the EGFR-mediated EMT signature (Mittal, 2018). It also suggests that the strong expressions of *ITGβ4* and laminin 5 at the leading edge of tumor might be associated with EMT or pEMT in HNSCC. Moreover, we observed a notable prevalence of *ITGβ4* expression in the outermost cells of tumor regions, which is strongly associated with a greater intensity of tumor budding in HNSCC primary tumors. Given the presence of tumor budding indicates that some cancer cells have gained the ability to invade to distant area and establish new tumor growths, tumor budding has been considered as a hallmark of local invasion and a prognostic factor in tumor progression (Ailia et al., 2022; Lugli et al., 2017; Qu et al., 2023; C. Xue et al., 2022). In our study, the association between *ITGβ4* expression in tumor protrusions and the intensity of tumor buds (**Fig 26**) further supports that *ITGβ4* plays a critical role in the early stage of local invasion and metastasis in HNSCC.

4.1.2 CD73 supports EGFR-mediated invasion in HPV-neg HNSCC

The identification of different types of EMT, including EGFR-EMT, as contributors to tumor progression in HNSCC, offers new options for progress, prediction, and treatment. These options are represented as gene signatures that correlate with different EMT states

in cancer cells. Given that Cetuximab has been approved for the treatment of advanced and recurrent HNSCC, the potential correlation between EGFR-mediated EMT with Cetuximab treatment resistance is particularly noteworthy. As one part of EGFR-mediated EMT gene signatures (Schinke, Shi, et al., 2022), CD73 has been reported to be recognized as an immune checkpoint in cancers and to be involved in EMT, migration and invasion through promoting ADO generation and interacting with ECM (Loi et al., 2013; X. L. Ma et al., 2019; Petruk et al., 2021; Reinhardt et al., 2017; F. Xue et al., 2022). Although CD73 has been identified in activating EGFR signaling pathway in HNSCC (Ren et al., 2016), the upregulation of CD73 through EGFR activation and the functional role of CD73 in EGFR-mediated EMT and invasion in HPV-neg HNSCC have not been investigated yet. Moreover, the prognostic relevance of CD73 in HNSCC remains uncertain in published data due to the absence of HPV stratification in these publications (X.-M. Chen et al., 2022; F. Xue et al., 2022; Yaoting Zhang et al., 2022). Hence, we focused on the assessment of functions of CD73 in EGFR-mediated EMT and local invasion and its ability as a predictive biomarker for Cetuximab treatment response in HPV-neg HNSCC.

It has been shown that CD73 is overexpressed and associated with the abilities of adhesion to ECM, migration and invasion in various tumors (Gelsleichter et al., 2023; Ghalamfarsa et al., 2019; Yang et al., 2018). In this thesis, CD73 was upregulated in EGFR-mediated EMT in HNSCC via activation of the EGFR-MAPK signaling pathway (**Fig 28**), which showed a *vice-versa* scenario compared with published data (Ren et al., 2016). Previous studies have documented the correlation between *CD73* with EMT scores in cancers (Iser et al., 2022). We have substantially expanded upon these discoveries and demonstrated a positive correlation between *CD73* and EGFR activity, MAPK signaling, EGFR-EMT signature, EMT hallmark and pEMT gene signature in malignant single cells and HNSCC bulk cohorts (**Fig 29**). Considering these EMT signatures are related to metastasis and poor OS in HNSCC, the associations between *CD73* and these signatures support the significant involvement of CD73 in EGFR-mediated invasion in HNSCC. In many cancers, activation of MAPK can upregulate CD73 expression, leading to migration and invasion (Reinhardt et al., 2017). It was described that *CD73* is associated with invadopodia formation and activation of the MAPK signaling pathway in HNSCC (F. Xue et al., 2022b). Our group has previously demonstrated that MAPK-ERK1/2 pathway is the main downstream signaling on EGFR-EMT in HNSCC. It indicated a potential positive feedback loop between EGFR and CD73, with convergence at the MAPK level,

influencing the regulation of EGFR-mediated EMT in HNSCC. In this thesis, we also observed inhibiting CD73 did not lead to notable changes in EGF-induced EMT in HNSCC (**Fig 31**), suggesting CD73 acts more as an effector than a regulator in the process of EGFR-mediated EMT in HNSCC.

Previous studies have revealed that overexpression of CD73 can enhance the abilities of adhesion to ECM, migration and invasion in breast cancer, which can be blocked by CD73 inhibitor adenosine 5'-(α,β -methylene)diphosphate (APCP) (Zhou et al., 2007). Suppressing CD73 using shRNA or inhibitors notably reduced cell viability and migration in TNBC (Petruk et al., 2021). In line with these data, we observed that blocking CD73 by the novel 22E6 CD73-antagonizing antibody significantly suppressed migration and invasion mediated by EGFR activation in a proliferation-independent manner in HNSCC (**Fig 32-33**). Notably, co-treatment of cells with 22E6 and Cetuximab at an inefficient concentration presented substantial effects on suppressing EGFR-mediated invasion area and invasive distance in FaDu cells (**Fig 34**). CD73 blockade by 22E6 at a powerless concentration resulted in a significant reduction in the functional IC50 of Cetuximab (**Fig 35**). This suggests that EGFR and CD73 have complementary roles in regulating local invasion in HNSCC. Moreover, loss- and gain-of-function experiments revealed effects of 22E6 are influenced by the presence or absence of CD73 expression (**Fig 38-39**). In HNSCC primary tissues, upregulation of CD73 was further observed compared with normal mucosa, and it was found to have a significant correlation with the intensity of tumor budding (**Fig 40A-C**), which is associated with local invasion, metastasis and recurrence (Lugli et al., 2021). Therefore, CD73 functions as an effector molecule in EGFR-mediated migration and invasion in vitro, and it shows a correlation with local dissemination within primary HNSCC tissues.

The correlation between overexpression of *CD73* and worse OS and disease-free survival (DFS) in HNSCC have been reported in previous publications (X.-M. Chen et al., 2022; F. Xue et al., 2022b; Yaoting Zhang et al., 2022). However, the association of *CD73* with clinical endpoints was analyzed without considering the HPV-status, even though it was acknowledged that there was a correlation between HPV infection and *CD73* expression (de Lourdes Mora-García et al., 2019). HPV-positive HNSCC typically exhibit better clinical outcome and lower median *CD73* expression levels when compared with HPV-negative HNSCC, which can be a confounding factor when assessing the prognostic significance of *CD73*. In our study, we examined the prognostic value of *CD73* expression in HPV-negative HNSCC patients in TCGA, FHCRC and GSE6585 cohorts.

A prognostic value for *CD73* in predicting HNSCC patients' clinical endpoints including OS and DFS in the full TCGA cohort comprised of HPV-positive and -negative HNSCC has been described by others. However, no significant association between *CD73* expression and OS in HPV-negative HNSCC-TCGA cohort (n=415) was observed in our study (**Fig 40D**), which indicated that HPV infection could influence the assessment of the prognostic value of *CD73* in HNSCC. Moreover, in the FHCRC cohort, higher *CD73* expression was significantly linked to poorer OS, a correlation not observed in the GSE65858 cohort. The FHCRC cohort comprises OSCC patients, the majority of whom are HPV-negative. Our finding of a correlation between *CD73* and clinical outcomes in FHCRC cohort aligns with findings reported in the OSCC-JKLOD cohort. Therefore, we infer that *CD73* may serve as a biomarker for OSCC but not necessarily for other HPV-negative HNSCC localizations.

4.2 *ITGβ4* and *CD73* as predictive biomarkers in HNSCC

HNSCC patients, who exhibit a pronounced EGFR-mediated EMT and are consequently at a heightened risk of experiencing local recurrences or metastases, are expected to derive the greatest benefit from Cetuximab treatment. However, Cetuximab therapy often results in the emergence of acquired resistance in the majority of HNSCC patients, frequently culminating in both local and distant treatment failures (Muraro et al., 2021; Sacco et al., 2021; Yao et al., 2022). Reliable predictive biomarkers of therapy response or cetuximab resistance are still lacking.

In this study, *ITGβ4* and *CD73*, as parts of EGFR-mediated EMT gene signatures, were demonstrated to be upregulated through EGFR-MAPK signaling and involved in EGFR-mediated invasion, which can be blocked by Cetuximab. These findings inspired us to further assess the predictive value of *ITGβ4* and *CD73* as biomarkers for Cetuximab response in HNSCC. In PDX-derived HNSCC models, it has been reported that a basal molecular subtype is associated with PDX responding to Cetuximab treatment in HNSCC (Klinghammer et al., 2017). We found that the expression of *CD73* is significantly increased in the Cetuximab responder group in this cohort (**Fig 41A-B**). Bossi *et al.* also reported on malignant transcriptomes in a cohort of cetuximab-treated HNSCC with recurrent-metastatic disease (Bossi, Bergamini, et al., 2016). In our study, we showed that compared with Cetuximab-treated patients with short PFS, patients with longer PFS showed a significant increase in *CD73* expression. Cetuximab-treated HNSCC with low *CD73* expression had a significantly increased odd for having short PFS in this cohort

(**Fig 41C**). Similarly, data published by our group also revealed that low ITG β 4 expression was significantly correlated with short PFS in Cetuximab-treated HNSCC patients (Schinke et al., 2022). Collectively, these findings indicate that both CD73 and ITG β 4 predict the efficacy of Cetuximab treatment in metastatic HNSCC.

Hence, CD73 and ITG β 4 may serve as an indicator of the EGFR-EMT status in cells, potentially acting as a sensor for aggressive, invasive cancer cells that respond to Cetuximab.

4.3 Rationale for ITG β 4 and CD73 as therapeutic targets in HNSCC

In recent years, there have been significant advancements in drug therapy for HNSCC, and multimodality approaches have been generally required in the treatment of HNSCC (Marur & Forastiere, 2016). Cetuximab, a monoclonal antibody targeting EGFR, is approved by the FDA as a radiation sensitizer. Cetuximab has been demonstrated to be useful in combination with chemotherapy and radiotherapy in recurrent-metastatic disease (Tejani et al., 2010). However, resistance to Cetuximab is one of the biggest challenges in the treatment of HNSCC and is associated with recurrence and poor clinical outcome in patients (Bhatia & Burtneess, 2023). The relevant mechanisms of cetuximab resistance include intrinsic factors such as genetic aberrations in EGFR gene, EGFR ligand abundance, activation of pathways related to tumor progression and induction of EMT, as well as extrinsic factors such as the acquisition of an immunosuppressive TME (C. Huang et al., 2021; Kitamura et al., 2021; Muraro et al., 2021). Hence, there is a tremendous need to identify new targets for adjuvant therapy in combination with Cetuximab in HNSCC.

In our study, the rationality for considering ITG β 4 and CD73 as a potential target to suppress local invasion and increase the response to Cetuximab treatment was as follows. Firstly, both *ITG β 4* and *CD73* are parts of the EGFR-EMT signature, which characterizes malignant cells' migration and invasion following EGF-induced EMT, suggesting their potential roles in regulating local invasion in HNSCC. Secondly, *ITG β 4* and *CD73* expression are positively associated with EGFR activation. It has been reported that overexpression of EGFR activates EGFR phosphorylation in a ligand-independent manner, leading to activation of MAPK and PI3K-AKT signaling pathways, which are involved in tumor growth, metastasis and treatment resistance (Stanoev et al., 2018). *ITG β 4* and *CD73* expression were positively associated with MAPK and PI3K-AKT

pathways, further supporting the rationale of being therapeutic targets. Thirdly, as transmembrane proteins, ITG β 4 and CD73 are extracellularly accessible and have druggability properties.

Accordingly, ASC8 antibody-mediated blocking ITG β 4 binding to laminin 5 or 22E6 antibody-mediated inhibition of the enzymatic activity of CD73 both significantly suppressed EGFR-mediated local invasion in HNSCC cells. Moreover, CD73-driven ADO is associated with suppressive TME in various cancers. The generation of suppressive TME is involved in the regulation of EMT, proliferation, migration, and angiogenesis (Y. Jiang & Zhan, 2020; L. Liu et al., 2021), which suggests that targeting CD73 may benefit response to treatment at several levels. Lastly, we observed strong expressions of ITG β 4 and CD73 in tumor buds, which supports that targeting ITG β 4 or CD73 may interfere with initial steps of local invasion and metastasis in HNSCC. Strong expression of ITG β 4 at the leading edge and leading invasive cells further validates its rationality for potential therapeutic targets. Therefore, we propose that ITG β 4 and CD73 represent potential targets in combination with Cetuximab in the treatment of HNSCC that would profit from a potential validation in pre-clinical animal models in the future.

5. References

- Aiello, N. M., Maddipati, R., Norgard, R. J., Balli, D., Li, J., Yuan, S., Yamazoe, T., Black, T., Sahmoud, A., Furth, E. E., Bar-, D., Stanger, B. Z., Division, G., & Family, A. (2019). *HHS Public Access*. 45(6), 681–695. <https://doi.org/10.1016/j.devcel.2018.05.027>.EMT
- Ailia, M. J., Thakur, N., Chong, Y., & Yim, K. (2022). Tumor Budding in Gynecologic Cancer as a Marker for Poor Survival: A Systematic Review and Meta-Analysis of the Perspectives of Epithelial-Mesenchymal Transition. *Cancers*, 14(6). <https://doi.org/10.3390/cancers14061431>
- Alcedo, K. P., Bowser, J. L., & Snider, N. T. (2021). The elegant complexity of mammalian ecto-5' -nucleotidase (CD73). *Trends in Cell Biology*, 31(10), 829–842. <https://doi.org/10.1016/j.tcb.2021.05.008>
- Allard, B., Longhi, M. S., Robson, S. C., & Stagg, J. (2017). The ectonucleotidases CD39 and CD73: Novel checkpoint inhibitor targets. *Immunological Reviews*, 276(1), 121–144. <https://doi.org/10.1111/imr.12528>
- Anguiano, M., Morales, X., Castilla, C., Pena, A. R., Ederra, C., Martínez, M., Ariz, M., Esparza, M., Amaveda, H., Mora, M., Movilla, N., Aznar, J. M. G., Cortés-Domínguez, I., & Ortiz-de-Solorzano, C. (2020). The use of mixed collagen-Matrigel matrices of increasing complexity recapitulates the biphasic role of cell adhesion in cancer cell migration: ECM sensing, remodeling and forces at the leading edge of cancer invasion. *PloS One*, 15(1), e0220019. <https://doi.org/10.1371/journal.pone.0220019>
- Arora, R., Cao, C., Kumar, M., Sinha, S., Chanda, A., McNeil, R., Samuel, D., Arora, R. K., Matthews, T. W., Chandarana, S., Hart, R., Dort, J. C., Biernaskie, J., Neri, P., Hyrcza, M. D., & Bose, P. (2023). Spatial transcriptomics reveals distinct and conserved tumor core and edge architectures that predict survival and targeted therapy response. *Nature Communications*, 14(1), 5029. <https://doi.org/10.1038/s41467-023-40271-4>
- Aumailley, M., El Khal, A., Knöss, N., & Tunggal, L. (2003). Laminin 5 processing and its integration into the ECM. *Matrix Biology : Journal of the International Society for Matrix Biology*, 22(1), 49–54. [https://doi.org/10.1016/s0945-053x\(03\)00013-1](https://doi.org/10.1016/s0945-053x(03)00013-1)
- Bakir, B., Chiarella, A. M., Pitarresi, J. R., & Rustgi, A. K. (2020). EMT, MET, Plasticity,

- and Tumor Metastasis. *Trends in Cell Biology*, 30(10), 764–776.
<https://doi.org/10.1016/j.tcb.2020.07.003>
- Baumeister, P., Zhou, J., Canis, M., & Gires, O. (2021). Epithelial-to-mesenchymal transition-derived heterogeneity in head and neck squamous cell carcinomas. *Cancers*, 13(21). <https://doi.org/10.3390/cancers13215355>
- Beaulieu, J.-F. (2019). Integrin $\alpha\beta 4$ in Colorectal Cancer: Expression, Regulation, Functional Alterations and Use as a Biomarker. *Cancers*, 12(1). <https://doi.org/10.3390/cancers12010041>
- Beaulieu, J. (2019). *Regulation, Functional Alterations and Use as a Biomarker*. 1–13.
- Benesch, M. G., Wu, R., Menon, G., & Takabe, K. (2022). High beta integrin expression is differentially associated with worsened pancreatic ductal adenocarcinoma outcomes. *American Journal of Cancer Research*, 12(12), 5403–5424.
- Bhatia, A., & Burtness, B. (2023). Treating Head and Neck Cancer in the Age of Immunotherapy: A 2023 Update. *Drugs*, 83(3), 217–248.
<https://doi.org/10.1007/s40265-023-01835-2>
- Bierie, B., Pierce, S. E., Kroeger, C., Stover, D. G., Pattabiraman, D. R., Thiru, P., Liu Donaher, J., Reinhardt, F., Chaffer, C. L., Keckesova, Z., & Weinberg, R. A. (2017). Integrin- $\beta 4$ identifies cancer stem cell-enriched populations of partially mesenchymal carcinoma cells. *Proceedings of the National Academy of Sciences of the United States of America*, 114(12), E2337–E2346.
<https://doi.org/10.1073/pnas.1618298114>
- Bossi, P., Bergamini, C., Siano, M., Cossu Rocca, M., Sponghini, A. P., Favales, F., Giannoccaro, M., Marchesi, E., Cortelazzi, B., Perrone, F., Pilotti, S., Locati, L. D., Licitra, L., Canevari, S., & De Cecco, L. (2016). Functional Genomics Uncover the Biology behind the Responsiveness of Head and Neck Squamous Cell Cancer Patients to Cetuximab. *Clinical Cancer Research: An Official Journal of the American Association for Cancer Research*, 22(15), 3961–3970.
<https://doi.org/10.1158/1078-0432.CCR-15-2547>
- Bossi, P., Resteghini, C., Paielli, N., Licitra, L., Pilotti, S., & Perrone, F. (2016). Prognostic and predictive value of EGFR in head and neck squamous cell carcinoma. *Oncotarget*, 7(45), 74362–74379. <https://doi.org/10.18632/oncotarget.11413>
- Botticelli, A., Cirillo, A., Strigari, L., Valentini, F., Cerbelli, B., Scagnoli, S., Cerbelli,

- E., Zizzari, I. G., Rocca, C. Della, D'Amati, G., Polimeni, A., Nuti, M., Merlano, M. C., Mezi, S., & Marchetti, P. (2021). Anti-PD-1 and Anti-PD-L1 in Head and Neck Cancer: A Network Meta-Analysis. In *Frontiers in immunology* (Vol. 12, p. 705096). <https://doi.org/10.3389/fimmu.2021.705096>
- Brabletz, S., Schuhwerk, H., Brabletz, T., & Stemmler, M. P. (2021). Dynamic EMT: a multi-tool for tumor progression. *The EMBO Journal*, *40*(18), e108647. <https://doi.org/10.15252/emj.2021108647>
- Cadassou, O., Raza, M.-Z., Machon, C., Gudefin, L., Armanet, C., Chettab, K., Guitton, J., Tozzi, M. G., Dumontet, C., Cros-Perrial, E., & Jordheim, L. P. (2021). Enhanced migration of breast and lung cancer cells deficient for cN-II and CD73 via COX-2/PGE2/AKT axis regulation. *Cellular Oncology (Dordrecht)*, *44*(1), 151–165. <https://doi.org/10.1007/s13402-020-00558-w>
- Caramel, J., Papadogeorgakis, E., Hill, L., Browne, G. J., Richard, G., Wierinckx, A., Saldanha, G., Osborne, J., Hutchinson, P., Tse, G., Lachuer, J., Puisieux, A., Pringle, J. H., Ansieau, S., & Tulchinsky, E. (2013). A switch in the expression of embryonic EMT-inducers drives the development of malignant melanoma. *Cancer Cell*, *24*(4), 466–480. <https://doi.org/10.1016/j.ccr.2013.08.018>
- Chaffer, C. L., Brueckmann, I., Scheel, C., Kaestli, A. J., Wiggins, P. A., Rodrigues, L. O., Brooks, M., Reinhardt, F., Suc, Y., Polyak, K., Arendt, L. M., Kuperwasser, C., Bierie, B., & Weinberg, R. A. (2011). Normal and neoplastic nonstem cells can spontaneously convert to a stem-like state. *Proceedings of the National Academy of Sciences of the United States of America*, *108*(19), 7950–7955. <https://doi.org/10.1073/pnas.1102454108>
- Chen, T., You, Y., Jiang, H., & Wang, Z. Z. (2017). Epithelial-mesenchymal transition (EMT): A biological process in the development, stem cell differentiation, and tumorigenesis. *Journal of Cellular Physiology*, *232*(12), 3261–3272. <https://doi.org/10.1002/jcp.25797>
- Chen, X.-M., Liu, Y.-Y., Tao, B.-Y., Xue, X.-M., Zhang, X.-X., Wang, L.-L., Zhong, H., Zhang, J., Yang, S.-M., & Jiang, Q.-Q. (2022). NT5E upregulation in head and neck squamous cell carcinoma: A novel biomarker on cancer-associated fibroblasts for predicting immunosuppressive tumor microenvironment. *Frontiers in Immunology*, *13*, 975847. <https://doi.org/10.3389/fimmu.2022.975847>

- Chowdhury, F. N., Reisinger, J., Gomez, K. E., Chimed, T.-S., Thomas, C. M., Le, P. N., Miller, B., Morton, J. J., Nieto, C. M., Somerset, H. L., Wang, X.-J., Keysar, S. B., & Jimeno, A. (2019). Leading edge or tumor core: Intratumor cancer stem cell niches in oral cavity squamous cell carcinoma and their association with stem cell function. *Oral Oncology*, *98*, 118–124. <https://doi.org/10.1016/j.oraloncology.2019.09.011>
- Ciardiello, F., & Tortora, G. (2008). EGFR antagonists in cancer treatment. *The New England Journal of Medicine*, *358*(11), 1160–1174. <https://doi.org/10.1056/NEJMra0707704>
- Citri, A., & Yarden, Y. (2006). EGF-ERBB signalling: Towards the systems level. *Nature Reviews Molecular Cell Biology*, *7*(7), 505–516. <https://doi.org/10.1038/nrm1962>
- Cobb, D. A., de Rossi, J., Liu, L., An, E., & Lee, D. W. (2022). Targeting of the alpha(v) beta(3) integrin complex by CAR-T cells leads to rapid regression of diffuse intrinsic pontine glioma and glioblastoma. *Journal for Immunotherapy of Cancer*, *10*(2). <https://doi.org/10.1136/jitc-2021-003816>
- Comprehensive genomic characterization of head and neck squamous cell carcinomas. (2015). *Nature*, *517*(7536), 576–582. <https://doi.org/10.1038/nature14129>
- Cooper, J., & Giancotti, F. G. (2019a). *Integrin Signaling in Cancer: Mechanotransduction, Stemness, Epithelial Plasticity, and Therapeutic Resistance*. *Cancer Cell*, *35*(3), 347–367. <https://doi.org/10.1016/j.ccell.2019.01.007>. Integrin
- Cooper, J., & Giancotti, F. G. (2019b). Integrin Signaling in Cancer: Mechanotransduction, Stemness, Epithelial Plasticity, and Therapeutic Resistance. *Cancer Cell*, *35*(3), 347–367. <https://doi.org/10.1016/j.ccell.2019.01.007>
- Dawood, S., Austin, L., & Cristofanilli, M. (2014). Cancer stem cells: implications for cancer therapy. *Oncology (Williston Park, N.Y.)*, *28*(12), 1101-1107,1110.
- De Craene, B., & Berx, G. (2013). Regulatory networks defining EMT during cancer initiation and progression. *Nature Reviews. Cancer*, *13*(2), 97–110. <https://doi.org/10.1038/nrc3447>
- de Lourdes Mora-García, M., López-Cisneros, S., Gutiérrez-Serrano, V., García-Rocha, R., Weiss-Steider, B., Hernández-Montes, J., Sánchez-Peña, H. I., Ávila-Ibarra, L. R., Don-López, C. A., Muñoz-Godínez, R., Pineda, D. B. T., Chacón-Salinas, R., Vallejo-Castillo, L., Pérez-Tapia, S. M., & Monroy-García, A. (2019). HPV-16 Infection Is Associated with a High Content of CD39 and CD73 Ectonucleotidases

- in Cervical Samples from Patients with CIN-1. *Mediators of Inflammation*, 2019, 4651627. <https://doi.org/10.1155/2019/4651627>
- Egloff, A. M., Rothstein, M. E., Seethala, R., Siegfried, J. M., Grandis, J. R., & Stabile, L. P. (2009). Cross-talk between estrogen receptor and epidermal growth factor receptor in head and neck squamous cell carcinoma. *Clinical Cancer Research : An Official Journal of the American Association for Cancer Research*, 15(21), 6529–6540. <https://doi.org/10.1158/1078-0432.CCR-09-0862>
- Enderle-Ammour, K., Bader, M., Ahrens, T. D., Franke, K., Timme, S., Csanadi, A., Hoepfner, J., Kulemann, B., Maurer, J., Reiss, P., Schilling, O., Keck, T., Brabletz, T., Stickeler, E., Werner, M., Wellner, U. F., & Bronsert, P. (2017). Form follows function: Morphological and immunohistological insights into epithelial-mesenchymal transition characteristics of tumor buds. *Tumour Biology: The Journal of the International Society for Oncodevelopmental Biology and Medicine*, 39(5), 1010428317705501. <https://doi.org/10.1177/1010428317705501>
- Fang, H., Ren, W., Cui, Q., Liang, H., Yang, C., Liu, W., Wang, X., Liu, X., Shi, Y., Feng, J., & Chen, C. (2023). Integrin $\beta 4$ promotes DNA damage-related drug resistance in triple-negative breast cancer via TNFAIP2/IQGAP1/RAC1. *ELife*, 12. <https://doi.org/10.7554/eLife.88483>
- Ferris, R. L., Spanos, W. C., Leidner, R., Gonçalves, A., Martens, U. M., Kyi, C., Sharfman, W., Chung, C. H., Devriese, L. A., Gauthier, H., Chiosea, S. I., Vujanovic, L., Taube, J. M., Stein, J. E., Li, J., Li, B., Chen, T., Barrows, A., & Topalian, S. L. (2021). Neoadjuvant nivolumab for patients with resectable HPV-positive and HPV-negative squamous cell carcinomas of the head and neck in the CheckMate 358 trial. *Journal for Immunotherapy of Cancer*, 9(6). <https://doi.org/10.1136/jitc-2021-002568>
- Frey, P., Devisme, A., Rose, K., Schrempp, M., Freißen, V., Andrieux, G., Boerries, M., & Hecht, A. (2022). SMAD4 mutations do not preclude epithelial-mesenchymal transition in colorectal cancer. *Oncogene*, 41(6), 824–837. <https://doi.org/10.1038/s41388-021-02128-2>
- Galeano Niño, J. L., Wu, H., LaCourse, K. D., Kempchinsky, A. G., Baryames, A., Barber, B., Futran, N., Houlton, J., Sather, C., Sicinska, E., Taylor, A., Minot, S. S., Johnston, C. D., & Bullman, S. (2022). Effect of the intratumoral microbiota on spatial and cellular heterogeneity in cancer. *Nature*, 611(7937), 810–817.

- <https://doi.org/10.1038/s41586-022-05435-0>
- Gan, L., Meng, J., Xu, M., Liu, M., Qi, Y., Tan, C., Wang, Y., Zhang, P., Weng, W., Sheng, W., Huang, M., & Wang, Z. (2018). Extracellular matrix protein 1 promotes cell metastasis and glucose metabolism by inducing integrin β 4/FAK/SOX2/HIF-1 α signaling pathway in gastric cancer. *Oncogene*, 37(6), 744–755. <https://doi.org/10.1038/onc.2017.363>
- Gao, Y., Zheng, H., Li, L., Feng, M., Chen, X., Hao, B., Lv, Z., Zhou, X., & Cao, Y. (2021). Prostate-Specific Membrane Antigen (PSMA) Promotes Angiogenesis of Glioblastoma Through Interacting With ITGB4 and Regulating NF- κ B Signaling Pathway. *Frontiers in Cell and Developmental Biology*, 9, 598377. <https://doi.org/10.3389/fcell.2021.598377>
- Gao, Z., Dong, K., & Zhang, H. (2014). The roles of CD73 in cancer. *BioMed Research International*, 2014, 460654. <https://doi.org/10.1155/2014/460654>
- García-Cabo, P., García-Pedrero, J. M., Villaronga, M. Á., Hermida-Prado, F., Granda-Díaz, R., Allonca, E., López, F., & Rodrigo, J. P. (2020). Expression of E-cadherin and β -catenin in Laryngeal and Hypopharyngeal Squamous Cell Carcinomas. *Acta Otorrinolaringologica Espanola*, 71(6), 358–366. <https://doi.org/10.1016/j.otorri.2019.12.002>
- Gelsleichter, N. E., Azambuja, J. H., Rubenich, D. S., & Braganhol, E. (2023). CD73 in glioblastoma: Where are we now and what are the future directions? *Immunology Letters*, 256–257, 20–27. <https://doi.org/10.1016/j.imlet.2023.03.005>
- Genduso, S., Freytag, V., Schetler, D., Kirchner, L., Schiecke, A., Maar, H., Wicklein, D., Gebauer, F., Bröker, K., Stürken, C., Milde-Langosch, K., Oliveira-Ferrer, L., Ricklefs, F. L., Ewald, F., Wolters-Eisfeld, G., Riecken, K., Unrau, L., Krause, L., Bohnenberger, H., ... Lange, T. (2023). Tumor cell integrin β 4 and tumor stroma E-/P-selectin cooperatively regulate tumor growth in vivo. *Journal of Hematology and Oncology*, 16(1), 1–24. <https://doi.org/10.1186/s13045-023-01413-9>
- Georgolios, A., Batistatou, A., Manolopoulos, L., & Charalabopoulos, K. (2006). Role and expression patterns of E-cadherin in head and neck squamous cell carcinoma (HNSCC). *Journal of Experimental & Clinical Cancer Research : CR*, 25(1), 5–14.
- Ghalanfarsa, G., Kazemi, M. H., Raoofi Mohseni, S., Masjedi, A., Hojjat-Farsangi, M., Azizi, G., Yousefi, M., & Jadidi-Niaragh, F. (2019). CD73 as a potential opportunity

- for cancer immunotherapy. *Expert Opinion on Therapeutic Targets*, 23(2), 127–142. <https://doi.org/10.1080/14728222.2019.1559829>
- Gil, S. G., Brown, T. A., Ryan, M. C., & Carter, W. G. (1994). Junctional epidermolysis bullosis: defects in expression of epiligrin/nicein/kalinin and integrin beta 4 that inhibit hemidesmosome formation. *The Journal of Investigative Dermatology*, 103(5 Suppl), 31S-38S. <https://doi.org/10.1111/1523-1747.ep12398953>
- Gillison, M. L., D'Souza, G., Westra, W., Sugar, E., Xiao, W., Begum, S., & Viscidi, R. (2008). Distinct risk factor profiles for human papillomavirus type 16-positive and human papillomavirus type 16-negative head and neck cancers. *Journal of the National Cancer Institute*, 100(6), 407–420. <https://doi.org/10.1093/jnci/djn025>
- Grigore, A. D., Jolly, M. K., Jia, D., Farach-Carson, M. C., & Levine, H. (2016). Tumor Budding: The Name is EMT. Partial EMT. *Journal of Clinical Medicine*, 5(5). <https://doi.org/10.3390/jcm5050051>
- Guo, W., & Giancotti, F. G. (2004). Integrin signalling during tumour progression. *Nature Reviews Molecular Cell Biology*, 5(10), 816–826. <https://doi.org/10.1038/nrm1490>
- Hallaj, S., Mirza-Aghazadeh-Attari, M., Arasteh, A., Ghorbani, A., Lee, D., & Jadidi-Niaragh, F. (2021). Adenosine: The common target between cancer immunotherapy and glaucoma in the eye. *Life Sciences*, 282, 119796. <https://doi.org/10.1016/j.lfs.2021.119796>
- Hamidi, H., & Ivaska, J. (2018). Every step of the way: Integrins in cancer progression and metastasis. *Nature Reviews Cancer*, 18(9), 533–548. <https://doi.org/10.1038/s41568-018-0038-z>
- Han, Y., Lee, T., He, Y., Raman, R., Irizarry, A., Martin, M. L., & Giaccone, G. (2022). The regulation of CD73 in non-small cell lung cancer. *European Journal of Cancer (Oxford, England : 1990)*, 170, 91–102. <https://doi.org/10.1016/j.ejca.2022.04.025>
- Harris, R. C., Chung, E., & Coffey, R. J. (2003). EGF receptor ligands. *Experimental Cell Research*, 284(1), 2–13. [https://doi.org/10.1016/s0014-4827\(02\)00105-2](https://doi.org/10.1016/s0014-4827(02)00105-2)
- Hay, E. D., & Zuk, A. (1995). Transformations between epithelium and mesenchyme: normal, pathological, and experimentally induced. *American Journal of Kidney Diseases : The Official Journal of the National Kidney Foundation*, 26(4), 678–690. [https://doi.org/10.1016/0272-6386\(95\)90610-x](https://doi.org/10.1016/0272-6386(95)90610-x)

- Ho, W. J., Jaffee, E. M., & Zheng, L. (2020). The tumour microenvironment in pancreatic cancer - clinical challenges and opportunities. *Nature Reviews. Clinical Oncology*, *17*(9), 527–540. <https://doi.org/10.1038/s41571-020-0363-5>
- Holz, C., Niehr, F., Boyko, M., Hristozova, T., Distel, L., Budach, V., & Tinhofer, I. (2011). Epithelial-mesenchymal-transition induced by EGFR activation interferes with cell migration and response to irradiation and cetuximab in head and neck cancer cells. *Radiotherapy and Oncology: Journal of the European Society for Therapeutic Radiology and Oncology*, *101*(1), 158–164. <https://doi.org/10.1016/j.radonc.2011.05.042>
- Hosen, N., Yoshihara, S., Takamatsu, H., Ri, M., Nagata, Y., Kosugi, H., Shimomura, Y., Hanamura, I., Fuji, S., Minauchi, K., Kuroda, J., Suzuki, R., Nishimura, N., Uoshima, N., Nakamae, H., Kawano, Y., Mizuno, I., Gomyo, H., Suzuki, K., ... Iida, S. (2021). Expression of activated integrin $\beta 7$ in multiple myeloma patients. *International Journal of Hematology*, *114*(1), 3–7. <https://doi.org/10.1007/s12185-021-03162-2>
- Huang, C., Chen, L., Savage, S. R., Eguez, R. V., Dou, Y., Li, Y., da Veiga Leprevost, F., Jaehnig, E. J., Lei, J. T., Wen, B., Schnaubelt, M., Krug, K., Song, X., Cieřlik, M., Chang, H.-Y., Wyczalkowski, M. A., Li, K., Colaprico, A., Li, Q. K., ... Zhang, B. (2021). Proteogenomic insights into the biology and treatment of HPV-negative head and neck squamous cell carcinoma. *Cancer Cell*, *39*(3), 361-379.e16. <https://doi.org/10.1016/j.ccell.2020.12.007>
- Huang, T., Song, X., Xu, D., Tiek, D., Goenka, A., Wu, B., Sastry, N., Hu, B., & Cheng, S.-Y. (2020). Stem cell programs in cancer initiation, progression, and therapy resistance. *Theranostics*, *10*(19), 8721–8743. <https://doi.org/10.7150/thno.41648>
- Hynes, N. E., & Lane, H. A. (2005). ERBB receptors and cancer: The complexity of targeted inhibitors. *Nature Reviews Cancer*, *5*(5), 341–354. <https://doi.org/10.1038/nrc1609>
- Iser, I. C., Vedovatto, S., Oliveira, F. D., Beckenkamp, L. R., Lenz, G., & Wink, M. R. (2022). The crossroads of adenosinergic pathway and epithelial-mesenchymal plasticity in cancer. *Seminars in Cancer Biology*, *86*(Pt 2), 202–213. <https://doi.org/10.1016/j.semcancer.2022.06.012>
- Jensen, D. H., Dabelsteen, E., Specht, L., Fiehn, A. M. K., Therkildsen, M. H., Jønson,

- L., Vikesaa, J., Nielsen, F. C., & von Buchwald, C. (2015). Molecular profiling of tumour budding implicates TGF β -mediated epithelial-mesenchymal transition as a therapeutic target in oral squamous cell carcinoma. *The Journal of Pathology*, 236(4), 505–516. <https://doi.org/10.1002/path.4550>
- Ji, H., Song, H., Wang, Z., Jiao, P., Xu, J., Li, X., Du, H., Wu, H., & Zhong, Y. (2021). FAM83A promotes proliferation and metastasis via Wnt/ β -catenin signaling in head neck squamous cell carcinoma. *Journal of Translational Medicine*, 19(1), 423. <https://doi.org/10.1186/s12967-021-03089-6>
- Jiang, X., Wang, J., Wang, M., Xuan, M., Han, S., Li, C., Li, M., Sun, X.-F., Yu, W., & Zhao, Z. (2021). ITGB4 as a novel serum diagnosis biomarker and potential therapeutic target for colorectal cancer. *Cancer Medicine*, 10(19), 6823–6834. <https://doi.org/10.1002/cam4.4216>
- Jiang, Y., & Zhan, H. (2020). Communication between EMT and PD-L1 signaling: New insights into tumor immune evasion. *Cancer Letters*, 468, 72–81. <https://doi.org/10.1016/j.canlet.2019.10.013>
- Johnson, D. E., Burtneess, B., Leemans, C. R., Lui, V. W. Y., Bauman, J. E., & Grandis, J. R. (2020). Head and neck squamous cell carcinoma. *Nature Reviews. Disease Primers*, 6(1), 92. <https://doi.org/10.1038/s41572-020-00224-3>
- Kang, J. J., Ko, A., Kil, S. H., Mallen-St Clair, J., Shin, D. S., Wang, M. B., & Srivatsan, E. S. (2023). EGFR pathway targeting drugs in head and neck cancer in the era of immunotherapy. *Biochimica et Biophysica Acta. Reviews on Cancer*, 1878(1), 188827. <https://doi.org/10.1016/j.bbcan.2022.188827>
- Kechagia, J. Z., & Ivaska, J. (2019). Integrins as biomechanical sensors of the microenvironment. *Nature Reviews Molecular Cell Biology*, 20(August). <https://doi.org/10.1038/s41580-019-0134-2>
- Keysar, S. B., Le, P. N., Anderson, R. T., Morton, J. J., Bowles, D. W., Paylor, J. J., Vogler, B. W., Thorburn, J., Fernandez, P., Glogowska, M. J., Takimoto, S. M., Sehr, D. B., Gan, G. N., Eagles-Soukup, J. R., Serracino, H., Hirsch, F. R., Lucia, M. S., Thorburn, A., Song, J. I., ... Jimeno, A. (2013). Hedgehog signaling alters reliance on EGF receptor signaling and mediates anti-EGFR therapeutic resistance in head and neck cancer. *Cancer Research*, 73(11), 3381–3392. <https://doi.org/10.1158/0008-5472.CAN-12-4047>

- Kirtonia, A., Pandey, A. K., Ramachandran, B., Mishra, D. P., Dawson, D. W., Sethi, G., Ganesan, T. S., Koeffler, H. P., & Garg, M. (2022). Overexpression of laminin-5 gamma-2 promotes tumorigenesis of pancreatic ductal adenocarcinoma through EGFR/ERK1/2/AKT/mTOR cascade. *Cellular and Molecular Life Sciences: CMLS*, 79(7), 362. <https://doi.org/10.1007/s00018-022-04392-1>
- Kitamura, N., Sento, S., Yoshizawa, Y., Sasabe, E., Kudo, Y., & Yamamoto, T. (2021). Current trends and future prospects of molecular targeted therapy in head and neck squamous cell carcinoma. *International Journal of Molecular Sciences*, 22(1), 1–13. <https://doi.org/10.3390/ijms22010240>
- Klinghammer, K., Otto, R., Raguse, J. D., Albers, A. E., Tinhofer, I., Fichtner, I., Leser, U., Keilholz, U., & Hoffmann, J. (2017). Basal subtype is predictive for response to cetuximab treatment in patient-derived xenografts of squamous cell head and neck cancer. *International Journal of Cancer*, 141(6), 1215–1221. <https://doi.org/10.1002/ijc.30808>
- Lambert, A. W., & Weinberg, R. A. (2021a). Linking EMT programmes to normal and neoplastic epithelial stem cells. *Nature Reviews Cancer*, 21(5), 325–338. <https://doi.org/10.1038/s41568-021-00332-6>
- Lambert, A. W., & Weinberg, R. A. (2021b). Linking EMT programmes to normal and neoplastic epithelial stem cells. *Nature Reviews. Cancer*, 21(5), 325–338. <https://doi.org/10.1038/s41568-021-00332-6>
- Lamouille, S., Xu, J., & Derynck, R. (2014a). Molecular mechanisms of epithelial–mesenchymal transition. *Nature Reviews Molecular Cell Biology*, 15(3), 178–196. <https://doi.org/10.1038/nrm3758>.Molecular
- Lamouille, S., Xu, J., & Derynck, R. (2014b). Molecular mechanisms of epithelial–mesenchymal transition. *Nature Reviews. Molecular Cell Biology*, 15(3), 178–196. <https://doi.org/10.1038/nrm3758>
- Leemans, C. R., Braakhuis, B. J. M., & Brakenhoff, R. H. (2011). The molecular biology of head and neck cancer. *Nature Reviews. Cancer*, 11(1), 9–22. <https://doi.org/10.1038/nrc2982>
- Leemans, C. R., Snijders, P. J. F., & Brakenhoff, R. H. (2018). The molecular landscape of head and neck cancer. *Nature Reviews. Cancer*, 18(5), 269–282. <https://doi.org/10.1038/nrc.2018.11>

- Leng, C., Zhang, Z.-G., Chen, W.-X., Luo, H.-P., Song, J., Dong, W., Zhu, X.-R., Chen, X.-P., Liang, H.-F., & Zhang, B.-X. (2016). An integrin beta4-EGFR unit promotes hepatocellular carcinoma lung metastases by enhancing anchorage independence through activation of FAK-AKT pathway. *Cancer Letters*, *376*(1), 188–196. <https://doi.org/10.1016/j.canlet.2016.03.023>
- Lengrand, J., Pastushenko, I., Vanuytven, S., Song, Y., Venet, D., Sarate, R. M., Bellina, M., Moers, V., Boinet, A., Sifrim, A., Rama, N., Ducarouge, B., Van Herck, J., Dubois, C., Scozzaro, S., Lemaire, S., Gieskes, S., Bonni, S., Collin, A., ... Blanpain, C. (2023). Pharmacological targeting of netrin-1 inhibits EMT in cancer. *Nature*, *620*(7973), 402–408. <https://doi.org/10.1038/s41586-023-06372-2>
- Leone, R. D., & Emens, L. A. (2018). Targeting adenosine for cancer immunotherapy. *Journal for Immunotherapy of Cancer*, *6*(1), 57. <https://doi.org/10.1186/s40425-018-0360-8>
- Li, S., Sampson, C., Liu, C., Piao, H., & Liu, H. X. (2023). Integrin signaling in cancer : bidirectional mechanisms and therapeutic opportunities. *Cell Communication and Signaling*, 1–19. <https://doi.org/10.1186/s12964-023-01264-4>
- Li, X.-L., Liu, L., Li, D.-D., He, Y.-P., Guo, L.-H., Sun, L.-P., Liu, L.-N., Xu, H.-X., & Zhang, X.-P. (2017). Integrin β 4 promotes cell invasion and epithelial-mesenchymal transition through the modulation of Slug expression in hepatocellular carcinoma. *Scientific Reports*, *7*, 40464. <https://doi.org/10.1038/srep40464>
- Li, Xiao Ling, Lu, X., Parvathaneni, S., Bilke, S., Zhang, H., Thangavel, S., Vindigni, A., Hara, T., Zhu, Y., Meltzer, P. S., Lal, A., & Sharma, S. (2014). Identification of RECQ1-regulated transcriptome uncovers a role of RECQ1 in regulation of cancer cell migration and invasion. *Cell Cycle (Georgetown, Tex.)*, *13*(15), 2431–2445. <https://doi.org/10.4161/cc.29419>
- Li, Xiao Long, Liu, L., Li, D. D., He, Y. P., Guo, L. H., Sun, L. P., Liu, L. N., Xu, H. X., & Zhang, X. P. (2017). Integrin β 4 promotes cell invasion and epithelial-mesenchymal transition through the modulation of Slug expression in hepatocellular carcinoma. *Scientific Reports*, *7*(July 2016), 1–12. <https://doi.org/10.1038/srep40464>
- Lin, K.-Y., Lu, D., Hung, C.-F., Peng, S., Huang, L., Jie, C., Murillo, F., Rowley, J., Tsai, Y.-C., He, L., Kim, D.-J., Jaffee, E., Pardoll, D., & Wu, T.-C. (2007). Ectopic

- expression of vascular cell adhesion molecule-1 as a new mechanism for tumor immune evasion. *Cancer Research*, 67(4), 1832–1841. <https://doi.org/10.1158/0008-5472.CAN-06-3014>
- Liu, C., Wang, M., Zhang, H., Li, C., Zhang, T., Liu, H., Zhu, S., & Chen, J. (2022). Tumor microenvironment and immunotherapy of oral cancer. *European Journal of Medical Research*, 27(1), 198. <https://doi.org/10.1186/s40001-022-00835-4>
- Liu, D., Skomorovska, Y., Song, J., Bowler, E., Harris, R., Ravasz, M., Bai, S., Ayati, M., Tamai, K., Koyuturk, M., Yuan, X., Wang, Z., Wang, Y., & Ewing, R. M. (2019). ELF3 is an antagonist of oncogenic-signalling-induced expression of EMT-TF ZEB1. *Cancer Biology & Therapy*, 20(1), 90–100. <https://doi.org/10.1080/15384047.2018.1507256>
- Liu, L., Lim, M. A., Jung, S.-N., Oh, C., Won, H.-R., Jin, Y. L., Piao, Y., Kim, H. J., Chang, J. W., & Koo, B. S. (2021). The effect of Curcumin on multi-level immune checkpoint blockade and T cell dysfunction in head and neck cancer. *Phytomedicine: International Journal of Phytotherapy and Phytopharmacology*, 92, 153758. <https://doi.org/10.1016/j.phymed.2021.153758>
- Liu, Y.-M., Ge, J.-Y., Chen, Y.-F., Liu, T., Chen, L., Liu, C.-C., Ma, D., Chen, Y.-Y., Cai, Y.-W., Xu, Y.-Y., Shao, Z.-M., & Yu, K.-D. (2023). Combined Single-Cell and Spatial Transcriptomics Reveal the Metabolic Evolvement of Breast Cancer during Early Dissemination. *Advanced Science (Weinheim, Baden-Wurttemberg, Germany)*, 10(6), e2205395. <https://doi.org/10.1002/advs.202205395>
- Loi, S., Pommey, S., Haibe-Kains, B., Beavis, P. A., Darcy, P. K., Smyth, M. J., & Stagg, J. (2013). CD73 promotes anthracycline resistance and poor prognosis in triple negative breast cancer. *Proceedings of the National Academy of Sciences of the United States of America*, 110(27), 11091–11096. <https://doi.org/10.1073/pnas.1222251110>
- Lu, Y., Liu, Y., Oeck, S., Zhang, G. J., Schramm, A., & Glazer, P. M. (2020). Hypoxia Induces Resistance to EGFR Inhibitors in Lung Cancer Cells via Upregulation of FGFR1 and the MAPK Pathway. *Cancer Research*, 80(21), 4655–4667. <https://doi.org/10.1158/0008-5472.CAN-20-1192>
- Lugli, A., Kirsch, R., Ajioka, Y., Bosman, F., Cathomas, G., Dawson, H., El Zimaity, H., Fléjou, J.-F., Hansen, T. P., Hartmann, A., Kakar, S., Langner, C., Nagtegaal, I.,

- Puppa, G., Riddell, R., Ristimäki, A., Sheahan, K., Smyrk, T., Sugihara, K., ... Quirke, P. (2017). Recommendations for reporting tumor budding in colorectal cancer based on the International Tumor Budding Consensus Conference (ITBCC) 2016. *Modern Pathology: An Official Journal of the United States and Canadian Academy of Pathology, Inc*, 30(9), 1299–1311. <https://doi.org/10.1038/modpathol.2017.46>
- Lugli, A., Zlobec, I., Berger, M. D., Kirsch, R., & Nagtegaal, I. D. (2021). Tumour budding in solid cancers. *Nature Reviews. Clinical Oncology*, 18(2), 101–115. <https://doi.org/10.1038/s41571-020-0422-y>
- Ma, S.-R., Liu, J.-F., Jia, R., Deng, W.-W., & Jia, J. (2023). Identification of a Favorable Prognostic Subgroup in Oral Squamous Cell Carcinoma: Characterization of ITGB4/PD-L1(high) with CD8/PD-1(high). *Biomolecules*, 13(6). <https://doi.org/10.3390/biom13061014>
- Ma, X. L., Hu, B., Tang, W. G., Xie, S. H., Ren, N., Guo, L., & Lu, R. Q. (2020). CD73 sustained cancer-stem-cell traits by promoting SOX9 expression and stability in hepatocellular carcinoma. *Journal of Hematology and Oncology*, 13(1), 1–16. <https://doi.org/10.1186/s13045-020-0845-z>
- Ma, X. L., Shen, M. N., Hu, B., Wang, B. L., Yang, W. J., Lv, L. H., Wang, H., Zhou, Y., Jin, A. L., Sun, Y. F., Zhang, C. Y., Qiu, S. J., Pan, B. S., Zhou, J., Fan, J., Yang, X. R., & Guo, W. (2019). CD73 promotes hepatocellular carcinoma progression and metastasis via activating PI3K/AKT signaling by inducing Rap1-mediated membrane localization of P110 β and predicts poor prognosis. *Journal of Hematology and Oncology*, 12(1), 1–17. <https://doi.org/10.1186/s13045-019-0724-7>
- Marur, S., & Forastiere, A. A. (2016). Head and Neck Squamous Cell Carcinoma: Update on Epidemiology, Diagnosis, and Treatment. *Mayo Clinic Proceedings*, 91(3), 386–396. <https://doi.org/10.1016/j.mayocp.2015.12.017>
- Mastelic-Gavillet, B., Navarro Rodrigo, B., Décombaz, L., Wang, H., Ercolano, G., Ahmed, R., Lozano, L. E., Ianaro, A., Derré, L., Valerio, M., Tawadros, T., Jichlinski, P., Nguyen-Ngoc, T., Speiser, D. E., Verdeil, G., Gestermann, N., Dormond, O., Kandalaf, L., Coukos, G., ... Vigano, S. (2019). Adenosine mediates functional and metabolic suppression of peripheral and tumor-infiltrating CD8(+) T cells. *Journal for Immunotherapy of Cancer*, 7(1), 257.

- <https://doi.org/10.1186/s40425-019-0719-5>
- Masugi, Y., Yamazaki, K., Emoto, K., Effendi, K., Tsujikawa, H., Kitago, M., Itano, O., Kitagawa, Y., & Sakamoto, M. (2015). Upregulation of integrin β 4 promotes epithelial-mesenchymal transition and is a novel prognostic marker in pancreatic ductal adenocarcinoma. *Laboratory Investigation; a Journal of Technical Methods and Pathology*, 95(3), 308–319. <https://doi.org/10.1038/labinvest.2014.166>
- Meng, X., Liu, P., Wu, Y., Liu, X., Huang, Y., Yu, B., Han, J., Jin, H., & Tan, X. (2020). Integrin beta 4 (ITGB4) and its tyrosine-1510 phosphorylation promote pancreatic tumorigenesis and regulate the MEK1-ERK1/2 signaling pathway. *Bosnian Journal of Basic Medical Sciences*, 20(1), 106–116. <https://doi.org/10.17305/bjbms.2019.4255>
- Mesia, R., Iglesias, L., Lambea, J., Martínez-Trufero, J., Soria, A., Taberna, M., Trigo, J., Chaves, M., García-Castaño, A., & Cruz, J. (2021). SEOM clinical guidelines for the treatment of head and neck cancer (2020). *Clinical & Translational Oncology : Official Publication of the Federation of Spanish Oncology Societies and of the National Cancer Institute of Mexico*, 23(5), 913–921. <https://doi.org/10.1007/s12094-020-02533-1>
- Mittal, V. (2018). Epithelial Mesenchymal Transition in Tumor Metastasis. *Annual Review of Pathology*, 13, 395–412. <https://doi.org/10.1146/annurev-pathol-020117-043854>
- Miyazaki, K. (2006). Laminin-5 (laminin-332): Unique biological activity and role in tumor growth and invasion. *Cancer Science*, 97(2), 91–98. <https://doi.org/10.1111/j.1349-7006.2006.00150.x>
- Mody, M. D., Rocco, J. W., Yom, S. S., Haddad, R. I., & Saba, N. F. (2021). Head and neck cancer. *Lancet (London, England)*, 398(10318), 2289–2299. [https://doi.org/10.1016/S0140-6736\(21\)01550-6](https://doi.org/10.1016/S0140-6736(21)01550-6)
- Muraro, E., Fanetti, G., Lupato, V., Giacomarra, V., Steffan, A., Gobitti, C., Vaccher, E., & Franchin, G. (2021). Cetuximab in locally advanced head and neck squamous cell carcinoma: Biological mechanisms involved in efficacy, toxicity and resistance. *Critical Reviews in Oncology/Hematology*, 164(June), 103424. <https://doi.org/10.1016/j.critrevonc.2021.103424>
- Nair, S., Bonner, J. A., & Bredel, M. (2022). EGFR Mutations in Head and Neck

- Squamous Cell Carcinoma. *International Journal of Molecular Sciences*, 23(7).
<https://doi.org/10.3390/ijms23073818>
- Nardi, C. E., Dedivitis, R. A., Camillo de Almeida, R., de Matos, L. L., & Cernea, C. R. (2018). The role of E-cadherin and β -catenin in laryngeal cancer. *Oncotarget*, 9(53), 30199–30209. <https://doi.org/10.18632/oncotarget.25680>
- Nassar, D., & Blanpain, C. (2016). Cancer Stem Cells: Basic Concepts and Therapeutic Implications. *Annual Review of Pathology*, 11, 47–76. <https://doi.org/10.1146/annurev-pathol-012615-044438>
- Nguyen, B. P., Ryan, M. C., Gil, S. G., & Carter, W. G. (2000). Deposition of laminin 5 in epidermal wounds regulates integrin signaling and adhesion. *Current Opinion in Cell Biology*, 12(5), 554–562. [https://doi.org/10.1016/s0955-0674\(00\)00131-9](https://doi.org/10.1016/s0955-0674(00)00131-9)
- Nguyen, Phuong T, Kudo, Y., Yoshida, M., Iizuka, S., Ogawa, I., & Takata, T. (2011). N-cadherin expression is correlated with metastasis of spindle cell carcinoma of head and neck region. *Journal of Oral Pathology & Medicine : Official Publication of the International Association of Oral Pathologists and the American Academy of Oral Pathology*, 40(1), 77–82. <https://doi.org/10.1111/j.1600-0714.2010.00966.x>
- Nguyen, Phuong Thao, Nguyen, D., Chea, C., Miyauchi, M., Fujii, M., & Takata, T. (2018). Interaction between N-cadherin and decoy receptor-2 regulates apoptosis in head and neck cancer. *Oncotarget*, 9(59), 31516–31530. <https://doi.org/10.18632/oncotarget.25846>
- Nicholson, R. I., Gee, J. M., & Harper, M. E. (2001). EGFR and cancer prognosis. *European Journal of Cancer (Oxford, England: 1990)*, 37 Suppl 4, S9-15. [https://doi.org/10.1016/s0959-8049\(01\)00231-3](https://doi.org/10.1016/s0959-8049(01)00231-3)
- Nie, H., Xie, X., Zhang, D., Zhou, Y., Li, B., Li, F., Li, F., Cheng, Y., Mei, H., Meng, H., & Jia, L. (2020). Use of lung-specific exosomes for miRNA-126 delivery in non-small cell lung cancer. *Nanoscale*, 12(2), 877–887. <https://doi.org/10.1039/c9nr09011h>
- Nieto, M. A., Huang, R. Y. Y. J., Jackson, R. A. A., & Thiery, J. P. P. (2016). Emt: 2016. *Cell*, 166(1), 21–45. <https://doi.org/10.1016/j.cell.2016.06.028>
- Nievers, M. G., Kuikman, I., Geerts, D., Leigh, I. M., & Sonnenberg, A. (2000). Formation of hemidesmosome-like structures in the absence of ligand binding by the $(\alpha)6(\beta)4$ integrin requires binding of HD1/plectin to the cytoplasmic

- domain of the (beta)4 integrin subunit. *Journal of Cell Science*, *113* (Pt 6, 963–973. <https://doi.org/10.1242/jcs.113.6.963>
- Pan, M., Schinke, H., Luxenburger, E., Kranz, G., Shakhtour, J., Libl, D., Huang, Y., Gaber, A., Pavšič, M., Lenarčič, B., Kitz, J., Jakob, M., Schwenk-Zieger, S., Canis, M., Hess, J., Unger, K., Baumeister, P., & Gires, O. (2018). EpCAM ectodomain EpEX is a ligand of EGFR that counteracts EGF-mediated epithelial-mesenchymal transition through modulation of phospho-ERK1/2 in head and neck cancers. *PLoS Biology*, *16*(9), e2006624. <https://doi.org/10.1371/journal.pbio.2006624>
- Pang, L., Ng, K. T.-P., Liu, J., Yeung, W.-H. O., Zhu, J., Chiu, T.-L. S., Liu, H., Chen, Z., Lo, C.-M., & Man, K. (2021). Plasmacytoid dendritic cells recruited by HIF-1 α /eADO/ADORA1 signaling induce immunosuppression in hepatocellular carcinoma. *Cancer Letters*, *522*, 80–92. <https://doi.org/10.1016/j.canlet.2021.09.022>
- Paolillo, M., & Schinelli, S. (2019). Extracellular Matrix Alterations in Metastatic Processes. *International Journal of Molecular Sciences*, *20*(19). <https://doi.org/10.3390/ijms20194947>
- Pastushenko, I., & Blanpain, C. (2019). EMT Transition States during Tumor Progression and Metastasis. *Trends in Cell Biology*, *29*(3), 212–226. <https://doi.org/10.1016/j.tcb.2018.12.001>
- Petruk, N., Tuominen, S., Åkerfelt, M., Mattsson, J., Sandholm, J., Nees, M., Yegutkin, G. G., Jukkola, A., Tuomela, J., & Selander, K. S. (2021a). CD73 facilitates EMT progression and promotes lung metastases in triple-negative breast cancer. *Scientific Reports*, *11*(1), 1–13. <https://doi.org/10.1038/s41598-021-85379-z>
- Petruk, N., Tuominen, S., Åkerfelt, M., Mattsson, J., Sandholm, J., Nees, M., Yegutkin, G. G., Jukkola, A., Tuomela, J., & Selander, K. S. (2021b). CD73 facilitates EMT progression and promotes lung metastases in triple-negative breast cancer. *Scientific Reports*, *11*(1), 6035. <https://doi.org/10.1038/s41598-021-85379-z>
- Psyrrri, A., Seiwert, T. Y., & Jimeno, A. (2013). Molecular pathways in head and neck cancer: EGFR, PI3K, and more. *American Society of Clinical Oncology Educational Book. American Society of Clinical Oncology. Annual Meeting*, 246–255. https://doi.org/10.14694/EdBook_AM.2013.33.246
- Pu, H., Collazo, J., Jones, E., Gayheart, D., Sakamoto, S., Vogt, A., Mitchell, B., &

- Kyprianou, N. (2009). Dysfunctional transforming growth factor-beta receptor II accelerates prostate tumorigenesis in the TRAMP mouse model. *Cancer Research*, *69*(18), 7366–7374. <https://doi.org/10.1158/0008-5472.CAN-09-0758>
- Puram, S. V., Mints, M., Pal, A., Qi, Z., Reeb, A., Gelev, K., Barrett, T. F., Gerndt, S., Liu, P., Parikh, A. S., Ramadan, S., Law, T., Mroz, E. A., Rocco, J. W., Adkins, D., Thorstad, W. L., Gay, H. A., Ding, L., Paniello, R. C., ... Tirosh, I. (2023). Cellular states are coupled to genomic and viral heterogeneity in HPV-related oropharyngeal carcinoma. *Nature Genetics*, *55*(4), 640–650. <https://doi.org/10.1038/s41588-023-01357-3>
- Puram, S. V., Parikh, A. S., & Tirosh, I. (2018). Single cell RNA-seq highlights a role for a partial EMT in head and neck cancer. *Molecular & Cellular Oncology*, *5*(3), e1448244. <https://doi.org/10.1080/23723556.2018.1448244>
- Puram, S. V., Tirosh, I., Parikh, A. S., Patel, A. P., Yizhak, K., Gillespie, S., Rodman, C., Luo, C. L., Mroz, E. A., Emerick, K. S., Deschler, D. G., Varvares, M. A., Mylvaganam, R., Rozenblatt-Rosen, O., Rocco, J. W., Faquin, W. C., Lin, D. T., Regev, A., & Bernstein, B. E. (2017). Single-Cell Transcriptomic Analysis of Primary and Metastatic Tumor Ecosystems in Head and Neck Cancer. *Cell*, *171*(7), 1611-1624.e24. <https://doi.org/10.1016/j.cell.2017.10.044>
- Qi, Z., Barrett, T., Parikh, A. S., Tirosh, I., & Puram, S. V. (2019). Single-cell sequencing and its applications in head and neck cancer. *Oral Oncology*, *99*, 104441. <https://doi.org/10.1016/j.oraloncology.2019.104441>
- Qu, Q., Wu, D., Li, Z., & Yin, H. (2023). Tumor budding and the prognosis of patients with metastatic colorectal cancer: a meta-analysis. *International Journal of Colorectal Disease*, *38*(1), 141. <https://doi.org/10.1007/s00384-023-04423-8>
- Rahimi, S. (2020). HPV-related squamous cell carcinoma of oropharynx: a review. *Journal of Clinical Pathology*, *73*(10), 624–629. <https://doi.org/10.1136/jclinpath-2020-206686>
- Rahimy, E., Gensheimer, M. F., Beadle, B., & Le, Q.-T. (2023). Lessons and Opportunities for Biomarker-Driven Radiation Personalization in Head and Neck Cancer. *Seminars in Radiation Oncology*, *33*(3), 336–347. <https://doi.org/10.1016/j.semradonc.2023.03.013>
- Rehmani, H. S., & Issaeva, N. (2020). *EGFR in head and neck squamous cell carcinoma* :

- exploring possibilities of novel drug combinations.* 8(10), 8–11.
<https://doi.org/10.21037/atm.2020.04.07>
- Reinhardt, J., Landsberg, J., Schmid-Burgk, J. L., Ramis, B. B., Bald, T., Glodde, N., Lopez-Ramos, D., Young, A., Ngiow, S. F., Nettersheim, D., Schorle, H., Quast, T., Kolanus, W., Schadendorf, D., Long, G. V., Madore, J., Scolyer, R. A., Ribas, A., Smyth, M. J., ... Holzel, M. (2017). MAPK signaling and inflammation link melanoma phenotype switching to induction of CD73 during immunotherapy. *Cancer Research*, 77(17), 4697–4709. <https://doi.org/10.1158/0008-5472.CAN-17-0395>
- Ren, Z.-H., Lin, C.-Z., Cao, W., Yang, R., Lu, W., Liu, Z.-Q., Chen, Y.-M., Yang, X., Tian, Z., Wang, L.-Z., Li, J., Wang, X., Chen, W.-T., Ji, T., & Zhang, C.-P. (2016). CD73 is associated with poor prognosis in HNSCC. *Oncotarget*, 7(38), 61690–61702. <https://doi.org/10.18632/oncotarget.11435>
- Rong, C., Muller, M. F., Xiang, F., Jensen, A., Weichert, W., Major, G., Plinkert, P. K., Hess, J., & Affolter, A. (2020). Adaptive ERK signalling activation in response to therapy and in silico prognostic evaluation of EGFR-MAPK in HNSCC. *British Journal of Cancer*, 123(2), 288–297. <https://doi.org/10.1038/s41416-020-0892-9>
- Ruan, S., Lin, M., Zhu, Y., Lum, L., Thakur, A., Jin, R., Shao, W., Zhang, Y., Hu, Y., Huang, S., Hurt, E. M., Chang, A. E., Wicha, M. S., & Li, Q. (2020). Integrin β 4-Targeted Cancer Immunotherapies Inhibit Tumor Growth and Decrease Metastasis. *Cancer Research*, 80(4), 771–783. <https://doi.org/10.1158/0008-5472.CAN-19-1145>
- Sacco, A. G., Chen, R., Worden, F. P., Wong, D. J. L., Adkins, D., Swiecicki, P., Chai-Ho, W., Oppelt, P., Ghosh, D., Bykowski, J., Molinolo, A., Pittman, E., Estrada, M. V., Gold, K., Daniels, G., Lippman, S. M., Natsuhara, A., Messer, K., & Cohen, E. E. W. (2021). Pembrolizumab plus cetuximab in patients with recurrent or metastatic head and neck squamous cell carcinoma: an open-label, multi-arm, non-randomised, multicentre, phase 2 trial. *The Lancet. Oncology*, 22(6), 883–892. [https://doi.org/10.1016/S1470-2045\(21\)00136-4](https://doi.org/10.1016/S1470-2045(21)00136-4)
- Saitoh, M. (2023). Transcriptional regulation of EMT transcription factors in cancer. *Seminars in Cancer Biology*. <https://doi.org/10.1016/j.semcancer.2023.10.001>
- Santos, F. M. Dos, Viani, G. A., & Pavoni, J. F. (2021). Evaluation of survival of patients

- with locally advanced head and neck cancer treated in a single center. *Brazilian Journal of Otorhinolaryngology*, 87(1), 3–10. <https://doi.org/10.1016/j.bjorl.2019.06.006>
- Schinke, H., Pan, M., Akyol, M., Zhou, J., Shi, E., Kranz, G., Libl, D., Quadt, T., Simon, F., Canis, M., Baumeister, P., & Gires, O. (2022). SLUG-related partial epithelial-to-mesenchymal transition is a transcriptomic prognosticator of head and neck cancer survival. *Molecular Oncology*, 16(2), 347–367. <https://doi.org/10.1002/1878-0261.13075>
- Schinke, H., Shi, E., Lin, Z., Quadt, T., Kranz, G., Zhou, J., Wang, H., Hess, J., Heuer, S., Belka, C., Zitzelsberger, H., Schumacher, U., Genduso, S., Riecken, K., Gao, Y., Wu, Z., Reichel, C. A., Walz, C., Canis, M., ... Gires, O. (2022a). A transcriptomic map of EGFR-induced epithelial-to-mesenchymal transition identifies prognostic and therapeutic targets for head and neck cancer. *Molecular Cancer*, 21(1), 1–25. <https://doi.org/10.1186/s12943-022-01646-1>
- Schinke, H., Shi, E., Lin, Z., Quadt, T., Kranz, G., Zhou, J., Wang, H., Hess, J., Heuer, S., Belka, C., Zitzelsberger, H., Schumacher, U., Genduso, S., Riecken, K., Gao, Y., Wu, Z., Reichel, C. A., Walz, C., Canis, M., ... Gires, O. (2022b). A transcriptomic map of EGFR-induced epithelial-to-mesenchymal transition identifies prognostic and therapeutic targets for head and neck cancer. *Molecular Cancer*, 21(1), 178. <https://doi.org/10.1186/s12943-022-01646-1>
- Sharma, M., Sah, P., Sharma, S. S., & Radhakrishnan, R. (2013). Molecular changes in invasive front of oral cancer. *Journal of Oral and Maxillofacial Pathology : JOMFP*, 17(2), 240–247. <https://doi.org/10.4103/0973-029X.119740>
- Sharon, S., Daher-Ghanem, N., Zaid, D., Gough, M. J., & Kravchenko-Balasha, N. (2023). The immunogenic radiation and new players in immunotherapy and targeted therapy for head and neck cancer. *Frontiers in Oral Health*, 4, 1180869. <https://doi.org/10.3389/froh.2023.1180869>
- Shen, A., Ye, Y., Chen, F., Xu, Y., Zhang, Z., Zhao, Q., & Zeng, Z.-L. (2022). Integrated multi-omics analysis identifies CD73 as a prognostic biomarker and immunotherapy response predictor in head and neck squamous cell carcinoma. *Frontiers in Immunology*, 13, 969034. <https://doi.org/10.3389/fimmu.2022.969034>
- Shen, T., Cai, L.-D., Liu, Y.-H., Li, S., Gan, W.-J., Li, X.-M., Wang, J.-R., Guo, P.-D.,

- Zhou, Q., Lu, X.-X., Sun, L.-N., & Li, J.-M. (2018). Ube2v1-mediated ubiquitination and degradation of Sirt1 promotes metastasis of colorectal cancer by epigenetically suppressing autophagy. *Journal of Hematology & Oncology*, *11*(1), 95. <https://doi.org/10.1186/s13045-018-0638-9>
- Sheng, W., Chen, C., Dong, M., Wang, G., Zhou, J., Song, H., Li, Y., Zhang, J., & Ding, S. (2017). Calreticulin promotes EGF-induced EMT in pancreatic cancer cells via Integrin/EGFR-ERK/MAPK signaling pathway. *Cell Death & Disease*, *8*(10), e3147. <https://doi.org/10.1038/cddis.2017.547>
- Shi, K., Wang, G., Pei, J., Zhang, J., Wang, J., Ouyang, L., Wang, Y., & Li, W. (2022). Emerging strategies to overcome resistance to third-generation EGFR inhibitors. In *Journal of Hematology and Oncology* (Vol. 15, Issue 1). BioMed Central. <https://doi.org/10.1186/s13045-022-01311-6>
- Shibue, T., & Robert A. Weinberg. (2017). EMT CSCs drug resistance. *Nat Rev Clin Oncol*, *14*(10), 611–629. <https://doi.org/10.1038/nrclinonc.2017.44.EMT>
- Shibue, T., & Weinberg, R. A. (2017). EMT, CSCs, and drug resistance: the mechanistic link and clinical implications. *Nature Reviews. Clinical Oncology*, *14*(10), 611–629. <https://doi.org/10.1038/nrclinonc.2017.44>
- Siegel, R. L., Miller, K. D., Wagle, N. S., & Jemal, A. (2023). Cancer statistics, 2023. *CA: A Cancer Journal for Clinicians*, *73*(1), 17–48. <https://doi.org/10.3322/caac.21763>
- Sigismund, S., Avanzato, D., & Lanzetti, L. (2018). Emerging functions of the EGFR in cancer. *Molecular Oncology*, *12*(1), 3–20. <https://doi.org/10.1002/1878-0261.12155>
- Skrypek, N., Goossens, S., De Smedt, E., Vandamme, N., & Berx, G. (2017). Epithelial-to-Mesenchymal Transition: Epigenetic Reprogramming Driving Cellular Plasticity. *Trends in Genetics : TIG*, *33*(12), 943–959. <https://doi.org/10.1016/j.tig.2017.08.004>
- Solomon, B., Young, R. J., & Rischin, D. (2018). Head and neck squamous cell carcinoma: Genomics and emerging biomarkers for immunomodulatory cancer treatments. *Seminars in Cancer Biology*, *52*(Pt 2), 228–240. <https://doi.org/10.1016/j.semcancer.2018.01.008>
- Stanoev, A., Mhamane, A., Schuermann, K. C., Grecco, H. E., Stallaert, W., Baumdick, M., Brüggemann, Y., Joshi, M. S., Roda-Navarro, P., Fengler, S., Stockert, R.,

- Roßmannek, L., Luig, J., Koseska, A., & Bastiaens, P. I. H. (2018). Interdependence between EGFR and Phosphatases Spatially Established by Vesicular Dynamics Generates a Growth Factor Sensing and Responding Network. *Cell Systems*, 7(3), 295-309.e11. <https://doi.org/10.1016/j.cels.2018.06.006>
- Stewart, R. L., & O'Connor, K. L. (2015a). Clinical significance of the integrin $\alpha 6\beta 4$ in human malignancies. *Laboratory Investigation*, 95(9), 976–986. <https://doi.org/10.1038/labinvest.2015.82>
- Stewart, R. L., & O'Connor, K. L. (2015b). Clinical significance of the integrin $\alpha 6\beta 4$ in human malignancies. *Laboratory Investigation; a Journal of Technical Methods and Pathology*, 95(9), 976–986. <https://doi.org/10.1038/labinvest.2015.82>
- Stransky, N., Egloff, A. M., Tward, A. D., Kostic, A. D., Cibulskis, K., Sivachenko, A., Kryukov, G. V, Lawrence, M. S., Sougnez, C., McKenna, A., Shefler, E., Ramos, A. H., Stojanov, P., Carter, S. L., Voet, D., Cortés, M. L., Auclair, D., Berger, M. F., Saksena, G., ... Grandis, J. R. (2011). The mutational landscape of head and neck squamous cell carcinoma. *Science (New York, N.Y.)*, 333(6046), 1157–1160. <https://doi.org/10.1126/science.1208130>
- Sun, X., Li, S., & Shen, B. (2016). Identification of Disease States and Response to Therapy in Humans by Utilizing the Biomarker EGFR for Targeted Molecular Imaging. *Current Protein & Peptide Science*, 17(6), 534–542. <https://doi.org/10.2174/1389203717666160101123610>
- Sung, H., Ferlay, J., Siegel, R. L., Laversanne, M., Soerjomataram, I., Jemal, A., & Bray, F. (2021). Global Cancer Statistics 2020: GLOBOCAN Estimates of Incidence and Mortality Worldwide for 36 Cancers in 185 Countries. *CA: A Cancer Journal for Clinicians*, 71(3), 209–249. <https://doi.org/10.3322/caac.21660>
- Sung, J. S., Kang, C. W., Kang, S., Jang, Y., Chae, Y. C., Kim, B. G., & Cho, N. H. (2020a). ITGB4-mediated metabolic reprogramming of cancer-associated fibroblasts. *Oncogene*, 39(3), 664–676. <https://doi.org/10.1038/s41388-019-1014-0>
- Sung, J. S., Kang, C. W., Kang, S., Jang, Y., Chae, Y. C., Kim, B. G., & Cho, N. H. (2020b). ITGB4-mediated metabolic reprogramming of cancer-associated fibroblasts. *Oncogene*, 39(3), 664–676. <https://doi.org/10.1038/s41388-019-1014-0>
- Takada, Y., Ye, X., & Simon, S. (2007). *Protein family review The integrins*. <https://doi.org/10.1186/gb-2007-8-5-215>

- Tam, W. L., & Weinberg, R. A. (2013). The epigenetics of epithelial-mesenchymal plasticity in cancer. *Nature Medicine*, *19*(11), 1438–1449. <https://doi.org/10.1038/nm.3336>
- Tejani, M. A., Cohen, R. B., & Mehra, R. (2010). The contribution of cetuximab in the treatment of recurrent and/or metastatic head and neck cancer. *Biologics : Targets & Therapy*, *4*, 173–185. <https://doi.org/10.2147/btt.s3050>
- Thiery, J. P., Acloque, H., Huang, R. Y. J., & Nieto, M. A. (2009). Epithelial-mesenchymal transitions in development and disease. *Cell*, *139*(5), 871–890. <https://doi.org/10.1016/j.cell.2009.11.007>
- Thomas, G. R., Gross, J. H., & Stubbs, V. C. (2022). Head and neck squamous cell carcinoma. *Genomic and Precision Medicine: Oncology, Third Edition*, *6*(1), 297–318. <https://doi.org/10.1016/B978-0-12-800684-9.00018-6>
- Tyler, M., & Tirosh, I. (2021). Decoupling epithelial-mesenchymal transitions from stromal profiles by integrative expression analysis. *Nature Communications*, *12*(1), 2592. <https://doi.org/10.1038/s41467-021-22800-1>
- Van den Bossche, V., Zaryouh, H., Vara-Messler, M., Vignau, J., Machiels, J.-P., Wouters, A., Schmitz, S., & Corbet, C. (2022). Microenvironment-driven intratumoral heterogeneity in head and neck cancers: clinical challenges and opportunities for precision medicine. *Drug Resistance Updates : Reviews and Commentaries in Antimicrobial and Anticancer Chemotherapy*, *60*, 100806. <https://doi.org/10.1016/j.drug.2022.100806>
- Vijayan, D., Young, A., Teng, M. W. L., & Smyth, M. J. (2017). Targeting immunosuppressive adenosine in cancer. *Nature Reviews. Cancer*, *17*(12), 709–724. <https://doi.org/10.1038/nrc.2017.86>
- Vu, T., & Datta, P. K. (2017). Regulation of EMT in Colorectal Cancer: A Culprit in Metastasis. *Cancers*, *9*(12). <https://doi.org/10.3390/cancers9120171>
- Vuoriluoto, K., Haugen, H., Kiviluoto, S., Mpindi, J.-P., Nevo, J., Gjerdrum, C., Tiron, C., Lorens, J. B., & Ivaska, J. (2011). Vimentin regulates EMT induction by Slug and oncogenic H-Ras and migration by governing Axl expression in breast cancer. *Oncogene*, *30*(12), 1436–1448. <https://doi.org/10.1038/onc.2010.509>
- Walcher, L., Kistenmacher, A.-K., Suo, H., Kitte, R., Dluczek, S., Strauß, A., Blandszun, A.-R., Yevsa, T., Fricke, S., & Kossatz-Boehlert, U. (2020). Cancer Stem Cells-

- Origins and Biomarkers: Perspectives for Targeted Personalized Therapies. *Frontiers in Immunology*, *11*, 1280. <https://doi.org/10.3389/fimmu.2020.01280>
- Wang, K., Zou, P., Zhu, X., & Zhang, T. (2019). Ziyuglycoside II suppresses the aggressive phenotype of triple negative breast cancer cells through regulating Src/EGFR-dependent ITGB4/FAK signaling. *Toxicology in Vitro : An International Journal Published in Association with BIBRA*, *61*, 104653. <https://doi.org/10.1016/j.tiv.2019.104653>
- Wolfe, K., Kamata, R., Coutinho, K., Inoue, T., & Sasaki, A. T. (2020). Metabolic Compartmentalization at the Leading Edge of Metastatic Cancer Cells. *Frontiers in Oncology*, *10*, 554272. <https://doi.org/10.3389/fonc.2020.554272>
- Wong, T.-S., Gao, W., & Chan, J. Y.-W. (2014). Interactions between E-cadherin and microRNA deregulation in head and neck cancers: the potential interplay. *BioMed Research International*, *2014*, 126038. <https://doi.org/10.1155/2014/126038>
- Wu, P., Wang, Y., Wu, Y., Jia, Z., Song, Y., & Liang, N. (2019). Expression and prognostic analyses of ITGA11, ITGB4 and ITGB8 in human non-small cell lung cancer. *PeerJ*, *7*, e8299. <https://doi.org/10.7717/peerj.8299>
- Wu, X., Gu, Z., Chen, Y., Chen, B., Chen, W., Weng, L., & Liu, X. (2019). Application of PD-1 Blockade in Cancer Immunotherapy. *Computational and Structural Biotechnology Journal*, *17*, 661–674. <https://doi.org/10.1016/j.csbj.2019.03.006>
- Xia, C., Yin, S., To, K. K. W., & Fu, L. (2023). CD39/CD73/A2AR pathway and cancer immunotherapy. *Molecular Cancer*, *22*(1), 44. <https://doi.org/10.1186/s12943-023-01733-x>
- Xu, M. J., Johnson, D. E., & Grandis, J. R. (2017). EGFR-targeted therapies in the post-genomic era. *Cancer Metastasis Reviews*, *36*(3), 463–473. <https://doi.org/10.1007/s10555-017-9687-8>
- Xu, Z., Gu, C., Yao, X., Guo, W., Wang, H., Lin, T., Li, F., Chen, D., Wu, J., Ye, G., Zhao, L., Hu, Y., Yu, J., Shi, J., Li, G., & Liu, H. (2020). CD73 promotes tumor metastasis by modulating RICS/RhoA signaling and EMT in gastric cancer. *Cell Death and Disease*, *11*(3). <https://doi.org/10.1038/s41419-020-2403-6>
- Xue, C., Du, Y., Li, Y., Xu, H., & Zhu, Z. (2022). Tumor budding as a predictor for prognosis and therapeutic response in gastric cancer: A mini review. *Frontiers in Oncology*, *12*, 1003959. <https://doi.org/10.3389/fonc.2022.1003959>

- Xue, F., Wang, T., Shi, H., Feng, H., Feng, G., Wang, R., Yao, Y., & Yuan, H. (2022a). CD73 facilitates invadopodia formation and boosts malignancy of head and neck squamous cell carcinoma via the MAPK signaling pathway. *Cancer Science*, *113*(8), 2704–2715. <https://doi.org/10.1111/cas.15452>
- Xue, F., Wang, T., Shi, H., Feng, H., Feng, G., Wang, R., Yao, Y., & Yuan, H. (2022b). CD73 facilitates invadopodia formation and boosts malignancy of head and neck squamous cell carcinoma via the MAPK signaling pathway. *Cancer Science*, *113*(8), 2704–2715. <https://doi.org/10.1111/cas.15452>
- Yang, J., Liao, X., Yu, J., & Zhou, P. (2018). Role of CD73 in Disease: Promising Prognostic Indicator and Therapeutic Target. *Current Medicinal Chemistry*, *25*(19), 2260–2271. <https://doi.org/10.2174/0929867325666180117101114>
- Yangguang Ou, Rachael E Wilson, and S. G. W. (2018). EMT, MET, plasticity and tumor metastasis Basil. *Annu Rev Anal Chem (Palo Alto Calif)*, *11*(1), 509–533. <https://doi.org/10.1016/j.tcb.2020.07.003.EMT>
- Yao, Y., Wang, Y., Chen, L., Tian, Z., Yang, G., Wang, R., Wang, C., Wu, Q., Wu, Y., Gao, J., Kang, X., Duan, S., Zhang, Z., & Sun, S. (2022). Clinical utility of PDX cohorts to reveal biomarkers of intrinsic resistance and clonal architecture changes underlying acquired resistance to cetuximab in HNSCC. *Signal Transduction and Targeted Therapy*, *7*(1), 73. <https://doi.org/10.1038/s41392-022-00908-0>
- Yegutkin, G. G., & Boison, D. (2022). ATP and Adenosine Metabolism in Cancer: Exploitation for Therapeutic Gain. *Pharmacological Reviews*, *74*(3), 797–822. <https://doi.org/10.1124/pharmrev.121.000528>
- Yu, C., Liu, Y., Huang, D., Dai, Y., Cai, G., Sun, J., Xu, T., Tian, Y., & Zhang, X. (2011). TGF- β 1 mediates epithelial to mesenchymal transition via the TGF- β /Smad pathway in squamous cell carcinoma of the head and neck. *Oncology Reports*, *25*(6), 1581–1587. <https://doi.org/10.3892/or.2011.1251>
- Yu, T., Tang, Q., Chen, X., Fan, W., Zhou, Z., Huang, W., & Liang, F. (2021). TGF- β 1 and IL-17A mediate the protumor phenotype of neutrophils to regulate the epithelial-mesenchymal transition in oral squamous cell carcinoma. *Journal of Oral Pathology & Medicine: Official Publication of the International Association of Oral Pathologists and the American Academy of Oral Pathology*, *50*(4), 353–361. <https://doi.org/10.1111/jop.13122>

- Zhang, H., Pan, Y.-Z., Cheung, M., Cao, M., Yu, C., Chen, L., Zhan, L., He, Z.-W., & Sun, C.-Y. (2019). LAMB3 mediates apoptotic, proliferative, invasive, and metastatic behaviors in pancreatic cancer by regulating the PI3K/Akt signaling pathway. *Cell Death & Disease*, *10*(3), 230. <https://doi.org/10.1038/s41419-019-1320-z>
- Zhang, N., Ng, A. S., Cai, S., Li, Q., Yang, L., & Kerr, D. (2021). Novel therapeutic strategies: targeting epithelial-mesenchymal transition in colorectal cancer. *The Lancet. Oncology*, *22*(8), e358–e368. [https://doi.org/10.1016/S1470-2045\(21\)00343-0](https://doi.org/10.1016/S1470-2045(21)00343-0)
- Zhang, Yan, Reif, G., & Wallace, D. P. (2020). Extracellular matrix, integrins, and focal adhesion signaling in polycystic kidney disease. *Cellular Signalling*, *72*, 109646. <https://doi.org/10.1016/j.cellsig.2020.109646>
- Zhang, Yaoting, Kadasah, S., Xie, J., & Gu, D. (2022). Head and Neck Squamous Cell Carcinoma: NT5E Could Be a Prognostic Biomarker. *Applied Bionics and Biomechanics*, *2022*, 3051907. <https://doi.org/10.1155/2022/3051907>
- Zhong, F., Lu, H.-P., Chen, G., Dang, Y.-W., Li, G.-S., Chen, X.-Y., Qin, Y.-Y., Yao, Y.-X., Zhang, X.-G., Liang, Y., Li, M.-X., Mo, M., Zhang, K.-L., Ding, H., Huang, Z.-G., & Wei, Z.-X. (2020). The clinical significance and potential molecular mechanism of integrin subunit beta 4 in laryngeal squamous cell carcinoma. *Pathology, Research and Practice*, *216*(2), 152785. <https://doi.org/10.1016/j.prp.2019.152785>
- Zhou, P., Zhi, X., Zhou, T., Chen, S., Li, X., Wang, L., Yin, L., Shao, Z., & Ou, Z. (2007). Overexpression of ecto-5' -nucleotidase (CD73) promotes T-47D human breast cancer cells invasion and adhesion to extracellular matrix. *Cancer Biology and Therapy*, *6*(3), 426–431. <https://doi.org/10.4161/cbt.6.3.3762>
- Zhu, L., Tian, Q., Gao, H., Wu, K., Wang, B., Ge, G., Jiang, S., Wang, K., Zhou, C., He, J., Liu, P., Ren, Y., & Wang, B. (2022). PROX1 promotes breast cancer invasion and metastasis through WNT/ β -catenin pathway via interacting with hnRNPK. *International Journal of Biological Sciences*, *18*(5), 2032–2046. <https://doi.org/10.7150/ijbs.68960>
- Zhuang, H., Zhou, Z., Ma, Z., Li, Z., Liu, C., Huang, S., Zhang, C., & Hou, B. (2020). Characterization of the prognostic and oncologic values of ITGB superfamily

- members in pancreatic cancer. *Journal of Cellular and Molecular Medicine*, 24(22), 13481–13493. <https://doi.org/10.1111/jcmm.15990>
- Zimmermann, M., Zouhair, A., Azria, D., & Ozsahin, M. (2006). *The epidermal growth factor receptor (EGFR) in head and neck cancer : its role and treatment implications*. 6, 1–6. <https://doi.org/10.1186/1748-717X-1-11>

6. Contribution statement

Immunohistochemistry and Immunofluorescence staining of HNSCC patients samples and 3D spheroids were performed by Gisela Kranz (Department of Otorhinolaryngology, Head and Neck Surgery, Grosshadern Medical Center, Ludwig-Maximilians-University, Munich, Germany). Quantification of immunohistochemistry staining and intensity of tumor budding was performed in collaboration with Tanja Quadt and Olivier Gires (Department of Otorhinolaryngology, Head and Neck Surgery, Grosshadern Medical Center, Ludwig-Maximilians-University, Munich, Germany).

RNAseq-related bioinformatic analysis was performed by Henrik Schinke (Department of Otorhinolaryngology, Head and Neck Surgery, Grosshadern Medical Center, Ludwig-Maximilians-University, Munich, Germany) and Zhengquan Wu (Walter Brendel Center for Experimental Medicine, University of Munich, Munich, Germany).

ITGB4 knockdown cells were generated by Prof. U. Schumacher and Dr. S. Gendus (UKE, Hamburg, Germany). WST8 assay and 22E6 treatment in 3D spheroids were performed by Birnur Sinem Karaoglan (Department of Otorhinolaryngology, Head and Neck Surgery, LMU University Hospital, LMU Munich, Munich, Germany). Examination of EMT markers by qPCR and co-treatment of mitomycin C with EGF were conducted by Sabina Schwenk-Zieger (Department of Otorhinolaryngology, Head and Neck Surgery, LMU University Hospital, LMU Munich, Munich, German).

7. List of publications

Parts of the results presented in this doctoral thesis have been published in:

A transcriptomic map of EGFR-induced epithelial-to-mesenchymal transition identifies prognostic and therapeutic targets for head and neck cancer.

Schinke, H. *, Shi, E. *, Lin, Z. *, Quadt, T., Kranz, G., Zhou, J., Wang, H., Hess, J., Heuer, S., Belka, C., Zitzelsberger, H., Schumacher, U., Genduso, S., Riecken, K., Gao, Y., Wu, Z., Reichel, C. A., Walz, C., Canis, M., Unger, K., Baumeister, P., Pan, M., Gires, O.

Molecular Cancer, 2022, 21(1): 178.

*These authors contributed equally to this work.

5'-Ectonucleotidase CD73/NT5E supports EGFR-mediated invasion of HPV-negative head and neck carcinoma cells.

Shi, E. *, Wu, Z. *, Karaoglan, B. S., Zieger, S. S., Kranz, G., Razak, N. A., Reichel, C. A., Canis, M., Baumeister, P., Zeidler, R., Gires, O.

Journal of Biomedical Science, 2023, 30(1): 72.

*These authors contributed equally to this work.

Additional work during my work as doctoral student warranted authorships in:

SLUG-related partial epithelial-to-mesenchymal transition is a transcriptomic prognosticator of head and neck cancer survival.

Schinke, H., Pan, M., Akyol, M., Zhou, J., Shi, E., Kranz, G., Libl, D., Quadt, T., Simon, F., Canis, M., Baumeister, P., Gires, O.

Molecular Oncology, 16(2), 347–367.

8. Acknowledge

I would like to express my sincere appreciation to everyone who contributed to the completion of my doctoral thesis.

First and foremost, I am deeply indebted to my supervisor, Prof. Olivier Gires, for his unwavering guidance, expertise, and continuous support throughout my three years of research. His mentorship has been invaluable in shaping the direction of my work and helping me navigate the challenges of academia. Under his supervision, I not only gained profound academic insights but also developed resilience and confidence.

I extend my heartfelt thanks to the other members of my thesis committee, Prof. Philipp Baumeister and Prof. Sebastian Kobold, for their insightful feedback, constructive criticism, and valuable suggestions that enriched the quality of my research.

Secondly, I sincerely thank my colleagues Henrik, Tanja, Yujing, and Jiefu for their teaching, guidance, and assistance when I first joined our lab. Their dedicated mentorship helped me integrate better into the lab and adapt smoothly to the new research environment. I'm also deeply grateful to my other colleagues, Vera, Alex, Darko, Gisela, and Sabina, for sharing their experiences and providing kind help with my doctoral project. Special acknowledgments to Dr. S. Genduso for their support in generating ITGB4 knockdown cells successfully, and to Prof. Reinhard Zeidler for providing me with the 22E6 antibody.

In addition, I express my gratitude to Sinem, Nilofer, Simrin, Ningyue, Zhongyang, Sharduli, Ana Marija, and Mahesh for their support and encouragement. Your camaraderie and shared experiences have made this academic endeavor more enjoyable.

I also want to acknowledge the financial support provided by the China Scholarship Council (CSC), which made my study possible. To my friends and family, your unwavering encouragement and belief in me have been a constant source of motivation. I am grateful for your patience and understanding during this demanding period.

Lastly, I want to express my heartfelt thanks to my partner, Zhengquan. During my studies in Germany, he not only provided emotional support, understanding, and companionship in my daily life but also actively participated in the bioinformatics analysis of my doctoral project. His love has consistently been an incredibly precious part of both my work and life.